

**TRANSVERSE STIFFENER REQUIREMENTS IN STRAIGHT
AND HORIZONTALLY CURVED STEEL I-GIRDERS**

A Thesis
Presented to
The Academic Faculty

By

Yoon Duk Kim

In Partial Fulfillment
Of the Requirements for the Degree
Master of Science in
Civil and Environmental Engineering

Georgia Institute of Technology
August 2004

**TRANSVERSE STIFFENER REQUIREMENTS IN STRAIGHT
AND HORIZONTALLY CURVED STEEL I-GIRDERS**

Approved by:

Dr. Donald W. White, Advisor

Dr. Kenneth M. Will

Dr. Rami M. Haj-Ali

August 19, 2004

ACKNOWLEDGEMENT

I would like to express my gratitude to all those who gave me the possibility to complete this thesis. Special thanks are due to my advisor Professor Donald W. White whose help, stimulating suggestions and encouragement helped me in all the time of research for and writing of this thesis. I am deeply indebted to my committee members, Professor Kenneth M. Will and Professor Rami M. Haj-Ali for all their help and support. Also, I would like to thank Dr. Min Xie for the suggestions and help that he provided for me.

I want to thank all my friends for all their help, support, interest and valuable hints. Especially I am obliged to Sekwon Jung for all his assistance and advice on this study.

Special thanks are due to my parents for their support and encouragement that makes this possible. I would like to thank more specially to my husband Yongjae whose patient love enabled me to complete this work.

TABLE OF CONTENTS

Acknowledgement	iii
List of Tables	vii
List of Figures	viii
List of Symbols	xiii
Summary	xvi
Chapter I Introduction	1
1.1 Background and Problem Statement	1
1.2 Organization	6
Chapter II Background	7
2.1 Transverse Stiffener Rigidity Requirements for Web Shear Buckling Strength	7
2.1.1 AASHTO (2004)	7
2.1.2 Bleich (1952)	8
2.1.3 Stanway et al. (1993)	10
2.1.4 Mariani et al. (1973)	15
2.2 Transverse Stiffener Rigidity Requirements for Web Shear Post-Buckling Strength	18
2.2.1 Stanway et al. (1993 and 1996)	18
2.2.2 Lee et al. (2002 and 2003)	24
2.2.3 Horne and Grayson (1983)	25
2.2.4 Nakai et al. (1984 and 1985)	27
2.3 Explicit Transverse Stiffener Strength Requirements	29
2.3.1 AASHTO (2004) Area Requirement	30
2.3.2 Eurocode 3 Requirements	36
2.3.3 Strength Requirements Based on Idealization of the Transverse Stiffeners as Flexural Elements	37
2.3.3.1 Stanway et al. (1993 and 1996)	37
2.3.3.2 Rahal and Harding (1990a, 1990b and 1991)	39
2.3.3.3 Xie (2000)	41

Chapter III Design of the Parametric Study	43
3.1 Design of Test Girders	43
3.1.1 Test Configuration	43
3.1.2 Test Variables	45
3.1.3 Selection of Girder Material and Geometry	46
3.2 Finite Element Models	50
3.2.1 Finite Element Discretization	50
3.2.2 Load and Displacement Boundary Conditions	50
3.2.3 Material Stress-Strain Characteristics	51
3.2.4 Residual Stresses and Geometric Imperfections	56
3.2.4.1 Residual Stresses	56
3.2.4.2 Geometric Imperfection Patterns, Straight I-Girders	56
3.2.4.3 Magnitude of the Geometric Imperfections	60
3.2.4.4 Geometric Imperfection Patterns and Inside versus Outside Location of One-Sided Transverse Stiffeners in Curved I- Girders	62
3.2.5 Comparison of FEA Predictions to Experimental Test Results	66
Chapter IV Parametric Study Results	79
4.1 Overview	79
4.2 I-Girder Shear Strength versus Stiffener Rigidity	80
4.3 Stiffener Strains	93
4.4 Sensitivity of the Shear Strength to the Geometric Imperfection Pattern	103
4.5 Web Behavior	105
4.6 Synthesis of Results	111
4.6.1 Stiffener Requirements for Development of the Shear Buckling Strength	111
4.6.2 Stiffener Requirements for Development of Shear Postbuckling Strength	112
4.6.2.1 The $I'_{scr(C=1)}$ Concept – Required Stiffener Size at the Largest Web Slenderness Corresponding to $C = 1$	112
4.6.2.2 Required Stiffener Sizes Relative to the Size Corresponding to $I'_{scr(C=1)}$	115
4.6.2.2.1 Comparisons to the Parametric Study Results from This Research	115
4.6.2.2.2 Comparisons to the Parametric Study Results from Prior Research	129

4.7 Consideration of General Stiffener Cross-Section Geometry	141
4.8 Stiffeners with $F_{ys} < F_{yw}$	142
4.9 Consideration of Cases with $V_u < \phi V_n$	143
4.10 Summary of Recommendations	144
Chapter V Summary	148
5.1 Summary	148
5.2 Future Work	154
List of References	157

LIST OF TABLES

Table 2.1.	Required J values for development of shear postbuckling strength from (Stanway et al. 1993).	20
Table 2.2.	Ratio of J required to achieve $\mu_u = 0.9$ to J required to achieve $\mu_{cr} = 0.9$, based on the solutions from (Stanway et al. 1993).	20
Table 2.3.	Comparison of required J values for development of the web postbuckling strength from Stanway et al. (1996 and 1993) to the J requirement in AASHTO (2004) for development of the web shear buckling load.	23
Table 3.1.	Summary of cross section dimensions and non-dimensional ratios for the test girders.	49
Table 3.2	True stress-strain data for the multilinear representations of the web-stiffener and flange materials for finite element analysis.	55
Table 3.3.	Dimensions of the test girders TGV7 and TGV8 (Rockey et al. 1981)	69
Table 3.4.	Material properties for test girders TGV7 and TGV8 (Rockey et al. 1981)	69
Table 3.5.	Key parameters pertinent to the design of the intermediate transverse stiffeners in girders TGV7 and TGV8	70
Table 4.1.	Summary of the approximate maximum knuckle values for I_s/I_{scr} .	93

LIST OF FIGURES

Figure 2.1a.	Required J values for development of the shear buckling strength emphasizing the requirements at $d_o/D = 0.5$.	12
Figure 2.1b.	Required J values for development of the shear buckling strength emphasizing the requirements for $d_o/D = 1$.	13
Figure 2.2.	Required J' values for development of the shear buckling strength emphasizing the requirements for $d_o/D = 1$.	16
Figure 2.3.	Free-body diagram at an intermediate transverse stiffener location.	31
Figure 2.4.	Stress Distribution in a stiffener	33
Figure 3.1.	Test configuration and shear and approximate moment diagrams	44
Figure 3.2.	Engineering stress-strain and true stress-strain curves for a representative HPS 485W tension coupon test (Wright 1997).	52
Figure 3.3.	Actual and multi-linear representations of the HPS 485W engineering and true stress-strain curves.	54
Figure 3.4.	Multi-linear representations of the web-stiffener and flange engineering and true stress-strain response	55
Figure 3.5.	Critical geometric imperfection pattern for nominally-flat webs with $d_o/D = 1, 1.5$ and 2.0 (Rahal and Harding 1991).	57
Figure 3.6.	Critical geometric imperfection pattern for nominally-flat webs with $d_o/D = 0.5$ (Rahal and Harding 1991).	57
Figure 3.7.	Critical geometric imperfection pattern for curved I-girders	66
Figure 3.8.	Geometric configuration of tests TGV7 and TGV8 (Rockey et al. 1981) ($d_{o1} = d_{o2} = d_{o12}/2$, $d_{o3} = d_{o4} = d_{o34}/2$).	68
Figure 3.9.	Load-deflection curves from finite element analysis of girder TGV7-2 and from experimental testing of girder TGV7-2 (Rockey et al. 1981).	71

Figure 3.10.	Load-deflection curves from finite element analysis of girder TGV8-1 and from experimental testing of girder TGV8-2 (Rockey et al. 1981).	72
Figure 3.11.	von Mises stress contours on the deformed geometry at the limit load in test TGV7-2 (view from the outside direction, deformation scale factor = 5).	74
Figure 3.12.	Lateral deflection contours on the deformed geometry when the vertical deflection at mid-span is 8 mm in test TGV7-2 (view from the outside direction, deformation scale factor = 1.0).	76
Figure 3.13.	von Mises stress contours on the deformed geometry at the limit load in test TGV8-1 (view from the outside direction, deformation scale factor = 10).	77
Figure 3.14.	Lateral deflection contours on the deformed geometry when the vertical deflection at mid-span is 4 mm in test TGV8-1 (view from the outside direction, deformation scale factor = 1.0).	78
Figure 4.1.	Strength versus stiffener rigidity for $d_o/D = 1$ and $D/t_w = 150$.	82
Figure 4.2.	Strength versus stiffener rigidity for $d_o/D = 1$ and $D/t_w = 300$.	83
Figure 4.3.	Strength versus stiffener rigidity for $d_o/D = 0.5$ and $D/t_w = 150$.	84
Figure 4.4.	Strength versus stiffener rigidity for $d_o/D = 0.5$ and $D/t_w = 300$.	85
Figure 4.5.	Strength versus stiffener rigidity for $d_o/D = 2$ and $D/t_w = 150$.	86
Figure 4.6.	Strength versus stiffener rigidity for $d_o/D = 3$ and $D/t_w = 150$.	87
Figure 4.7.	Strength versus stiffener rigidity for $d_o/D = 1.5$ and $D/t_w = 300$.	88
Figure 4.8a.	Variation of stiffener mid-height strains at maximum shear strength for $d_o/D = 1.0$, $D/t_w = 150$ and $I_s/I_{scr} = 8$.	95
Figure 4.8b.	Variation of stiffener end strains at maximum shear strength for $d_o/D = 1.0$, $D/t_w = 150$ and $I_s/I_{scr} = 8$.	95
Figure 4.9a.	Variation of stiffener mid-height strains at maximum shear strength for $d_o/D = 1.0$ and $D/t_w = 300$.	98
Figure 4.9b.	Variation of stiffener end strains at maximum shear strength for $d_o/D = 1.0$ and $D/t_w = 300$ (at stiffener end having the largest strain).	98

Figure 4.10.	Stiffener mid-height strains versus shear force, curved girder with two-sided stiffeners, $d_o/D = 1$, $D/t_w = 150$ and $I_s/I_{scr} = 8$.	100
Figure 4.11.	Stiffener mid-height strains versus shear force, straight girder with one-sided stiffeners on outside, $d_o/D = 1$, $D/t_w = 300$ and $I_s/I_{scr} = 50$.	101
Figure 4.12.	Stiffener mid-height strains versus shear force, straight girder with two-sided stiffeners, $d_o/D = 1$, $D/t_w = 300$ and $I_s/I_{scr} = 21$.	102
Figure 4.13.	Effect of geometric imperfection pattern for curved girders with $d_o/D = 1$, $D/t_w = 300$ and one-sided stiffeners.	104
Figure 4.14.	von Mises stress at web mid-thickness for $V = V_{max}$, straight girder with one-sided stiffener on outside, $d_o/D = 1$, $D/t_w = 150$ and $I_s/I_{scr} = 1$ (deformation scale factor = 10).	106
Figure 4.15.	Equivalent plastic strain at web mid-thickness for $V = V_{max}$, straight girder with one-sided stiffener on outside, $d_o/D = 1$, $D/t_w = 150$ and $I_s/I_{scr} = 1$ (deformation scale factor = 10).	106
Figure 4.16.	Lateral deflection contours at $V = V_{max}$, straight girder with one-sided stiffener on outside, $d_o/D = 1$, $D/t_w = 150$ and $I_s/I_{scr} = 1$ (deformation scale factor = 10).	107
Figure 4.17.	von Mises stress contours for $V = V_{max}$, curved girder with one-sided stiffener, $d_o/D = 1$, $D/t_w = 150$ and $I_s/I_{scr} = 8$ (deformation scale factor = 10).	108
Figure 4.18.	Equivalent plastic strain contours for $V = V_{max}$, curved girder with one-sided stiffener, $d_o/D = 1$, $D/t_w = 150$ and $I_s/I_{scr} = 8$ (deformation scale factor = 10).	109
Figure 4.19.	Lateral deflection contours at $V = V_{max}$, curved girder with one-sided stiffener, $d_o/D = 1$, $D/t_w = 150$ and $I_s/I_{scr} = 8$ (deformation scale factor = 10).	110
Figure 4.20.	Lateral deflection contours at $V = V_{max}$, curved girder with two-sided stiffener, $d_o/D = 1$, $D/t_w = 150$ and $I_s/I_{scr} = 8$ (deformation scale factor = 10).	110
Figure 4.21a.	Required stiffener sizes, girders with one-sided stiffeners, $d_o/D = 1$, $F_{yw} = 485$ MPa (70ksi).	116

Figure 4.21b.	Required stiffener sizes, girders with two-sided stiffeners, $d_o/D = 1$, $F_{yw} = 485$ MPa (70ksi).	117
Figure 4.22a.	Required stiffener sizes, girders with one-sided stiffeners, $d_o/D = 0.5$, $F_{yw} = 485$ MPa (70ksi).	118
Figure 4.22b.	Required stiffener sizes, girders with two-sided stiffeners, $d_o/D = 0.5$, $F_{yw} = 485$ MPa (70ksi).	119
Figure 4.23a.	Required stiffener sizes, girders with one-sided stiffeners, $d_o/D = 2$, $F_{yw} = 485$ MPa (70ksi).	120
Figure 4.23b.	Required stiffener sizes, girders with two-sided stiffeners, $d_o/D = 2$, $F_{yw} = 485$ MPa (70ksi).	121
Figure 4.24a.	Required stiffener sizes, girders with one-sided stiffeners, $d_o/D = 3$, $F_{yw} = 485$ MPa (70ksi).	122
Figure 4.24b.	Required stiffener sizes, girders with two-sided stiffeners, $d_o/D = 3$, $F_{yw} = 485$ MPa (70ksi).	123
Figure 4.25a.	Required stiffener sizes, girders with one-sided stiffeners, $d_o/D = 1.5$, $F_{yw} = 485$ MPa (70ksi).	124
Figure 4.25b.	Required stiffener sizes, girders with two-sided stiffeners, $d_o/D = 1.5$, $F_{yw} = 485$ MPa (70ksi).	125
Figure 4.26a.	Required stiffener sizes, girders with one-sided stiffeners, $d_o/D = 1$, $F_{yw} = 245$ MPa (36ksi).	130
Figure 4.26b.	Required stiffener sizes, girders with two-sided stiffeners, $d_o/D = 1$, $F_{yw} = 245$ MPa (36ksi).	131
Figure 4.27a.	Required stiffener sizes, girders with one-sided stiffeners, $d_o/D = 0.5$, $F_{yw} = 245$ MPa (36ksi).	132
Figure 4.27b.	Required stiffener sizes, girders with two-sided stiffeners, $d_o/D = 0.5$, $F_{yw} = 245$ MPa (36ksi).	133
Figure 4.28a.	Required stiffener sizes, girders with one-sided stiffeners, $d_o/D = 2$, $F_{yw} = 245$ MPa (36ksi).	134
Figure 4.28b.	Required stiffener sizes, girders with two-sided stiffeners, $d_o/D = 2$, $F_{yw} = 245$ MPa (36ksi).	135

- Figure 4.29. Shear buckling coefficient for an infinitely long plate subdivided by equidistant stiffeners with $I_s = I'_{scr(C=1)}$ versus the AASHTO (2004) k value, $d_o/D = 0.5$. 140
- Figure 4.30. Elastic and inelastic buckling solutions $C_{el} = V_{cr,el}/V_p$ and $C = V_{cr}/V_p$ from Bleich (1952) for an infinitely long plate subdivided by equidistant stiffeners with $I_s = I'_{scr(C=1)}$, $d_o/D = 0.5$ and $F_{yw} = 230$ MPa (33 ksi). 140

LIST OF SYMBOLS

A_s	= area of a transverse stiffener
$A_{s,reqd}$	= area of a transverse stiffener required by the AASHTO (2004) area requirement
A_w	= area of the web participating to the stiffener
b	= smaller dimension of the panel (equal to the minimum of d_o and D)
b_f	= width of a flange
b_s	= width of a transverse stiffener
$b_{scr(C=1)}$	= stiffener width corresponding to $I_{scr(C=1)}$
$b'_{scr(C=1)}$	= stiffener width corresponding to $I'_{scr(C=1)}$
c	= curvature parameter
C	= ratio of the shear buckling stress to the shear yield strength
C_{el}	= ratio of the shear elastic buckling stress to the shear yield strength
D	= depth of the web plate
d_o	= spacing of transverse stiffeners
E	= modulus of elasticity of steel, taken as 200 GPa (29000 ksi)
e	= strain of a specified point on transverse stiffener
e_y	= yield strain, F_{ys}/E
F_{crs}	= stiffener local buckling stress
F_{nl}	= ratio of q_{pb}/q_{pbcr} at $y = D/2$, where q_{pb} is from nonlinear analyses with an imperfection fully affined to the first point-symmetric buckling mode, and q_{pbcr} is from the first point-symmetric critical buckling mode (Stanway et al. 1996)
F_n	= nominal flexural resistance in terms of stress
F_u	= ultimate tensile strength of material
F_{yf}	= specified minimum yield strength of a flange
F_{ys}	= specified minimum yield strength of a transverse stiffener
F_{yw}	= specified minimum yield strength of a web
f_l	= maximum elastically computed flange lateral bending stress within the unbraced length under consideration
I_s	= moment of inertia of a stiffener
I_{scr}	= moment of inertia of a stiffener required for critical buckling by AASHTO (2004)
I_{sR}	= moment of inertia of a stiffener required based on the final recommendations of this study
I_{sA1}	= moment of inertia of a stiffener which satisfies the AASHTO (2004) area requirement for single-plate transverse stiffeners
I_{sA2}	= moment of inertia of a stiffener which satisfies the AASHTO (2004) area requirement for two-sided transverse stiffeners
I'_{scr}	= moment of inertia of transverse stiffener for critical buckling required by the modified equation in this thesis
J	= the required ratio of rigidity of one transverse stiffener to that of a web plate

k	= shear buckling coefficient
k_λ	= $0.375 (D/b) + 0.625$ (Stanway et al. 1996)
k_0	= shear buckling coefficient for the plate with $I_s = 0$
k_∞	= shear buckling coefficient for the plate with $I_s = \infty$
k_{cro}	= non-dimensional buckling stress coefficient for the design model (Stanway et al. 1996)
L_b	= unbraced length
M_n	= nominal moment capacity
M_o	= M_s caused by the out-of-plane component of the rigid link forces, acting on a stiffener with the total deflection w_{os} ($w_s = 0$) (Stanway et al. 1996)
M_{pb}	= stiffener moment resulting from q_{pb} (Stanway et al. 1996)
M_{pbcr}	= M_{pb} from critical buckling analysis (Stanway et al. 1996)
M_s	= stiffener bending moment (Stranway et al. 1996)
P_s	= axial force in a transverse stiffener
R	= radius of curvature
R_b	= web bend-buckling parameter
S_s	= section modulus of a transverse stiffener
S_x	= elastic section modulus
t_f	= thickness of a flange
t_s	= thickness of a transverse stiffener
t_w	= thickness of a web
V	= applied shear load in finite element analysis in this study
V_{cr}	= theoretical elastic buckling resistance of the web panels
V_p	= plastic shear capacity
$V_{cr,el}$	= theoretical elastic shear buckling strength of a simply-supported web panel
V_u	= applied shear at the strength load level
V_n	= nominal shear resistance
V_{max}	= shear limit load of finite element analysis in this study
$V_{n(AASHTO)}$	= nominal shear resistance of the web given by the AASHTO (2004) shear strength equations
w_{os}	= initial imperfection of a transverse stiffener
w_{op}	= initial imperfection of a web
w_p	= web panel lateral deflection
w_{pbcr}	= w_p in critical buckling analysis (Stanway et al. 1996)
w_s	= stiffener lateral deflection
X	= modification factor on the required rigidity for development of the buckling strength of curved web panels
X_u	= modification factor on the rigidity required by JSHB for development of the postbuckling strength of curved web panels (Nakai et al. 1985)
Z	= curvature parameter
σ	= true stress
ϵ	= true strain
σ_{nom}	= engineering stress
ϵ_{nom}	= engineering strain
ρ_t	= maximum of F_{yw}/F_{crs} and 1

γ	= stiffener flexural rigidity parameter
ϕ	= strength reduction factor
α	= web aspect ratio
σ_t	= tension field stress, given by $\sigma_t = (1 - C)F_{yw}$
θ	= orientation of the tension field
$\tau_{u\infty}$	= maximum shear strength corresponding to $I_s = \infty$
τ_{u0}	= maximum shear strength corresponding to $I_s = 0$
μ_{cr}	= $\frac{k - k_0}{k_\infty - k_0}$
μ_u	= $\frac{t_u - t_{u0}}{t_{u\infty} - t_{u0}}$
ν	= Poisson's ratio

SUMMARY

Recent research studies have confirmed that curved I-girders are capable of developing substantial shear postbuckling resistance due to tension field action and have demonstrated that the AASHTO LRFD equations for the tension field resistance in straight I-girders may be applied to curved I-girders within specific limits. However, the corresponding demands on intermediate transverse stiffeners in curved I-girders are still largely unknown. Furthermore, a number of prior research studies have demonstrated that transverse stiffeners in straight I-girders are loaded predominantly by bending induced by their restraint of web lateral deflections at the shear strength limit state, not by in-plane tension field forces. This is at odds with present Specification approaches for the design of transverse stiffeners, which are based on (1) providing sufficient stiffener bending rigidity only to develop the shear buckling strength of the web and (2) providing sufficient stiffener area to resist the in-plane tension field forces. In this research, the behavior of one- and two-sided intermediate transverse stiffeners in straight and horizontally curved steel I-girders is investigated by refined full nonlinear finite element analysis. Variations in stiffener rigidity, panel aspect ratio, panel slenderness, and stiffener type are considered. New recommendations for design of transverse stiffeners in straight and curved I-girder bridges are developed by combining the solutions from the above FEA studies with the results from prior research.

CHAPTER I

INTRODUCTION

1.1 Background and Problem Statement

Existing methods for the design of intermediate transverse stiffeners in steel bridge I-girders vary widely in concept and in the resulting stiffener requirements. The AASHTO (1998) provisions for the design of transverse stiffeners in straight I-girders are based on two criteria:

- (1) A moment of inertia requirement developed to ensure that the stiffener is able to maintain a line of near zero lateral deflection at the web shear buckling load, and
- (2) For webs that are designed including tension-field action, an area requirement based on an estimate of the in-plane forces transmitted by the postbuckled web plate to the transverse stiffeners. This requirement is intended to ensure that the stiffeners are able to act as the vertical members of an effective Pratt truss in resisting shear forces larger than the web shear buckling load.

Neither of these requirements addresses the effects of out-of-plane forces on the transverse stiffeners caused by initial imperfections within fabrication tolerances (at pre or postbuckling load levels), nor do they address the effects of out-of-plane forces on the transverse stiffeners due to the shear postbuckling response of the web panels. Various independent research studies (Horne and Grayson 1983; Rahal and Harding 1990a, 1990b and 1991; Stanway et al. 1993 and 1996; Xie 2000; Lee et al. 2002 and 2003) have demonstrated that, at least for webs with a slenderness up to about $D/t_w = 250$, the stiffeners are loaded predominantly by bending induced by their restraint of web lateral

deflections at the shear strength limit state, not by in-plane tension field forces. Each of these investigations propose models and/or design equations that address the lateral bending effects in different ways and with different results. Refined finite element solutions from the above studies show that in some cases, stiffeners designed according to AASHTO (1998) are deformed substantially at the limit load and the shear strengths associated with tension field action are not fully realized. Unfortunately, only a few experimental studies have been conducted to quantify the demands placed on transverse stiffeners in straight I-girders (Rockey et al. 1981; Tang and Evans 1984; Lee et al. 2003). Typically, the transverse stiffeners in experimental shear tests are designed conservatively to ensure that the transverse stiffener size is not a significant parameter influencing the test results.

For curved I-girder design, the AASHTO (2003) transverse stiffener design provisions are based solely on the AASHTO (1998) moment of inertia requirement multiplied by an additional factor, $X \geq 1$, which accounts for larger demands on the stiffeners in certain cases to develop the larger elastic shear buckling strengths of curved web panels (Mariani et al. 1973). However, in all the cases considered by Mariani et al. (1973), a curved web is able to develop the smaller elastic buckling strength of an equivalent flat web panel using a smaller stiffener stiffness than that required for the flat web. Stated alternately, for a given stiffener rigidity, the elastic buckling strength of a curved web panel is always greater than the corresponding buckling strength for an equivalent flat panel. The equation for X in AASHTO (2003) is valid only for panels with the aspect ratio $d_o/D \leq 1.0$ (Mariani et al. 1973), where d_o is a distance between stiffeners. Also, X is specified as 1.0 for $d_o/D \leq 0.78$.

The AASHTO (2003) rules for the shear design of curved I-girders limit the nominal shear resistance to the AASHTO (1998) shear buckling strength. Hence, it can be questioned whether the additional requirement of $X > 1$ for curved girders with $0.78 < d_o/D < 1.0$ is strictly necessary.

Recent research studies (Lee and Yoo 1999; White et al. 2001; Zureick et al. 2002; Jung and White 2003; White and Barker 2004) have demonstrated that there is some reduction in the maximum shear strength of transversely stiffened I-girders due to horizontal curvature. However, these investigators have observed that this reduction is small and may be neglected within the following limits:

- $d_o/D \leq 3$,
- $D/t_w \leq 160$, and
- $L_b/R \leq 0.1$ in the final constructed configuration, where L_b is the arc length between the brace locations and R is the radius of the curvature.

The last limit ensures that $d_o/R \leq 0.1$ for all curved I-girders, since the web is stiffened by connection plates at cross-frame locations. Based on these findings, the unified AASHTO LRFD (2004) provisions use the tension field action shear resistance equations of AASHTO (1998) for the design of both straight and curved I-girder bridges. Also, based on assessment of prior research and the fact that the AASHTO (1998) provisions for the shear design of longitudinally stiffened straight girders assume that longitudinal stiffeners are ineffective at strength load levels, the AASHTO (1998) tension field action shear resistance equations have been extended to longitudinally stiffened curved I-girders as well. The AASHTO (1998) shear resistance equations were originally developed by Basler (1961), with the exception that a simplified equation is used for the shear buckling

coefficient. The AASHTO (1998) shear buckling coefficient was first proposed by Vincent (1969).

Although the above research studies demonstrate that the AASHTO (1998) straight I-girder shear resistance equations are applicable for the design of curved I-girders, the corresponding demands on intermediate transverse stiffeners are largely unknown. In the experimental studies by Zureick et al. (2002), the intermediate transverse stiffeners were designed conservatively to ensure that the shear strength limit state was not influenced by a failure of these components. Nakai et al. (1985) conducted analytical studies of the demands placed on transverse stiffeners in curved I-girders for development of the web shear postbuckling strength. Nakai and Yoo (1988) give a summary of the model development. These researchers created a beam-column model to estimate the axial force and bending moment in transverse stiffeners of curved girders, including the influence of a radial loading component from the web tension field. They estimated this radial loading effect by assuming that the web tension field acts along a chord between transverse stiffeners. They compared their analytical predictions to the results from experiments conducted by Nakai et al. (1984), in which premature failure of a transverse stiffener occurred in one of the tests. However, the transverse stiffener in this test does not satisfy the AASHTO (1998) rigidity requirements for straight I-girders. Also, the influence of the stiffener size was studied only for $d_o/D = 0.5$ in the studies by Nakai et al. (1984).

Based on their studies, Nakai et al. (1985) recommended a multiplier on the transverse stiffener rigidity for straight I-girders from JSHB (1980), applicable for $d_o/D \leq$

1. For the largest value of the curvature parameter¹

$$c = \frac{d_o^2}{8Rt_w} \quad (1.1)$$

equal to 1.31 and web panel aspect ratio $d_o/D = 1.0$ considered in their research, this multiplier requires a stiffener moment of inertia of 23 times that required by AASHTO (1998) for an equivalent flat web panel. Nakai and Yoo (1988) state that the required rigidity of the transverse stiffeners is too large for use in design when d_o/D is greater than 1.0 and indicate that this conclusion was also reached by Mariani et al. (1973). The Mariani et al. paper does not contain any evidence of this conclusion.

The assumption by Nakai et al. (1985) that the transverse stiffeners are subjected to a radial load based on the web tension field forces acting along a chord between the ends of the panels is likely to provide a conservative estimate of the lateral bending in the transverse stiffeners due to horizontal curvature. However, in the limit of a straight girder, the predicted lateral bending effects are equal to zero in the model proposed by Nakai et al. (1985). Based on the research studies by Horne and Grayson (1983), Rahal and Harding (1990a, b and 1991), Stanway et al. (1993 and 1996), Xie (2000) and Lee et al. (2002 and 2003), the demands on the transverse stiffeners are dominated by lateral bending effects in straight girders.

Research is needed to better understand the demands on intermediate transverse stiffeners in both straight and curved bridge I-girders. Ideally, the resulting transverse

¹ The parameter c is a small angle approximation of the out-of-flatness of the web panel due to the horizontal curvature divided by the web thickness.

stiffener requirements should address both straight and curved cases as a continuum. The requirements in both transversely as well as longitudinally stiffened curved I-girders should be tested up to the maximum limits allowed by AASHTO (2004). These limits are $d_o/D = 3$ and $D/t_w = 150$ for transversely stiffened girders and $d_o/D = 1.5$ and $D/t_w = 300$ for longitudinally stiffened members. This thesis addresses this need by the execution of and interpretation of the results from refined full nonlinear finite element analyses (FEA) for a range of representative straight and curved I-girders. The solutions from these FEA studies are combined with results from prior research to arrive at recommendations for the design of intermediate transverse stiffeners in straight and curved I-girder bridges.

1.2 Organization

Chapter II provides a detailed review of prior research and the present state-of-the-art (2004) with respect to the behavior and design of intermediate transverse stiffeners in straight and horizontally curved I-girders.

Chapter III summarizes the design and organization of the parametric studies conducted in this research. Also, the detailed attributes of the finite element models used in this work are described, and their effectiveness for predicting the strength limit states in one set of experimental tests is demonstrated.

In Chapter IV, the results of the parametric studies are presented. The influence of stiffener size on the girder maximum shear strengths and the strength limit states behavior are considered. Chapter IV concludes with recommendations for the design of intermediate transverse stiffeners. Chapter V summarizes the results of this research and discusses additional research needs.

CHAPTER II

BACKGROUND

2.1 Transverse Stiffener Rigidity Requirements for Web Shear Buckling Strength

2.1.1 AASHTO (2004)

AASHTO (2004) requires that the moment of inertia of the transverse stiffeners must satisfy:

$$I_s \geq I_{scr} \quad (2.1)$$

where

$$I_{scr} = d_o t_w^3 J \quad (2.2)$$

and

$$J = \frac{2.5}{\left(\frac{d_o}{D}\right)^2} - 2.0 \geq 0.5 \quad (2.3)$$

This requirement is carried forward from prior AASHTO Specifications including AASHTO (1998). Equation (2.1) ensures that transverse stiffeners have sufficient rigidity to maintain a line of near zero lateral deflection throughout their height for loads up to the elastic shear buckling load. For panel aspect ratios less than one, the value of J increases substantially with decreasing d_o/D , while for panel aspect ratios greater than one, J is constant at 0.5. The moment of inertia of the transverse stiffener I_s is taken about the edge in contact with the web for one-sided or single-plate stiffeners and about the mid-thickness of the web for two-sided stiffeners (i.e., stiffener pairs). Therefore,

$$I_s = \frac{b_s^3 t_s}{3} \quad (2.4a)$$

for single-plate stiffeners, and

$$I_s \cong \frac{2b_s^3 t_s}{3} \quad (2.4b)$$

for two-sided plate stiffeners (neglecting the small contribution from the thickness of the web). Unless noted otherwise, the moment of inertia for the transverse stiffeners is computed in this way in all of the approaches considered in this thesis.

2.1.2 Bleich (1952)

Equations (2.1) to (2.3) are based on the research by Stein and Fralich (1949) on the elastic shear buckling of simply-supported, infinitely long plates reinforced by equidistant transverse stiffeners of equal bending rigidity. Bleich (1952) explains that the solutions by these investigators are significantly more accurate than other approximate solutions available prior to their work, and develops the following expression for the required normalized rigidity of transverse stiffeners as a curve fit to their results (valid for $d_o/D \leq 1$):

$$\gamma = (k - 5.34)^3 \frac{4 \left[\frac{7}{(d_o/D)^2} - 5 \right]}{\left[\frac{5.5}{(d_o/D)^2} - 0.6 \right]^3} \quad (2.5)$$

where

$$\gamma = \frac{12(1 - \nu^2)I_s}{t_w^3 d_o} \quad (2.6)$$

and k is the shear buckling coefficient. Bleich also presents an equation for the shear buckling coefficient k as a function of the normalized stiffener rigidity γ , based on the solutions from Stein and Fralich. However, Equation (2.5) is the relevant expression for the required transverse stiffener moment of inertia. The stiffener rigidity necessary to

develop the AASHTO (2004) shear buckling load may be determined by substituting the AASHTO (2004) shear buckling coefficient (originally proposed by Vincent (1969)),

$$k = 5 + \frac{5}{(d_o/D)^2} \quad (2.7)$$

into Equation (2.5).

Bleich (1952) also presents equations that address the demands on the intermediate transverse stiffeners for them to hold a line of near zero lateral deflection in plates that are loaded above their proportional limit (taken equal to $0.8V_p$ in AASHTO (2004) and $0.76V_p$ by Bleich (1952)), i.e., for plates governed by inelastic shear buckling. However, the calculations required by these equations are somewhat elaborate and involve subtle interpretations. To the knowledge of the author, neither AASHTO (2004) nor any other international standards for steel design implement these equations. AASHTO (2004) simply reduces the shear buckling strength of the plate-stiffener assembly relative to the elastic shear buckling load to account for inelastic actions. Furthermore, AASHTO (2004) requires a transverse stiffener moment of inertia sufficient to develop the theoretical elastic shear buckling strength of a simply-supported web panel, $V_{cr,el}$, even for combinations of D/t_w and d_o/D such that $V_{cr,el}$ is more than three times V_p . The conservatism of this approach is discussed further in Sections 2.2.1, 4.6 and 4.10.

It is useful to express Equation (2.5) in the form of a J requirement, where J is the required value of $I_s/d_o t_w^3$, for comparison to Equation (2.3). This form is

$$J = \frac{(k - 5.34)^3}{3(1 - \nu^2)} \frac{\left[\frac{7}{(d_o/D)^2} - 5 \right]}{\left[\frac{5.5}{(d_o/D)^2} - 0.6 \right]^3} \quad (2.8)$$

Equations (2.3) and (2.8) are compared in the following discussions.

The Engineer should note that even for an initially perfect flat plate, there is no finite stiffener rigidity for which the stiffener lateral displacement is zero within the buckling mode of the plate-stiffener assembly. Correspondingly, the solutions by Stein and Fralich (1949) for the shear buckling coefficient k , which is proportional to the shear buckling load, approach their maximum values asymptotically as the specified J or γ values approach infinity. These maximum values, denoted by the symbol k_{∞} , are generally greater than the k values specified by Equation (2.7). For $d_o/D = 0.5$, $k_{\infty} = 28.71$ whereas Equation (2.7) gives $k = 25$, and for $d_o/D = 1.0$, $k_{\infty} = 10.86$ whereas Equation (2.7) gives $k = 10$. For $J = I_s/d_o t_w^3$ values larger than specified by the combination of Equations (2.7) and (2.8), the shear buckling strength is for all practical purposes constant with any increase in the stiffener rigidity.

2.1.3 Stanway et al. (1993)

Stanway et al. (1993) studied the elastic shear buckling of simply-supported plates with a single intermediate transverse stiffener subdividing the plate into two equal-width panels. They generated FEA solutions as well as series solutions retaining a large number of terms, and obtained converged results from each approach that were within one percent of one another. They studied the influence of the stiffener flexural rigidity, with the torsional rigidity of the stiffener set equal to zero (note that the solutions by Stein and Fralich (1949) also do not account for any torsional resistance of the transverse

stiffeners)¹. Stanway et al. present their results in the form of the γ required to obtain different values of the parameter μ_{cr} , defined as

$$\mu_{cr} = \frac{k - k_0}{k_{\infty} - k_0} \quad (2.9)$$

where k_{∞} is the shear buckling coefficient for the plate with $I_s = \infty$ and k_0 is the shear buckling coefficient for the plate with $I_s = 0$. Figures 2.1a and 2.1b compare the results from Stanway et al. (1993) for $\mu_{cr} = 0.95, 0.90$ and 0.80 , written in terms of the required $J = I_s/d_o t_w^3$, to Equation (2.3) from AASHTO (2004) and to Equation (2.8) from Bleich (1952). These figures show the same solutions, but Figure 2.1a has a larger scale for the J axis to illustrate the large required J value determined by Stanway et al. for $d_o/D = 0.5$ and $\mu_{cr} = 0.95$ whereas Figure 2.1b has a smaller scale to emphasize the J requirements for $d_o/D \geq 1$. The requirements specified by Timoshenko and Gere (1961) are also shown in these figures.

One can observe that the AASHTO (2004) J expression (Equation (2.3)) matches well with Bleich's approximate equation. Bleich's equation also matches well with the required J values for $\mu_{cr} = 0.90$ determined by Stanway et al. (1993) at $d_o/D = 0.5$ and 1.0 . Furthermore, it can be seen that the AASHTO (2004) J curve given by Equation (2.3) generally falls between the required J values for $\mu_{cr} = 0.90$ and $\mu_{cr} = 0.95$ from Stanway et al. (1993). In contrast, the k values from Equation (2.7) of 25 for $d_o/D = 0.5$ and 10 for $d_o/D = 1.0$ both correspond to $\mu_{cr} = 0.84$ in Equation (2.9), using the k_{∞} values from Stein and Fralich (1949) along with their k_0 value of 5.34. This indicates that possibly the AASHTO (2004) equation is slightly more conservative than necessary.

¹ Stanway et al. (1993) also considered the effect of transverse stiffener torsional rigidity in a separate section of their studies.

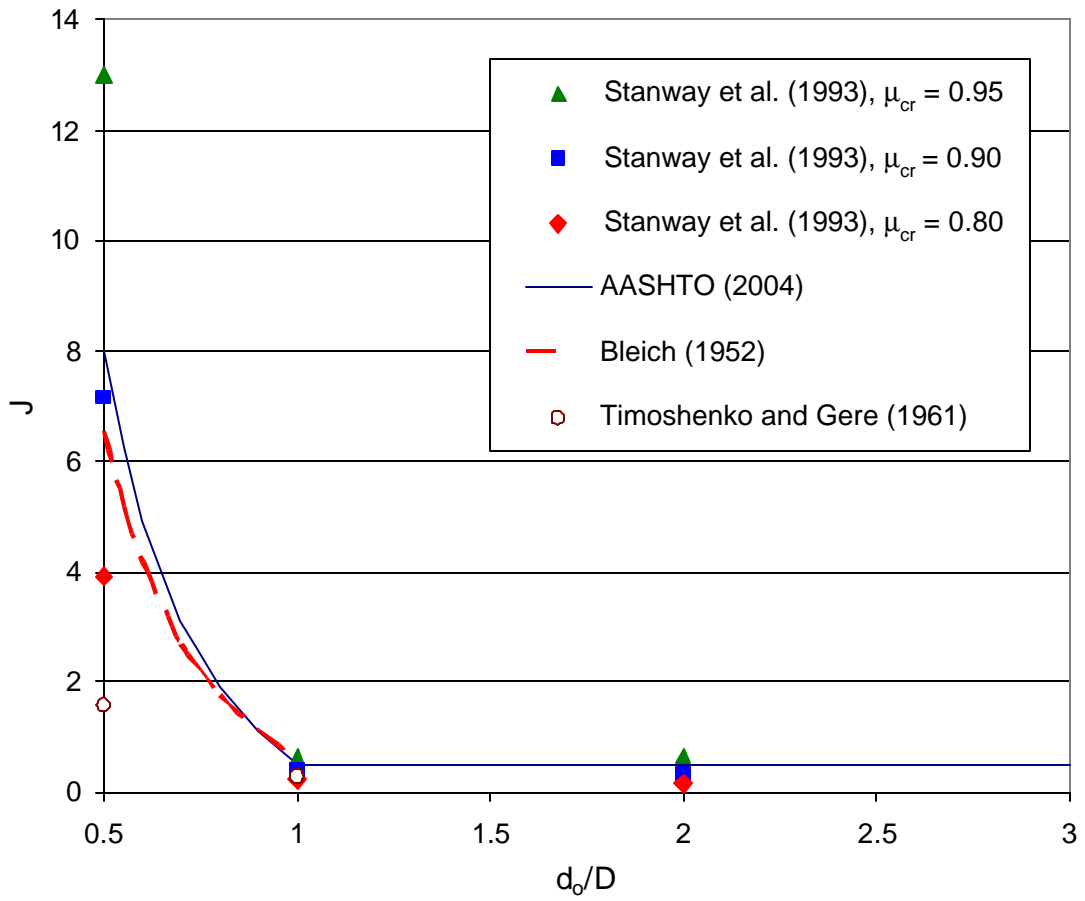


Figure 2.1a. Required J values for development of the shear buckling strength emphasizing the requirements at $d_o/D = 0.5$.

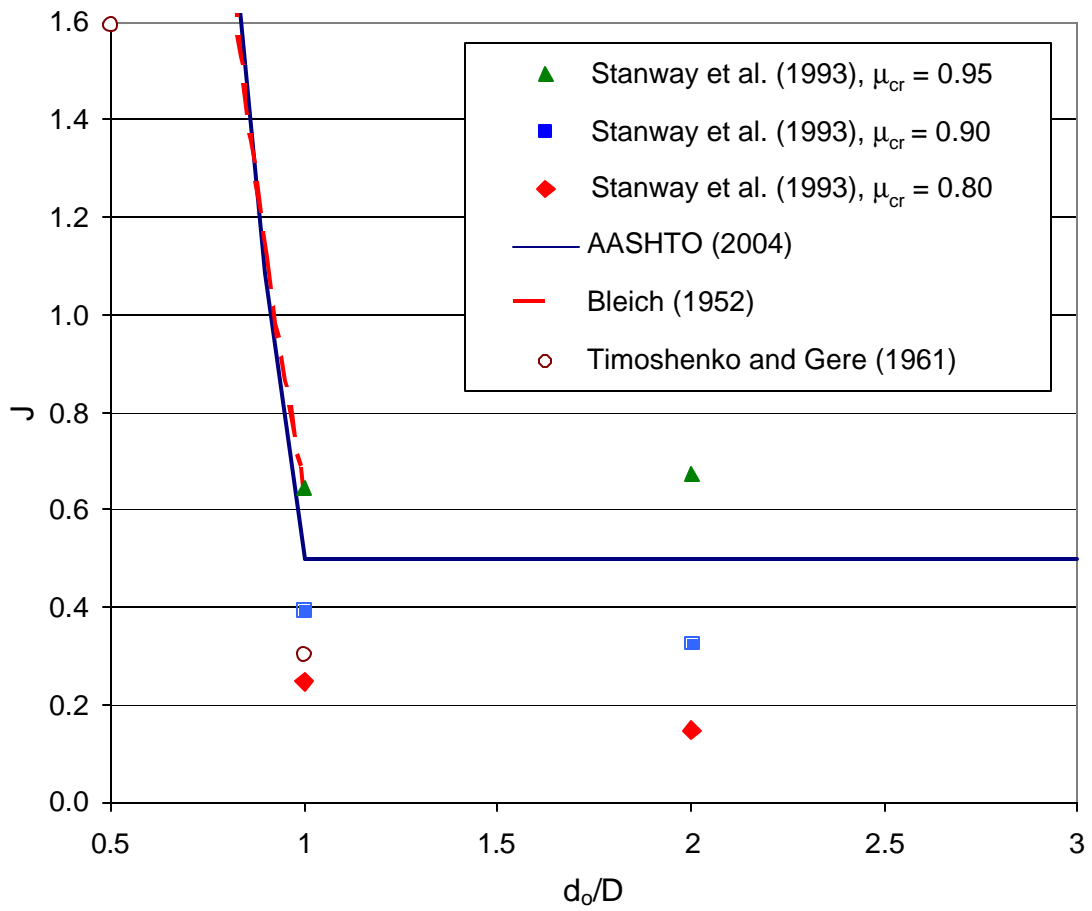


Figure 2.1b. Required J values for development of the shear buckling strength emphasizing the requirements for $d_o/D = 1$.

The stiffener rigidity requirements specified by Timoshenko and Gere (1961) are substantially smaller than those specified by Bleich (1952) and by AASHTO (2004), particularly for $d_o/D = 0.5$. Bleich comments on the solutions presented by Timoshenko and Gere, and indicates that considerable errors are possible because the limited number of terms employed in the series expansion used in their development is not suitable to represent the deformation of the stiffened plate.

It is apparent that the demands on the transverse stiffeners for Equation (2.7) to be valid are significantly larger for $d_o/D < 1$, where d_o is the smaller dimension of the web panels, whereas these demands are more minor for $d_o/D > 1$, where the smaller dimension of the web panels is the distance between the flanges D . This is because the shear buckling waves within the web plate are modified by the transverse stiffeners to a lesser extent as d_o/D increases above one. In fact, at $d_o/D = 3$, Equation (2.7) gives $k = 5.56$ whereas Bleich (1952) shows that $k = 5.34$ is applicable for a simply-supported infinitely long web plate without any transverse stiffeners at all. The difference between these two shear buckling coefficients is compensated for easily by the most minor restraint from the flanges and/or torsional rigidity of the transverse stiffeners. Therefore, for $d_o/D = 3$, one can conclude that the required J value is zero. Furthermore, for $d_o/D = 2$, $k = 6.25$ from Equation (2.7). Lee et al. (1996), Bradford (1996) and White et al. (2001) show that typical I-girder webs with $d_o/D = 2$ have k values close to 10 due to the restraint provided by the flanges (assuming adequate transverse stiffeners).

Also, from Figure 2.1b, one can observe that the implied μ_{cr} value from the AASHTO (2004) equation for $d_o/D = 2$ is slightly more conservative (i.e., larger) than the implied

μ_{cr} value for $d_o/D = 1$ and 0.5 . In as such, it is worthwhile to consider a potential modification of Equation (2.1) to the form

$$I_s \geq I'_{scr} \quad (2.10a)$$

where

$$I'_{scr} = b t_w^3 J' \quad (2.10b)$$

$$b = \min (d_o, D) \quad (2.10c)$$

and Equation (2.3) is still employed to calculate J' (the prime on J is used to emphasize the different values determined by rigorous solutions for this coefficient if Equation (2.10a) is used rather than Equation (2.1)). Figure 2.2 shows the required $J' = I_s/bt_w^3$ values based on Stanway et al. (1993) versus Equation (2.3). Assuming that μ_{cr} between 0.80 and 0.90 is acceptable, Equation (2.10a) is a better (more liberal) expression for the stiffener rigidity requirement for $d_o/D = 2$. The acceptability of Equation (2.10a) for $d_o/D > 1$ is addressed further in Section 2.2.1 and also subsequently in Sections 4.6 and 4.10.

2.1.4 Mariani et al. (1973)

Mariani et al. (1973) studied the required stiffener rigidity to develop the elastic shear buckling strength of a long simply-supported curved plate, subdivided into panels of equal width by intermediate transverse stiffeners of equal bending rigidity. They found that for $0.78 < d_o/D < 1.0$, the stiffener rigidity necessary to develop an elastic shear buckling strength equal to that of an isolated simply-supported curved web panel of the same dimensions increases with the curvature approximately by the ratio:

$$X = 1 + \frac{1}{1775} \left(\frac{d_o}{D} - 0.78 \right) Z^4 \quad (2.11)$$

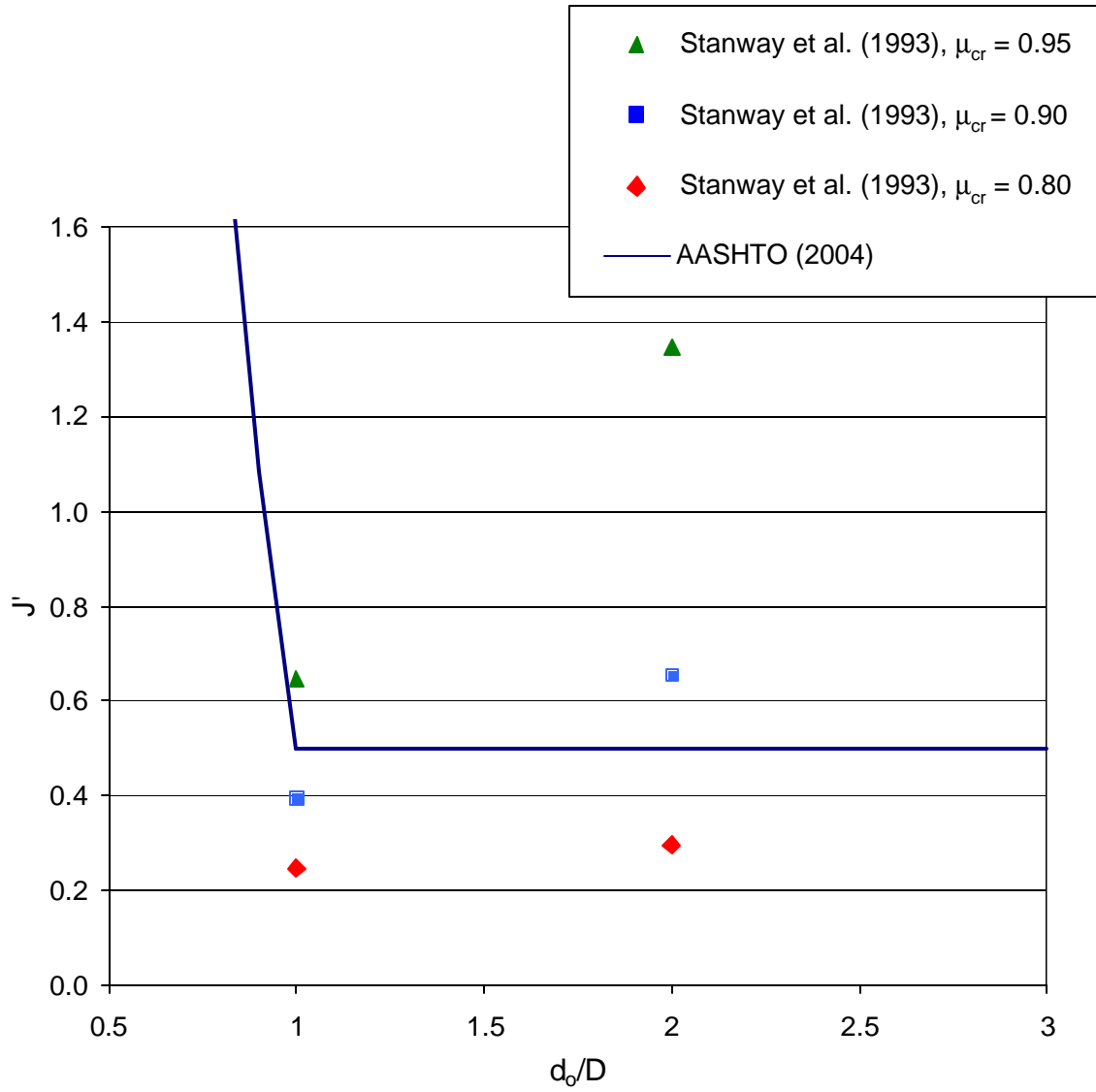


Figure 2.2. Required J' values for development of the shear buckling strength emphasizing the requirements for $d_o/D = 1$.

where Z is a curvature parameter defined as

$$Z = \frac{d_o^2}{R t_w} \sqrt{1 - \nu^2} = 8c \sqrt{1 - \nu^2} \quad (2.12)$$

(the parameter c is defined by Equation (1.1)). They also found that the above ratio is less than one if the panel aspect ratio d_o/D is less than 0.78. However, it was decided that curved girder stiffener requirements should not be less than the requirements for straight girders. Therefore for $d_o/D \leq 0.78$, they recommended $X = 1$. This study was limited to $0 \leq Z \leq 10$ (or $0 \leq c \leq 1.31$).

Although their design recommendations were limited to $d_o/D \leq 1$, Mariani et al. (1973) also considered panel aspect ratios up to $d_o/D = 1.5$ in their research. The suggested limit of $d_o/D \leq 1$ appears to be related to: (a) the fact that the AASHTO Standard Specifications in effect at the time of their work limited the panel aspect ratios of transversely-stiffened I-girders to this value, and (b) the research indicated that a function much different than Equation (2.11) would be needed for $d_o/D = 1.5$. Mariani et al. (1973) found that for a web with $d_o/D = 1.5$, a maximum rigidity of 2.4 times that required for the corresponding straight-girder was necessary, and that this requirement occurred at $Z = 5$. However, the required rigidity for $d_o/D = 1.5$ reduces to the value for straight girders as Z approaches 0 or 10. Equation (2.11) gives a maximum required value of $X = 2.24$ at $d_o/D = 1$ and $Z = 10$. Therefore, the maximum rigidity requirement determined by Mariani et al. (1973) for panels with $d_o/D = 1.5$ is not significantly larger than the maximum for $d_o/D = 1$.

It should be emphasized that Equation (2.11) is based on the development of an elastic shear buckling strength ($V_{cr,el}$) in a long curved plate divided into panels by N

transverse stiffeners equal to the corresponding $V_{cr,el}$ of a comparable isolated simply-supported curved web panel. Mariani et al. (1973) show that in all cases, the elastic shear buckling load of an isolated simply-supported curved web panel is larger than the elastic shear buckling load of an isolated simply-supported flat web panel of the same dimensions. Also, the elastic buckling strengths obtained from their models of long stiffened plates are always increased for larger panel curvatures. Of key importance to the requirements for the transverse stiffeners, the stiffener rigidity necessary to develop a given buckling load is always smaller in curved stiffened plates than in the corresponding flat stiffened plate. AASHTO (2003) adopts Equation (2.11) as an additional requirement on intermediate transverse stiffeners in curved I-girders. However, these Specifications neglect the increase in the elastic shear buckling strength due to the horizontal curvature in that they use the AASHTO (1998) shear buckling equations in all cases. Since the AASHTO (2003) Specifications do not rely on larger elastic buckling capacities for curved web panels, it can be questioned whether the additional requirement of $X \geq 1$ for $0.78 < d_o/D < 1.0$ is strictly necessary. In any case, Equation (2.11) is not applicable for $d_o/D > 1.0$.

2.2 Transverse Stiffener Rigidity Requirements for Web Shear Post-Buckling Strength

2.2.1 Stanway et al. (1993 and 1996)

The above studies address only the development of the web shear buckling strength. The development of postbuckling strength, i.e., tension field action, and its influence on the transverse stiffeners is not considered. However, Stanway et al. (1993) also conducted full nonlinear finite element analyses to quantify the required rigidity of

transverse stiffeners to develop the shear post-buckling strengths of flat web panels. The geometrical characteristics of the panels studied are the same as those used in their elastic buckling solutions. That is, the plate is simply-supported along its exterior edges and is subdivided into two equal width subpanels by an intermediate transverse stiffener.

Uniform shear tractions are applied along the exterior edges of the plate. Its left and right sides are constrained to remain straight but these edges are otherwise free to translate and rotate within the plane of the problem. The top and bottom sides of the plate are free to displace within the plane of the problem, i.e., there is zero in-plane restraint normal to the edge of the plate. The yield strength of the plate and the stiffener are taken as 245 MPa (36 ksi). Isoparametric shell finite elements are used for the web and beam elements are used for the stiffener.

The results from Stanway's finite element analyses are presented in Table 2.1. These results are shown in a form similar to that used in Figures 2.1 and 2.2. The stiffener J values ($J = I_s/d_o t_w^3$) necessary to develop different values of the parameter μ_u , defined as

$$\mu_u = \frac{\tau_u - \tau_{u0}}{\tau_{u\infty} - \tau_{u0}} \quad (2.13)$$

are considered, where τ_u is the maximum strength of the plate expressed in terms of the applied uniform edge tractions for a given stiffener flexural rigidity, and $\tau_{u\infty}$ and τ_{u0} are the corresponding maximum strengths for $I_s = \infty$ and $I_s = 0$ respectively². Table 2.1³

² The prior solutions are presented in the form $J = I_s/d_o t_w^3$ to facilitate comparison to the AASHTO (2004) transverse stiffener requirements. The corresponding J' values, where J' is the required value of I_s/bt_w^3 from the rigorous solutions and b is given by Equation (2.10b), are as follows:

$$J' = J \text{ for } d_o \leq D$$

$$J' = J (d_o/D) \text{ for } d_o > D.$$

³ Stanway et al. (1993) also consider webs with d_o/D as small as 0.2. Values of d_o/D less than 0.5 are not considered as practical for bridge I-girders, but are believed to address very deep girders such as may be used in offshore structures.

shows solutions for three different web slenderness ratios $b/t_w = \min(d_o, D)/t_w$. The solutions in Figures 2.1 and 2.2 are independent of the web slenderness. Also, Table 2.2 shows the ratio of the J required to achieve $\mu_u = 0.9$ to J required to achieve $\mu_{cr} = 0.9$.

Table 2.1. Required J values for development of shear postbuckling strength from (Stanway et al. 1993).

d_o/D	b/t_w	J for given μ_u from Finite Element Analysis		
		$\mu_u = 0.8$	0.9	0.95
0.5	180	21	30	57
	120	12	18	36
	80	5.0	7.3	13
1	180	2.1	3.2	5.4
	120	0.69	1.1	2.0
	80	0.13	0.21	0.55
2	180	0.99	1.2	1.7
	120	0.33	0.56	1.1
	80	0.11	0.26	0.41

Table 2.2. Ratio of J required to achieve $\mu_u = 0.9$ to J required to achieve $\mu_{cr} = 0.9$, based on the solutions from (Stanway et al. 1993)

b/t_w	$J(\mu_u = 0.9) / J(\mu_{cr} = 0.9)$		
	$d_o/D = 0.5$	1	2
180	4.2	8.1	3.7
120	2.5	2.7	1.7
80	1.0	0.5	0.8

One can observe from Table 2.2 that for the stockier plates with $b/t_w = 80$, the $J(\mu_u = 0.9) / J(\mu_{cr} = 0.9)$ necessary to develop the maximum shear strength, including the contribution from postbuckling or tension field action, is less than or equal to 1.0. This is logical since for $F_{yw} = 245$ MPa and $d_o/D = 0.5$, the AASHTO (2004) shear buckling provisions predict that the web is able to develop its fully plastic shear strength V_p

without the need for any postbuckling strength at $b/t_w = 80$ (or $D/t_w = 160$), that is $C = V_{cr}/V_p = 1.0$. Also, for $F_{yw} = 245$ MPa and $d_o/D = 1$, the AASHTO (2004) shear buckling provisions give $C = 1.0$ at $D/t_w = b/t_w = 100$. Finally, for $F_{yw} = 245$ MPa and $d_o/D = 2$, the AASHTO (2004) provisions give $C = 1.0$ at $b/t_w = D/t_w = 80$. Since no postbuckling shear resistance is needed in these cases, no additional demands are placed on the transverse stiffener. Furthermore, for $d_o/D = 1$ and $b/t_w = 80$, the theoretical elastic buckling resistance of the web panels, V_{cr} , is equal to $2V_p$ based on the AASHTO (2004) equations. In as such, the stiffener rigidity necessary to develop the maximum shear strength is smaller than that required to develop the theoretical elastic shear buckling resistance, i.e., $J(\mu_u = 0.9) / J(\mu_{cr} = 0.9) = 0.5$ in Table 2.2. The transverse stiffener rigidities required to develop $\mu_u = 0.8$ are substantially smaller (see Table 2.1).

Conversely, for the larger web slenderness values ($b/t_w = 120$ and 180), significantly larger stiffeners are required to develop the shear postbuckling strengths. The largest additional demands are observed for the panels with $d_o/D = 1$. For the case with $b/t_w = D/t_w = 180$ and $d_o/D = 1$, the stiffener moment of inertia must be increased 8.1 times relative to $J(\mu_{cr} = 0.9)$ to ensure that the panels are able to develop $\mu_u = 0.9$. The question of whether J values this large are necessary is addressed subsequently in this thesis.

Based on their findings in (Stanway et al. 1993), Stanway et al. (1996) recommend an analytical model for calculation of the demands on transverse stiffeners in straight I-girders designed based on tension field action. An important attribute of this model is that it is based on two separate criteria:

- (1) Stiffness – the provision of sufficient flexural rigidity of the transverse stiffeners such that the stiffener lateral deflections are small enough to “ensure effective subdivision of the plate.”
- (2) Strength – the provision of an elastic section modulus for the transverse stiffeners sufficient to ensure that the stiffeners do not yield prior to the failure of the web panels.

Both of these criteria stem from the observations by Stanway (1993 and 1996) and others that transverse stiffeners in straight I-girders are loaded predominantly by the bending induced by their restraint of the web lateral deflections at the shear strength limit state, not by in-plane tension field forces.

A detailed discussion of Stanway’s strength criterion is presented in Section 2.3.3.1. Stanway’s stiffness (or flexural rigidity) requirement is based on an explicit estimate of the magnitude of the stiffener and web panel lateral deflections at the strength limit state, represented by the symbols w_s and w_p respectively. Given these estimates, Stanway et al. (1996) require

$$w_s \leq \frac{0.125 w_p}{1 - \cos\left(\frac{\pi k_\lambda b}{2D}\right)} \quad (2.13)$$

where

$$k_\lambda = 0.375 \frac{D}{b} + 0.625 \quad (2.14)$$

for $d_o/D > 1/3$, with the exception that w_s is not required to be any smaller than $D/1000$ nor is it allowed to be any larger than $D/200$. For $d_o/D = 1$, Equation (2.13) amounts to a requirement that the stiffener lateral deflection must be less than or equal to one-eighth of the panel lateral deflection. The term within the denominator of Equation (2.13) relaxes

this limit for $d_o/D < 1$. For $d_o/D = 0.5$, Equation (2.13) requires that the stiffener lateral deflection must be less than or equal to approximately one-quarter of the panel lateral deflection.

Table 2.3 compares the required values for $J = I_s/d_o t_w^3$ based on Stanway's analytical model, as well as the J values to obtain a specified μ_u using Stanway's FEA solutions (from Table 2.2), to the J values specified by Equation (2.3) from AASHTO (2004). The required J values from Stanway's analytical model closely match Stanway's FEA results for $\mu_u = 0.95$. All of Stanway's solutions are based on $F_{ys} = F_{yw} = 245$ MPa.

Table 2.3. Comparison of required J values for development of the web postbuckling strength from Stanway et al. (1996 and 1993) to the J requirement in AASHTO (2004) for development of the web shear buckling load.

d_o/D	b/t_w	J values from Stiffener Analytical Model (Stanway et al. 1996) ⁽¹⁾		J values from FEA for a given μ_u (Stanway et al. 1993)			J from AASHTO (2004), Eq. (2.3)
		J_1 / J_2	J_{max}	$\mu_u = 0.8$	0.9	0.95	
0.5	180	1.18	58	21	30	57	8
	120	1.11	29	12	18	36	8
	80	1.72	14	5.0	7.3	13	8
1	180	1.21	5.7	2.1	3.2	5.4	0.5
	120	1.30	2.8	0.69	1.1	2.0	0.5
	80	1.65	1.1	0.13	0.21	0.55	0.5
2	180	0.69	2.9	0.99	1.2	1.7	0.5
	120	0.74	1.5	0.33	0.56	1.1	0.5
	80	1.16	0.62	0.11	0.26	0.41	0.5

⁽¹⁾ J_1 = The J required to satisfy Stanway's stiffness criterion; J_2 = The J required to satisfy Stanway's strength criterion; $J_{max} = \max(J_1, J_2)$.

For $b/t_w = 80$, one can observe that the required $J(\mu_u = 0.9)$ from Stanway's FEA solutions is smaller than the J requirement specified by AASHTO (2004) for each of the d_o/D values considered. If Equations (2.10) are used as an alternative representation of the stiffener moment of inertia needed to develop the web shear buckling strength, the J'

values are unchanged relative to the values reported in Table 2.3 for $d_o/D = 0.5$ and 1, but all the J' values in the fourth through seventh columns are increased by a factor of two for $d_o/D = 2$. Therefore, if Equations (2.10) are used, one can conclude that the AASHTO (2004) expression (Equation (2.3)) is an accurate to somewhat conservative representation of the J' requirement to achieve $\mu_u = 0.9$ for webs with $b/t_w = 80$. Equation (2.3) is the most liberal relative to $J'(\mu_u = 0.9)$ for $d_o/D = 2$, where Equation (2.3) gives a value of 0.5 and $J'(\mu_u = 0.9) = 2 * 0.26 = 0.52$. However, as noted previously, significantly larger J or J' values are necessary for larger b/t_w .

2.2.2 Lee et al. (2002 and 2003)

Lee et al. (2002 and 2003) also observed that larger stiffener rigidities are needed for the web to develop postbuckling strength than to develop the shear buckling strength. Lee et al. (2002) conducted FEA studies of web panels with $D/t_w = 200$ and $d_o/D = 1$ using single plate stiffeners with three different projecting widths. They also varied the stiffener thickness for each of these widths. Furthermore, Lee et al. (2002) studied one example involving a two-sided stiffener. Also, Lee et al. (2003) present the results of six experimental tests with $D/t_w = 187$ and 150, $d_o/D = 1$ and 0.75, and in which the transverse stiffeners violate the AASHTO (2004) area requirement⁴. Also, they conducted additional FEA parametric studies of webs with one-sided stiffeners and $D/t_w = 125$ to 250, $d_o/D = 0.5$ to 3.0, and $F_{yw} = 345$ to 690 MPa. For each combination of these parameters, they considered three different stiffener widths and varied the stiffener thickness for each of these widths (as in (Lee et al. 2002)). Based on their two studies, Lee et al. (2003) concluded that in general:

⁴ The AASHTO (2004) area requirement is reviewed within Section 2.3.1.

- In I-girders designed based on the shear postbuckling strength, the rigidity of the transverse stiffeners must be larger than that specified by the AASHTO (2004) rigidity requirement (Equation (2.1)),
- The AASHTO (2004) area requirement can be violated substantially without having a significant impact on the web maximum shear strengths, as long as the stiffeners have sufficient bending rigidity, and
- The stiffener responses at the strength limit state are dominated by bending actions due to lateral loading from the web panels, and not by axial loading effects associated with tension field action.

Lee et al. (2003) recommend that a J requirement of six times that specified by Equation (2.3) is necessary and sufficient to develop the web shear postbuckling strength in cases in which the web shear buckling is elastic, i.e., $C = V_{cr}/V_p < 0.8$. For webs in which C is greater than 0.8, they suggest that the AASHTO (2004) rigidity requirement given by Equation (2.3) is sufficient. Also, they recommend that the AASHTO (2004) area requirement is not needed if these rigidity requirements are satisfied.

2.2.3 Horne and Grayson (1983)

Interestingly, Horne and Grayson (1983) also proposed a transverse stiffener rigidity requirement targeted at ensuring the development of the web shear postbuckling strength. They developed an empirical formula from full nonlinear FEA parametric studies that may be written in terms of a J requirement as

$$J = \frac{0.6}{12(1-\nu^2)(d_o/D)} \left[23.7 \frac{D}{t_w} \sqrt{\frac{F_{yw}}{E}} - 50 \right] \leq \frac{0.8}{12(1-\nu^2)} \left(23.7 \frac{D}{t_w} \sqrt{\frac{F_{yw}}{E}} - 50 \right) \quad (2.15)$$

This equation is targeted at ensuring that nominally flat web panel postbuckling strengths are not less than that of an isolated simply-supported web panel of the same dimensions.

Also, Horne and Grayson (1983) studied the influence of single versus multiple transverse stiffeners, concentric (two-sided) versus eccentric (single-sided) stiffeners, residual stresses, various patterns for the web plate out-of-flatness, and the effect of potential anchorage of the tension field by the flanges. They offer the following observations regarding these factors:

- The maximum strength for a given stiffener rigidity and panel dimensions is virtually the same in plates with one and three stiffeners as long as the stiffener rigidity is large enough such that the strength is essentially unchanged for larger stiffener moments of inertia.
- The ratio of the maximum strengths for panels with one-sided versus two-sided stiffeners with the same stiffener bending rigidity had a difference in mean strengths of only about three percent with a standard deviation of about one percent.
- The effect of residual stresses on the required stiffener rigidities can be neglected in all cases.
- The pattern of out-of-flatness assumed within the web panels has a discernable although small effect on the maximum shear strength.
- Anchorage of the tension field from the flanges has virtually no effect on the value of the stiffener rigidity required to achieve the target web panel capacities.

Also, Horne and Grayson (1983) show solutions for the stiffener axial force and bending moment at the mid-depth of their shear panels. Even in cases where the stiffeners are substantially larger than required to attain an approximate plateau in shear strength versus

stiffener rigidity plots, the stiffener responses are dominated by bending rather than axial compression from the tension field. Of further note, Horne and Grayson state that parametric studies conducted for applied loading conditions other than pure shear show that their proposed design formula may be used as a safe estimate of the required stiffener rigidity for all possible combinations of web loading. Horne and Grayson (1983) show solutions for D/t_w ranging from 160 to 240 and $d_o/D = 0.5$ and 1.0 , but unfortunately, they do not present any results for $d_o/D > 1$. Therefore, additional studies that consider the behavior for wider stiffener spacings would be useful.

2.2.4 Nakai et al. (1984 and 1985)

Nakai et al. (1984 and 1985) studied the demands placed on transverse stiffeners in horizontally curved I-girders necessary to develop the curved web postbuckling strength. These researchers developed an analytical beam-column model to estimate the axial force and bending moment developed in transverse stiffeners of curved I-girders. Their model includes a radial loading component from the tension field estimated based on the assumption that the tension field acts along a chord between the transverse stiffeners. Nakai and Yoo (1988) give a summary of the model development. Using their beam-column model for the transverse stiffeners along with a strength limit equal to the nominal first-yield strength of the stiffeners under bending and axial compression, Nakai et al. (1985) derived a multiplier applicable to the base stiffener rigidity requirement in JSHB (1980) for development of the web postbuckling strength. This multiplier may be written as

$$X_u = \begin{cases} 1.0 + (\alpha - 0.69)Z[9.38\alpha - 7.67 - (1.479\alpha - 1.78)Z] & \text{for } 0.69 \leq \alpha \leq 1.0 \\ 1.0 & \text{for } \alpha < 0.69 \end{cases} \quad (2.16)$$

for one-sided stiffeners, and as

$$X_u = \begin{cases} 1.0 + (\alpha - 0.65)Z[12.67\alpha - 10.42 - (1.99\alpha - 2.49)Z] & \text{for } 0.65 \leq \alpha \leq 1.0 \\ 1.0 & \text{for } \alpha < 0.65 \end{cases} \quad (2.17)$$

for two-sided stiffeners, where $\alpha = d_o/D$ and Z is given by Equation (2.12). Furthermore, the JSHB (1980) base stiffener rigidity requirement is equivalent to

$$J = \frac{0.73}{\left(\frac{d_o}{D}\right)^2} \quad (2.18)$$

which is slightly larger than Equation (2.3) for $d_o/D > 0.94$ but is substantially less than Equation (2.3) at $d_o/D = 0.5$. For the largest value of Z considered in their research ($Z = 10$, or $c = 1.31$ from Equation (1.1)) and $d_o/D = 1.0$, Equation (2.16) gives $X_u = 15.6$. This results in a rigidity requirement that is 23 times that of Equation (2.1). However, for $Z = 10$ and $d_o/D = 0.5$, Equations (2.16) and (2.18) require a stiffener moment of inertia that is only 0.36 of the value specified by AASHTO (2004) for development of just the shear buckling strength.

Nakai and Yoo (1988) state that the required rigidity of the transverse stiffeners is too large for use in design when d_o/D is greater than 1.0 and indicate that this conclusion was also reached by Mariani et al. (1973). The Mariani et al. paper does not contain any evidence of this conclusion. The assumption by Nakai et al. (1985) that the transverse stiffeners are subjected to a radial load based on the web tension field forces acting along a chord between the ends of the panels is likely to provide a conservative estimate of the lateral bending in the transverse stiffeners due to horizontal curvature. However, in the limit of a straight I-girder, the predicted lateral bending effects are equal to zero in the model proposed by Nakai et al. (1985). Based on the research studies by Horne and Grayson (1983), Rahal and Harding (1990a, b and 1991), Stanway et al. (1993 and 1996),

Xie (2000) and Lee et al. (2002 and 2003), the demands on the transverse stiffeners are dominated by lateral bending effects in straight I-girders.

2.3. Explicit Transverse Stiffener Strength Requirements

Although stiffness or deflection considerations may govern in certain structural design situations, structures in general cannot be designed solely based on stiffness. The Engineer must in general also ensure that structures and their components have adequate strength to resist the internal forces induced at the strength load levels. For instance, it is well established that the stability bracing for beam and column members must satisfy both stiffness and strength criteria (AISC 1999; Galambos 1998; Yura 1993 and 1995).

In steel I-girders where the applied shear force does not exceed the shear buckling load of the web panels, it is generally accepted that the intermediate transverse stiffeners need not be checked for separate strength requirements. That is, AASHTO (2004) assumes implicitly that if the stiffeners satisfy Equation (2.1) and if the applied shear force is less than the shear buckling resistance of the web panels, the stiffener strengths are large enough such that lateral bending stresses induced by their restraint of web out-of-plane deflections are small enough to be neglected.

Conversely, for I-girders designed to take advantage of the inherent web postbuckling strength associated with tension field action, the majority of the prior research studies conclude that explicit transverse stiffener strength considerations need to be addressed in addition to stiffness criteria. To the knowledge of the author, all of the present international standards for the design of I-girders for tension field action specify a stiffener area requirement of some sort. This requirement is generally based on an estimate of the in-plane forces transmitted by the postbuckled web plate to the transverse

stiffeners, such that the tension diagonal of the web and the transverse stiffeners act as a Pratt truss in resisting forces larger than the shear buckling load. To the knowledge of the author, none of the international standards consider the influence of lateral loading on the transverse stiffeners due to the restraint they provide to the lateral deflection of the web panels. However, as noted previously, multiple research studies indicate that this is a predominant effect, that is, postbuckled web panels load the transverse stiffeners more in bending than in axial compression at least up to a web slenderness of about $D/t_w = 250$ (approximately the maximum limit of these investigations). In a few of these research studies, models have been developed for checking stiffener strengths explicitly in terms of bending resistance or section modulus.

The following two sections review the basis for the area requirement in AASHTO (2004) as well as other similar requirements in Eurocode 3. This is followed by an overview of several models that consider the stiffeners as flexural elements.

2.3.1 AASHTO (2004) Area Requirement

The tension field theory adopted by AASHTO (2004) is based on the seminal research by Basler (1961). Basler developed a free body diagram at the location of an intermediate transverse stiffener that allows the calculation of the stiffener axial compression caused by the tension field (see Figure 2.3). This axial force is

$$P_s = (\sigma_t t_w d_o \sin \theta) \sin \theta = \sigma_t \left(\frac{t_w d_o}{2} \right) \left[1 - \frac{d_o/D}{\sqrt{1 + (d_o/D)^2}} \right] \quad (2.19)$$

where σ_t is the tension field stress, given by the approximation

$$\sigma_t = (1 - C) F_{yw} \quad (2.20)$$

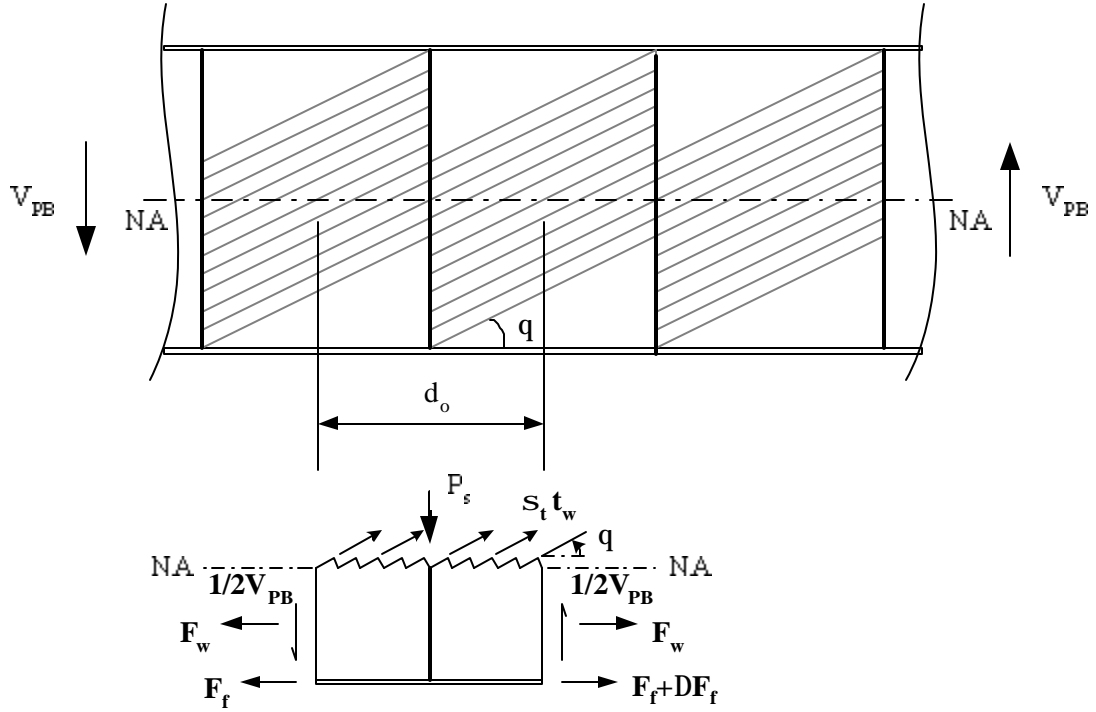


Figure 2.3. Free-body diagram at an intermediate transverse stiffener location.

and θ is the orientation of the tension field determined by Basler's theory. The corresponding increase in the shear resistance above the web shear buckling load is represented by the symbol V_{PB} in the figure. The parameter C in Equation (2.20) is the ratio of the shear buckling load (elastic or inelastic) to the fully-plastic shear resistance of the web, i.e., $C = V_{cr}/V_p$. After substituting Equation (2.20) and performing some minor algebraic manipulation, Equation (2.19) can be written as

$$P_s = \frac{1}{2} F_{yw} t_w D \left[\frac{d_o}{D} - \frac{(d_o/D)^2}{\sqrt{1 + (d_o/D)^2}} \right] (1 - C) \quad (2.21)$$

Vincent (1969) suggests a simplification to Equation (2.21) by considering that the expression within the brackets varies between 0.21 and 0.3 for the practical range of d_o/D

between 1/3 and 1.5. He uses $d_o/D = 0.8$ within this expression, which gives the maximum (conservative) value equal to 0.3. Interestingly, in current practice (2004), it is not uncommon for I-girders with d_o/D of 2 to 3 to be designed including tension-field action. For $d_o/D = 3$, the expression within the brackets of Equation (2.21) is equal to 0.15, only one-half of the maximum value.

Furthermore, Vincent (1969) states that when the tension field is not fully developed, the force P_s is reduced by the ratio V_u/V_n , where V_u is the applied shear at the strength load level and V_n is the nominal shear resistance of the web based on tension field action. This is an ad hoc liberalization of Basler's original equation, which is expected to be conservative since the in-plane axial forces from the tension field tend to increase at a higher rate as the maximum strength of the web is approached and the tension field develops. Basler (1961) originally suggested that P_s could be assumed to increase in proportion to $(V_u - V_{cr}) / (V_n - V_{cr})$. The ratio V_u/V_n is conservative relative to Basler's recommendation. Given the above adjustments, Equation (2.21) becomes

$$P_s = 0.15F_{yw} D t_w (1 - C) \frac{V_u}{V_n} \quad (2.22)$$

Basler (1961) assumed that when the tension field has formed, the web is already yielded in the vicinity of the transverse stiffener such that it cannot support any additional stresses associated with the stiffener axial force P_s . Therefore, according to Basler, the axial force P_s can only be resisted by the actual area of the transverse stiffener, A_s . However, Vincent (1969) indicated that Basler's area requirement could be liberalized by assuming that a portion of the web acts with the stiffener in resisting the force P_s , which was the practice in AASHTO (1969) at the time of his research.

Based on the assumption that P_s is resisted by the stiffener and a portion of the web, and that the material is stressed to its yield point as shown in Figure 2.4, force equilibrium along the line of the stiffener requires that

$$P_s = A_w F_{yw} + A_1 F_{ys} - (A_s - A_1) F_{ys} = (2A_1 - A_s) F_{ys} + A_w F_{yw} \quad (2.23)$$

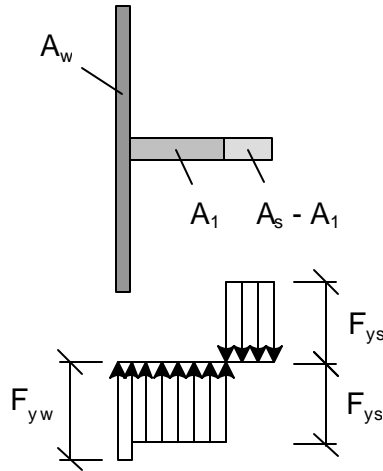


Figure 2.4. Stress Distribution in a stiffener.

By equating this expression to Equation (2.22), the required area of the stiffener can be written as

$$A_s = \left[0.15 F_{yw} D t_w (1 - C) \frac{V_u}{V_n} - A_w \right] \frac{F_{yw}}{F_{ys}} B \quad (2.24)$$

where

$$B = \frac{1}{2 \frac{A_1}{A_s} - 1} \quad (2.25)$$

If two stiffeners are placed symmetrically, one on each side of the web plate, there is no eccentricity of P_s with respect to the stiffener area and thus $A_1 = A$ and $B = 1.0$. However,

for a one-sided plate stiffener, moment equilibrium based on the application of P_s at the centerline of the web plate requires $A_1 = A/\sqrt{2}$, and therefore $B = 2.4$. This value for B is independent of the area of the web that participates with the stiffener.

Vincent (1969) suggests that

$$A_w = \frac{18t_w^2}{B} \quad (2.26)$$

can be assumed to act with the stiffeners in resisting the force P_s . He explains that very little information is available on the effective width of the web that works with the stiffener in resisting P_s , but that the contribution of the web is thought to be less for a one-sided stiffener. He shows a table that compares the theoretical stiffener axial force P_s from Equation (2.22) to the axial force calculated as the measured stress on the stiffener adjacent to the failed panel multiplied by the stiffener area ($\sigma_s A_s$) in eight of the tests from Basler (1960) as partial justification of Equation (2.26). The ratio $\sigma_s A_s / P_s$ ranges from zero to 0.56. More recently, Xie and Chapman (2003) have recommended an equation for the axial force transferred by the actual stiffener area that is applicable for a wide range of girder geometries. Their equation typically predicts stiffener axial forces significantly smaller than the more rigorous theoretical estimate of the forces from Basler's Equation (2.21). Interestingly, they find that the axial force in a stiffener with infinite rigidity is close to the result from Equation (2.21). Also, Yoo et al. (2004) provide FEA solutions that illustrate the development of significant normal stresses along the line of the stiffener within a representative web panel. These solutions confirm the assertion that a portion of the web adjacent to the stiffener participates significantly with the stiffener in transferring the tension field forces.

Two other modifications to Basler's original derivation are invoked to obtain the AASHTO (2004) equation for the transverse stiffener area. AASHTO allows stiffener width-to-thickness ratios b_s/t_s up to 16. However, particularly for transverse stiffeners with large F_{ys} , potential local buckling (or "tripping") of the stiffener is a concern at this high of a width-to-thickness ratio. To guard against local buckling of these types of transverse stiffeners, AASHTO (2004) uses a conservative expression for the stiffener local buckling stress

$$F_{crs} = \frac{0.31E}{\left(\frac{b_s}{t_s}\right)^2} \leq F_{ys} \quad (2.27)$$

in place of F_{ys} within its equation for the area requirement. This equation is based on a conservative elastic buckling coefficient of $k_s = 0.35$. This conservative solution for the stiffener elastic local buckling stress intersects the yield strength F_{ys} at a value of b_s/t_s that is an accepted limit in AISC (1999) for which an unstiffened plate can develop its yield strength in uniform compression. For $b_s/t_s = 13.5$, which corresponds to the AISC (1999) width-to-thickness limit for $F_{ys} = 345$ MPa (50 ksi), Equation (2.27) limits F_{crs} to this value of the yield strength. That is, for a transverse stiffener with $b_s/t_s = 13.5$, there is no advantage to using a yield strength greater than $F_{ys} = 345$ MPa. The effective yield strength of the stiffener is limited to $F_{crs} = 345$ MPa regardless of the actual yield strength of the stiffener.

The last modification involves the use of the ratio $V_u/\phi V_n$ in place of V_u/V_n within Equation (2.24). The resulting area requirement in AASHTO (2004) is written as

$$A_s \geq t_w^2 \frac{F_{yw}}{F_{crs}} \left(0.15B \frac{D}{t_w} (1 - C) \frac{V_u}{\phi V_n} - 18 \right) \quad (2.28)$$

2.3.2 Eurocode 3 Requirements

It is interesting to note that the rules for intermediate transverse stiffener design in Eurocode 3 (CEN 1993) are quite similar in terms of broad concepts to the approach taken in AASHTO (2004). That is, the stiffeners are designed by two criteria:

- (1) A moment of inertia requirement intended to ensure that the stiffener is able to maintain a line of near zero lateral deflection at the web shear buckling load, and
- (2) An axial force requirement (equivalent to an area requirement) based on an estimate of the in-plane forces transmitted to the stiffeners by the postbuckled web plate.

Similar to the AASHTO (2004) provisions, the Eurocode 3 idealization does not address the effects of out-of-plane forces on the transverse stiffeners caused by the shear postbuckling response of the web panels. The Eurocode 3 rigidity requirement is similar in magnitude to the AASHTO (2004) rule for $0.9 = d_o/D = 1.4$, but it is increasingly more liberal for $d_o/D < 0.9$ and $d_o/D > 1.4$. The Eurocode axial force requirement is based on the simple approximation

$$P_s = V_u - V_{cr} \quad (2.29)$$

where V_u is the shear force at strength load levels, and V_{cr} is the smaller web shear buckling resistance of the two panels adjacent to the stiffener. An area of the web of $30t_w \sqrt{235/F_{yw}}$ is assumed to act with the transverse stiffeners in resisting this force (with F_{yw} expressed in units of MPa), except at member ends or web openings, where $15t_w \sqrt{235/F_{yw}}$ is to be used. The stiffeners are required in general to be designed as beam-columns with an effective length greater than or equal to $0.75D$, recognizing the eccentricity of the force P_s with respect to the effective stiffener cross-section.

One of the earliest investigations of an approach similar to the Eurocode 3 method was by Rockey et al. (1981). These researchers considered the one-sided stiffener behavior in 11 experimental shear strength tests, all with $d_o/D = 1$ and $D/t_w = 300$. Rockey et al. found that an assumed participation from the web of $40t_w$ was necessary to obtain a reasonable estimate of the axial forces from the experimental measurements using the Cardiff theory (Porter 1975) to calculate V_n . Also, significant bending strains are apparent within plots they provide illustrating acceptable stiffener behavior (i.e., the stiffener is “effectively straight” and the girders have a “satisfactory post-peak w/δ curve” where w and δ represent the applied mid-span load and mid-span vertical deflection in their tests; however, the gradient in the strains across the stiffener is significantly larger than the axial strain near the juncture of the stiffener with the web). Lastly, Rockey et al. found that although part of the transverse stiffener has yielded, the remaining elastic part of the stiffener still can be effective. In as such, they conclude that it would be uneconomical to keep the transverse stiffeners elastic at the shear strength limit state of the web.

2.3.3 Strength Requirements Based on Idealization of the Transverse Stiffeners as Flexural Elements

2.3.3.1 Stanway et al. (1993 and 1996)

As noted previously, Stanway (1993) observed that transverse stiffeners in typical straight I-girders are loaded predominantly by bending effects induced by the lateral forces transmitted from the web panels they restrain. Also, Stanway et al. (1996) observed that similar web strengths and stiffener behavior are obtained when the stiffeners are modeled as “unattached” components that restrain the out-of-plane

deflection of the plate but have no in-plane attachment. In as such, Stanway et al. (1996) proposed an analytical model based on combined stiffness and strength criteria that idealizes the stiffeners solely as flexural components. In the previous Section 2.2, the key attributes of Stanway's stiffness criterion have been described. This section addresses Stanway's strength criterion.

Stanway et al. (1996) developed expressions for the stiffener bending moment M_s caused by two distinct effects: (1) out-of-plane forces transferred from the web panels due to out-of-plane bending and (2) overall buckling of the stiffener and web assembly. They state that overall buckling is not a major consideration for $d_o/D \geq 1/3$. Given the estimated stiffener moment, they proportion the intermediate transverse stiffeners for strength by providing an elastic section modulus such that the stiffeners are not yielded at the maximum strength limit state of the web panels.

Stanway et al. (1996) provide the following expression to estimate the stiffener moment caused by panel bending:

$$M_{pb} = \left(\frac{M_{pbcr}}{w_{pcr}} \right) w_p F_{nl} \quad (2.30)$$

where M_{pbcr}/w_{pcr} is the ratio of the moment (M_{pbcr}) derived from a buckling analysis of plates with a rigid straight knife edge support at the intermediate transverse stiffener to the corresponding maximum panel out-of-plane deflection (w_{pcr}), w_p is the maximum panel out-of-plane deflection at the strength limit state, and $F_{nl} = q_{pb}/q_{pbcr}$ where q_{pb} is the distributed lateral force on the stiffener, derived from nonlinear FEA solutions with straight knife edge supports at the stiffener, and q_{pbcr} represents the lateral distributed force corresponding to M_{pbcr} and w_{pcr} in the above buckling analysis. The web panel

deflection w_p is given by an equation developed by curve-fitting nonlinear elastic FEA results.

The stiffener moment from the overall buckling effect is expressed as:

$$M_o = \frac{V_n \pi^2 w_{os}}{k_{cro}} \quad (2.31)$$

where V_n is the shear strength of the idealized web panel considered by Stanway et al. (1993 and 1996) in their FEA solutions, including the development of tension field action, w_{os} is the stiffener initial imperfection, and k_{cro} is the overall buckling stress coefficient, derived by idealization of the web panels as rigid links that are connected into the flexible intermediate transverse stiffener.

Given the above two fundamental contributions to the stiffener bending moment, the total stiffener moment M_s is calculated as

$$M_s = \frac{M_o + M_{pb}}{1 - V_n / V_{cro}} \quad (2.32)$$

where

$$V_{cro} = k_{cro} D t_w \frac{E I_s}{D^3 t_w} \quad (2.33)$$

is the buckling load of the idealized assembly of the stiffener along with the rigid link representation of the web panels.

2.3.3.2 Rahal and Harding (1990a, 1990b and 1991)

Rahal and Harding (1990a, 1990b and 1991) performed extensive finite element studies of transversely-stiffened girder webs, and recommended an approach in which the stiffener is designed as a beam subjected to a transverse distributed force with a half sine wave distribution. These investigators studied the influence of tension field anchorage

from the flanges, geometric imperfection patterns, plate slenderness, panel aspect ratio, stiffener size, and yield strength in flat panels subdivided by a single transverse stiffener.

In their (1990a) paper, they state conclusively that:

“... the important panel influence on the stiffener is lateral loading induced by panel buckling. For panels bounded by actual flange members there is evidence of a significant tension field loading on the stiffener, but the effect of this, even for the more slender plates considered, is less than the beneficial effect resulting from the lateral stiffener bending restraint provided by the flange. This indicates that bending rigidity rather than axial stiffness is the most important parameter for the design of the stiffener, which supports the emphasis placed on stiffener rigidity in the study by Horne and Grayson.”

Rahal and Harding (1990b and 1991) develop an empirical equation for the magnitude of the transverse distributed force acting on the stiffeners from the web plate, based on FEA solutions of plates with non-deflecting stiffeners over the ranges $0.5 = d_o/D = 2$ and $60 = D/t_w = 240$. They consider the effects of not only the web shear force, but also web stresses due to bending moment and axial force within the I-girder in their solutions. Rahal and Harding (1990b) conclude:

“With this approach, there is no need to introduce the modest effects of tension field forces for the design of web stiffeners with panel slendernesses typical of those found in bridge structures.”

Similar to Stanway et al. (1996), the basic strength criterion adopted by Rahal and Harding is that the stiffeners should remain elastic at the maximum shear strength limit state of the web plate. Rahal and Harding (1990b) observe that the peak shear capacity of

stiffened web panels is extremely close to the point at which first yielding occurs within the stiffener.

The approach taken by Rahal and Harding is very promising and appealing, but unfortunately, their transverse load equation has constants that have dimensions, and the resulting stiffener strength requirements are girder size dependent. Therefore, the Rahal and Harding (1990b; 1991) model is not considered further in this work. However, their findings regarding the most critical geometric imperfection patterns are used as a point of departure for the author's study in Section 3.2.4.2, and a number of their findings are discussed in conjunction with the results from the current research study in Chapter IV.

2.3.3.3 Xie (2000)

Possibly the most complete model for calculation of the demands on intermediate transverse stiffeners is one developed by Xie (2000). Xie takes an approach similar to that of Stanway et al. (1996) for calculation of stiffener bending moments. However, he generalizes Stanway's equations to include web plates that are subjected not only to shear, but also plates that are subjected to shear, axial loading and bending. Furthermore, Xie develops equations that provide an estimate of the axial loads within the stiffeners by themselves. These equations, summarized in Xie and Chapman (2003), show that the stiffener axial force is a function of the ratio of the applied web shear force to the shear buckling load (V/V_{cr}), the web panel aspect ratio (d_o/D) and the area of the stiffener relative to the corresponding web plate area (expressed by the parameter $\Omega = A_s/d_o t_w$). Xie (2000) utilizes the above stiffener moment and axial force to check the transverse stiffeners as beam-columns based on a first-yield condition for strength and based on deflection limit equations similar to those developed by Stanway et al. (1996) for

stiffness. At the time of the writing of this thesis, improvements to the above model are being evaluated (Xie 2004), and therefore the model has not been finalized as of yet. Furthermore, although comprehensive in nature, Xie's model is not amenable to basic design calculations other than via the potential development of design charts or tables. It is desirable to consider whether the design of transverse stiffeners in both curved and straight I-girders can be achieved with a simpler approach such as that proposed by Horne and Grayson (1983). Therefore, the model developed by Xie (2000) is not considered further in this work.

CHAPTER III

DESIGN OF THE PARAMETRIC STUDY

3.1. Design of Test Girders

3.1.1. Test Configuration

The test configuration utilized for this research is shown in Figure 3.1. All the girders are laterally braced by ideally rigid braces (zero lateral displacement) at the top and bottom flanges at four locations, subdividing them into three equal unbraced lengths denoted by the symbol L_b . Both straight and curved I-girders are considered. For the curved I-girders, L_b corresponds to the arc length between the brace locations and the braces are oriented in the radial direction. All the girders are supported by an idealized knife edge at position 1L and by a roller at position 2R. They are loaded by a downward load of $P_2 = 3P$ at location 2L and by a downward load of $P_1 = P$ at location 1R. These loading and support conditions produce a large shear force and a small maximum major-axis bending moment, equal to $2P$ and PL_b respectively, within the center unbraced length of the girders. All the girders are designed using the AASHTO (2004) provisions such that their maximum capacity is governed by the shear resistance of the center unbraced length. Bearing stiffeners are located at each of the loading and support points, and an intermediate transverse stiffener is placed at the middle of each of the unbraced lengths. Therefore, $d_o = L_b/2$, where d_o is the width of the web panels. In Figure 3.1, the

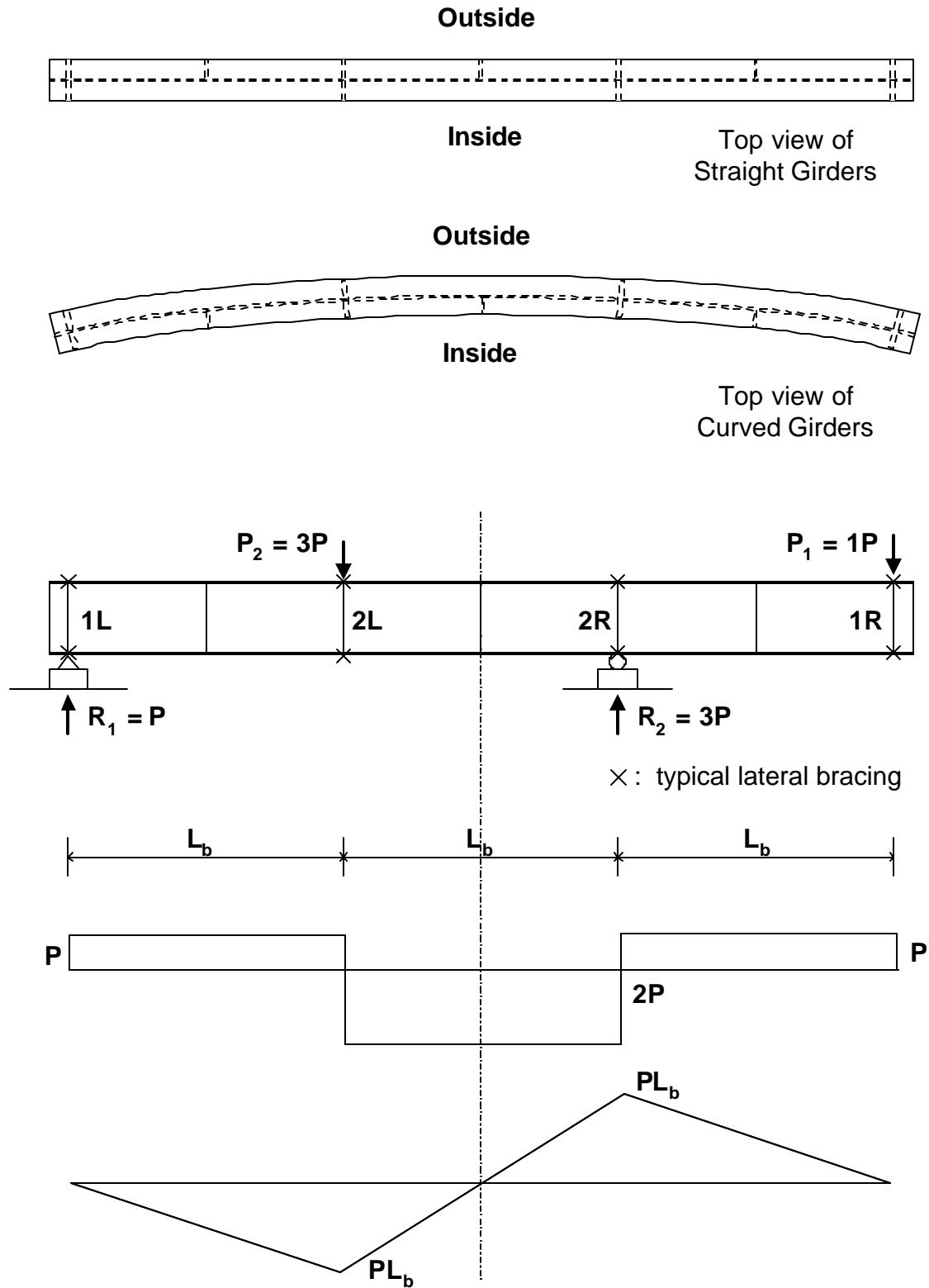


Figure 3.1 Test configuration and shear and approximate moment diagrams.

representative top views of straight and curved girders show the location of the stiffeners along the length of the girders. Both double- and single-sided stiffeners are considered in this research for all of the girder geometries. The location of single-sided transverse stiffeners relative to assumed panel geometric imperfections, and/or the inside or outside of the web with respect to the center of the horizontal curvature, is addressed in detail in Section 3.2.4.

3.1.2. Test Variables

This thesis focuses on the influence of the size and geometry (one- or two-sided) of intermediate transverse stiffeners on the maximum shear strength for a range of girder geometries. Specifically, these studies focus on the influence of the intermediate transverse stiffener within the center unbraced length of the configuration shown in Figure 3.1. The following girder geometry parameters are varied in these tests:

1. The web slenderness, D/t_w . Values of $D/t_w = 150$ and 300 are considered. The value $D/t_w = 150$ is the largest web slenderness allowed for transversely stiffened I-girders in AASHTO (2004). The value $D/t_w = 300$ is the largest web slenderness allowed for longitudinally stiffened I-girders in these Specifications. It is assumed that girders with the largest D/t_w values place the most severe demands on the transverse stiffeners (this assumption is based on results from prior work discussed in Chapter II and is subsequently verified).
2. The web panel aspect ratio d_o/D . Values of $d_o/D = 0.5, 1, 2$ and 3 are considered for girders with $D/t_w = 150$, and values of $d_o/D = 0.5, 1,$ and 1.5 are considered for $D/t_w = 300$. AASHTO (2004) restricts d_o/D to a maximum of three for transversely stiffened I-girders and to a maximum of 1.5 for longitudinally stiffened I-girders. The value

- $d_o/D = 0.5$ is a reasonable practical minimum value for the web panel aspect ratio in bridge I-girders.
- Both curved and straight I-girders are considered for each of the above geometries. For the curved girders, the radius of curvature is taken as a minimum value determined as explained within the following section.
 - Both one-sided and two-sided transverse stiffeners are considered for each of the above geometries.

3.1.3. Selection of Girder Material and Geometry

The webs and stiffeners are assumed to have a nominal yield strength of $F_{yw} = F_{ys} = 485$ MPa (70 ksi) in all of these studies. The postbuckling strength is generally a larger proportion of the total shear strength in Grade 485 versus Grade 345 webs. Grade 690 webs are considered to be unusual for I-girder bridge construction, and therefore F_{yw} and F_{ys} greater than 485 MPa are not addressed. However, the flanges of all the girders considered in these studies are designed with $F_{yf} = 690$ MPa (100 ksi). This results in smaller flanges and in turn tends to minimize the elastic restraint provided to the girder webs and transverse stiffeners by the flanges.

The I-girder web depths are taken equal to 2438 mm (96 in) in all cases. The selection of this absolute dimension is tied to the selection of a maximum $d_o/R = 0.1$ in these studies. The value $d_o/R = 0.1$ is the maximum ratio of the web panel length to the radius of curvature considered in the prior studies by Zureick et al. (2002) and by Jung and White (2003). It is desired to study curved I-girders with d_o/R values equal or close to this maximum, such that any radial loading effects induced in the critical transverse stiffener by web postbuckling action are maximized. Also, the AASHTO (2003 and

2004) Specifications restrict the horizontal radius of curvature to $R = 30.48$ m (100 ft). The value $D = 2438$ mm is selected as a reasonable approximate upper-bound web depth of transversely stiffened I-girders in which the maximum $d_o/R = 0.1$ can be achieved for $d_o/D = 1.5, 2$ and 3 without violating this minimum limit on R . For the test girders with $d_o/D = 1$ and 0.5 , the minimum R of 30.48 m applies and the corresponding d_o/R values are 0.08 and 0.04 respectively. For the curved girders, the subtended angle between the brace points L_b/R is equal to $2d_o/R$ in all cases. As a result, all the girders except the ones with $d_o/D = 0.5$ exceed the AASHTO (2004) requirement of $L_b/R = 0.1$ for bridges in their final constructed configuration. However, AASHTO (2004) allows the use of $L_b/R > 0.1$ during construction.

All of the test girder cross-sections are doubly-symmetric. Also, all of the girders are transversely stiffened only, even for $D/t_w = 300$. The AASHTO (2004) provisions for the shear strength of longitudinally stiffened I-girders do not consider any positive influence of the longitudinal stiffeners on the shear and flexural strengths, with the exception that if web bend-buckling is prevented at the strength limit due to the longitudinal stiffening of the web, the web bend-buckling parameter R_b is taken equal to one. This approach to longitudinally stiffened I-girder design is used because the longitudinal stiffener proportioning requirements in AASHTO (2004) are based only on the development of the web buckling strengths. They are not in general sufficient for the stiffener to maintain a line of near zero lateral deflection once the web is loaded into its postbuckling range (Galambos 1998). Therefore, to parallel the AASHTO (2004) approach, and also to simplify the interpretation of the parametric study results, the longitudinal stiffeners are not included within the finite element studies conducted in this research.

All of the transverse stiffeners of the test girders have a width-to-thickness ratio $b_s/t_s = 10$. The value of $b_s/t_s = 10$ is selected as a representative value for typical plate stiffeners. The implications of other b_s/t_s values are addressed subsequently. Various moments of inertia of the stiffener are obtained by changing the stiffener width b_s while b_s/t_s is held constant. The bearing stiffeners are designed conservatively such that the girder strengths are effectively independent of the size of these elements. All of the bearing stiffeners are a pair of 228.6 mm by 54.61 mm (9.00 in by 2.15 in) plates.

The flanges of the test girders are sized such that the maximum internal bending moment PL_b is less than $0.75M_n$, where M_n is the nominal moment capacity of the girders calculated based on the one-third rule of AASHTO (2004) and accounting for the flange lateral bending effects in the curved I-girders. That is, M_n is calculated as

$$M_n = \left(F_n - \frac{1}{3} f_\ell \right) S_x \quad (3.1)$$

where:

F_n = nominal flexural resistance, taken as the smaller value corresponding to flange local or lateral-torsional buckling,

f_ℓ = maximum elastically computed flange lateral bending stress within the unbraced length under consideration, determined by conducting a first-order analysis of the test girders using open-walled section beam theory, then amplifying the maximum first-order lateral bending stress by the amplification factor specified in AASHTO (2004), and

S_x = elastic section modulus.

A curved and a straight configuration are considered for each of the girder cross-sections, and the same flange size is employed for both configurations. By restricting the maximum moment to $0.75M_n$, it is expected that the effects of any interaction between

the flexural and shear strengths is negligible. The Engineer should note that in some cases, F_n is governed by lateral-torsional buckling of the outside unbraced segments in Figure 3.1. Also, the flanges are sized such that the amplified maximum flange lateral bending stress is limited to $0.6F_{yf}$ as specified in AASHTO (2004).

The flange proportions are selected such that the flanges are compact by AASHTO (2004). The flange slenderness $b_f/2t_f$ is slightly less than 6.47, except for the girders with $d_o/D = 3$, where a slightly smaller $b_f/2t_f$ (larger t_f) is employed to limit the magnitude of the lateral bending stresses. The flanges are sized close to the minimum that satisfies $0.75M_n$ from Equation (3.1) as well as the limit $f_\ell \leq 0.6F_{yf}$.

Table 3.1 summarizes the primary dimensions and non-dimensional ratios for the test girders utilized in this study, including the horizontal radius of curvature for the curved geometry cases. For the girders with $d_o/D = 0.5$, the flexural design requirements are satisfied with relatively small flanges such that $D/b_f = 6$, the smallest I-girder cross-section aspect ratio allowed within the AASHTO (2004) provisions. For the girders with $d_o/D = 3$, larger flanges are necessary to satisfy the flexural design requirements.

Table 3.1. Summary of cross section dimensions and non-dimensional ratios for the test girders.

D/t_w	t_w (mm)	d_o/D	d_o (mm)	R (m)	d_o/R	b_f (mm)	t_f (mm)	$b_f/2t_f$	D/b_f
150	16.27	0.5	1219	30.48	0.04	406.4	31.75	6.40	6
		1	2438	30.48	0.08	457.2	35.56	6.43	5.33
		2	4877	48.77	0.1	660.4	51.56	6.40	3.69
		3	7315	73.15	0.1	863.6	86.36	5.00	2.82
300	8.13	0.5	1219	30.48	0.04	406.4	31.75	6.40	6
		1	2438	30.48	0.08	457.2	35.56	6.43	5.33
		1.5	3658	36.58	0.1	508	39.62	6.41	4.80

3.2. Finite Element Models

3.2.1. Finite Element Discretization

The finite element models are constructed with the ABAQUS 6.3 analysis system (HKS 2002) using the S4R element for the web and the B31 element for the flanges, the bearing stiffeners and the transverse stiffeners. The S4R element is a general purpose four-node quadrilateral displacement-based shell element with reduced integration. Five integration points are used through the thickness of the shell elements (trapezoidal rule). The B31 element is two-node linear-order beam element based on Reissner-Mindlin beam theory. The beam cross-section is modeled using a five point trapezoidal integration rule through its thickness and width.

In all the specimens, thirty two shell elements are used through the depth of the web. All of the shell elements have an aspect ratio of one except the elements located at the top and bottom of the web. These elements have an aspect ratio slightly greater than one depending on the thickness of the flanges. That is, their height is equal to $D/32 + t_f/2$. This mesh density is approximately two times that found in previous studies to provide acceptable convergence of the load-displacement results (e.g., see (Aydemir 2001)), thus providing a relatively accurate approximation of the localized web and transverse stiffener strains.

3.2.2. Load and Displacement Boundary Conditions

The exterior vertical support at location 1L (see Figure 3.1) is modeled by restraining the displacement in the vertical and longitudinal directions at the corresponding flange node. The longitudinal direction is taken as the direction tangent to the curved flange in the curved girders. The interior vertical support at location 2R is an ideal roller support

modeled by restraining the displacement in the vertical direction only. The girders are free to move along the longitudinal direction at this location. The lateral displacements are restrained at the juncture of the web with the top and bottom flange at each of the loading and support locations (1L, 2L, 2R and 1R). In the curved girders, the lateral direction is the radial direction perpendicular to the curved longitudinal axis of the member.

With regard to the force boundary conditions used in the analysis, concentrated loads are applied having a total magnitude of 3P at the interior brace location 2L and P at the end brace location 1R. These loads are placed at the top web-flange juncture. The self weight of the test girders and of the bracing members is not included in the analysis.

3.2.3. Material Stress-Strain Characteristics

Since the S4R and B31 elements in ABAQUS are based on a large strain formulations, the material response must be defined in terms of true stress and true strain. For the finite element analysis, multi-linear curves representative of the true stress-strain response of the assumed physical materials are determined as follows. The stress-strain curve from a representative HPS 485W tension coupon test (Wright 1997), expressed in terms of the engineering (or nominal) stress and strain, serves as the starting point. Given this engineering stress-strain curve (σ_{nom} versus ϵ_{nom}), the true stress-strain response (σ versus ϵ) is calculated by applying the following equations :

$$\sigma = \sigma_{nom}(1 + \epsilon_{nom}) \quad (3.2)$$

$$\epsilon = \ln(1 + \epsilon_{nom}) \quad (3.3)$$

Figure 3.2 shows the measured engineering and the calculated true stress-strain curves from the representative coupon test. The static yield strength in this HPS 485W

test is 527.1 MPa (76 ksi). However, it is desired to use a nominal yield strength of $F_y = 485$ MPa (70 ksi) within the parametric study solutions. Therefore, nominal stress-strain curves for the web and the stiffeners with $F_{yw} = F_{ys} = 485$ MPa are obtained by scaling the ordinate of the engineering and true stress-strain curves in Figure 3.2 by $485/527.1$. The strains for the stress-strain data points are not modified by this scaling process, with the exception that the yield strain is still taken as F_y/E . The modulus of elasticity E is taken as 200 GPa (29,000 ksi) throughout this research.

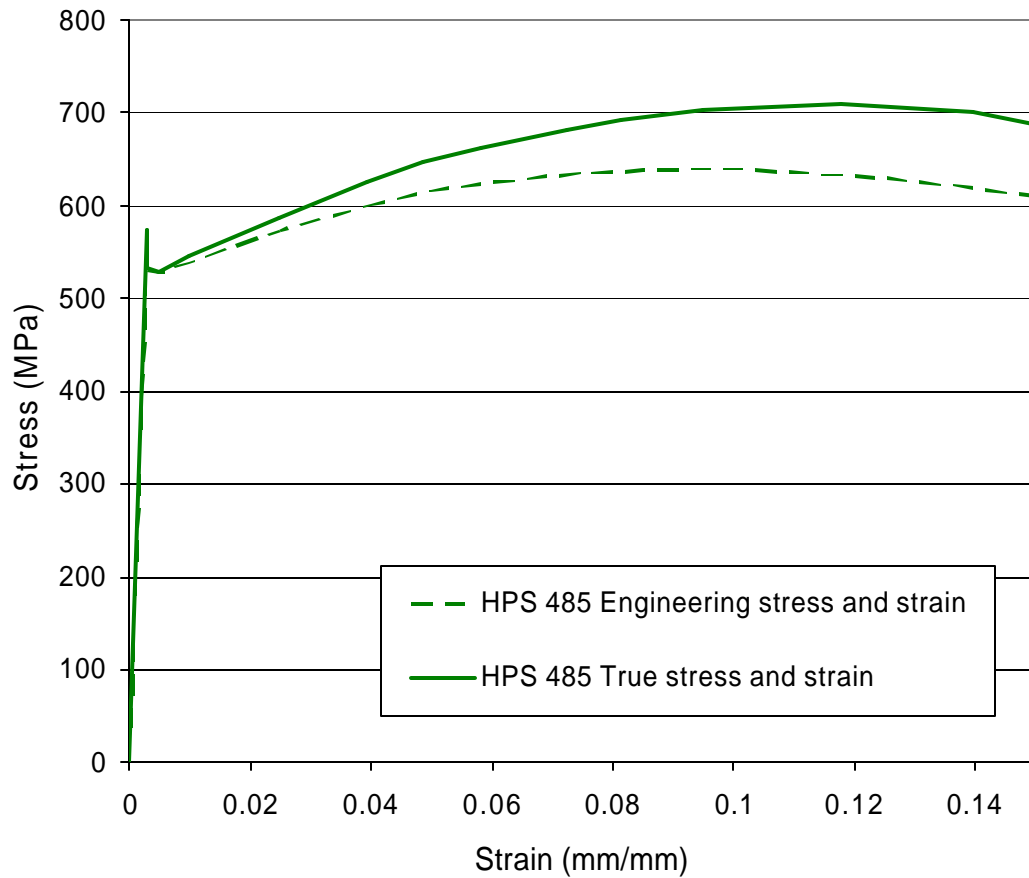


Figure 3.2 Engineering stress-strain and true stress-strain curves for a representative HPS 485W tension coupon test (Wright 1997).

Representative nominal stress-strain curves for the flanges, which are assumed to have $F_{yf} = 690$ MPa (100 ksi), are obtained by scaling the stress-strain curves from the HPS 485W coupon test by $690/527.1$. This is justified based on the fact that the resulting ultimate tensile strength (on the scaled engineering stress-strain curve) is $F_u = 840$ MPa. This value is within the range specified for the ultimate tensile strength of 760 to 900 MPa (110 to 130 ksi) for ASTM A514 material having a specified minimum yield strength of 690 MPa (ASTM 1993) as well for HPS 690W material (Krouse 2004). Also, it should be noted that the yield plateau of the HPS 485W stress-strain curve shown in Figure 3.2 is relatively short. ASTM A514 steel does not exhibit a well defined yield point, and HPS 690W material also typically does not have an extended yield plateau.

Multi-linear representations of the scaled engineering and true stress-strain curves are defined for the finite element analysis using four points selected from the test data. The first point is the initial yield point of the material, and therefore has a plastic strain value of zero. The second point is defined at the onset of strain hardening. The third and fourth points are arbitrarily selected at points that allow for a close fit to the scaled representative stress-strain curves. The true stress is assumed to be constant for strains larger than those associated with the last point. Multi-linear curves representing the engineering and the true stress-strain response of the representative HPS 485W coupon test are shown in Figure 3.3. The final scaled multi-linear curves for the web-stiffener and flange materials are shown in Figure 3.4¹. Table 3.2 summarizes the true strain-stress data for these curves.

¹ The same scaled multi-linear true stress-strain curves are obtained by (1) scaling the ordinate of the engineering stress-strain curves, then converting to true stress-strain, or by (2) converting to true stress-strain and then scaling the ordinate of the curves.

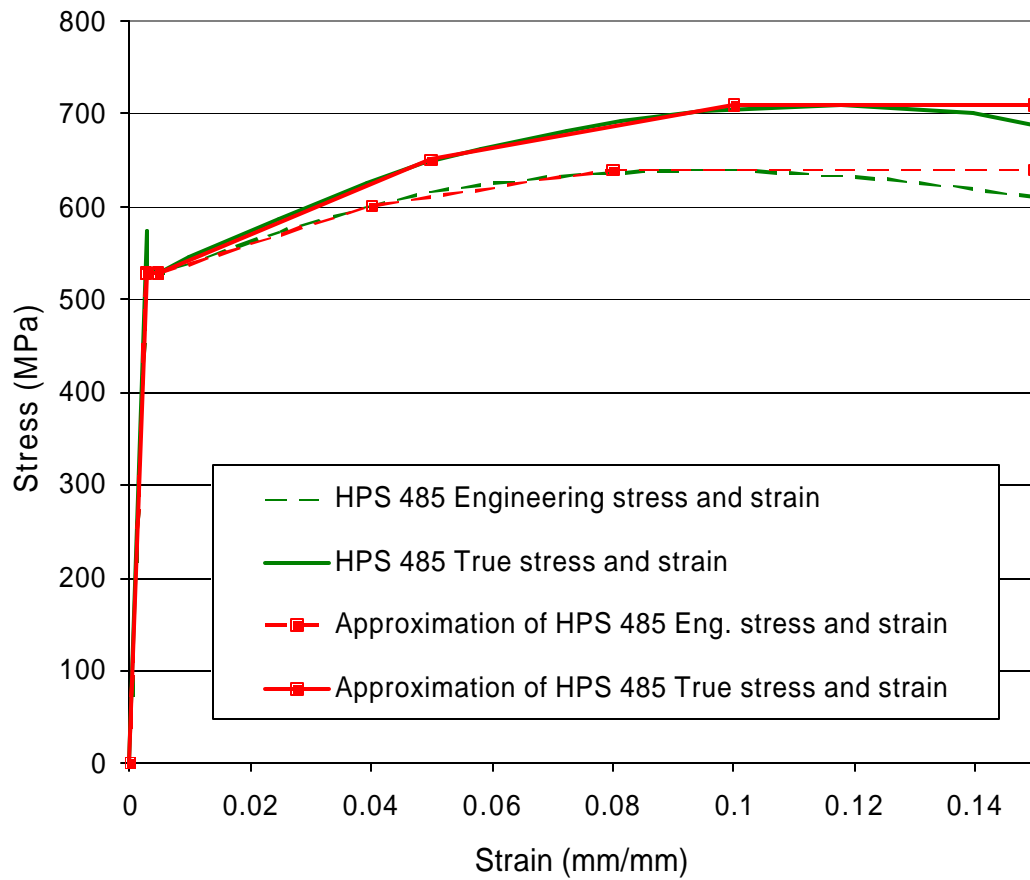


Figure 3.3. Actual and multi-linear representations of the HPS 485W engineering and true stress-strain curves.

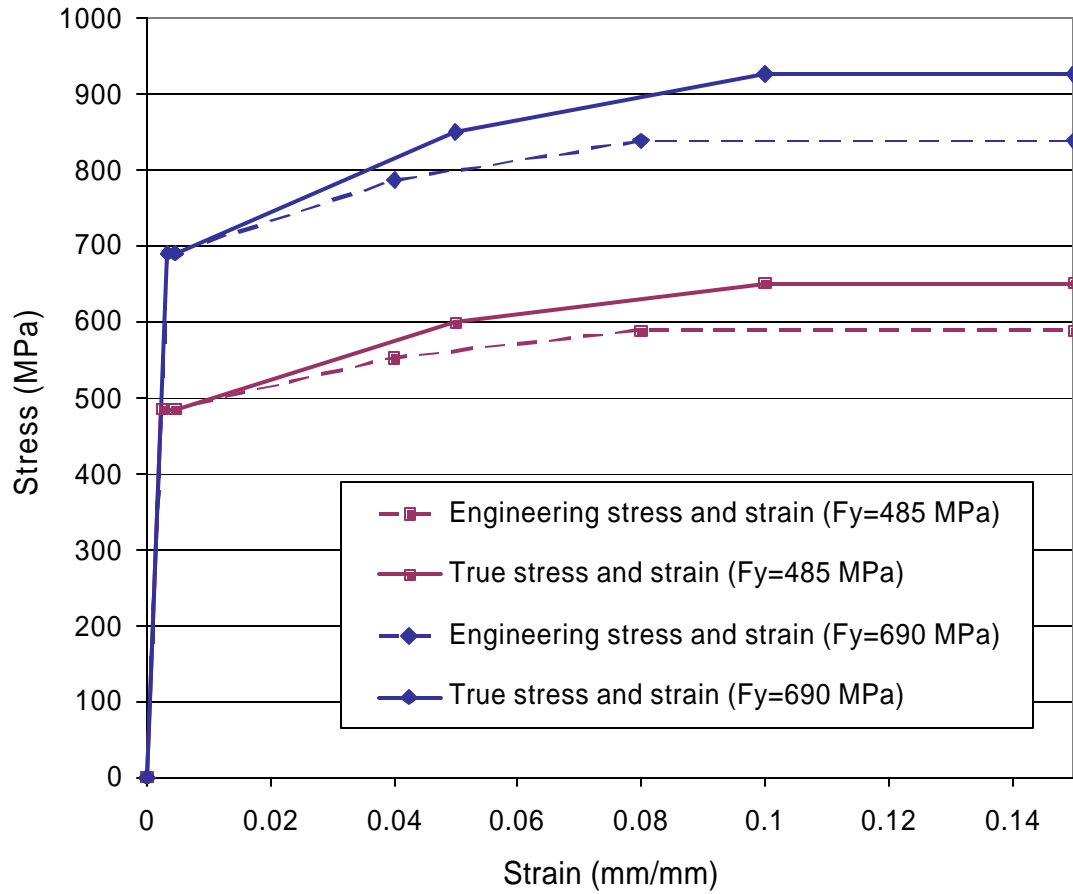


Figure 3.4 Multi-linear representations of the web-stiffener and flange engineering and true stress-strain response.

Table 3.2. True stress-strain data for the multilinear representations of the web-stiffener and flange materials for finite element analysis.

Web and Stiffeners $F_{yw} = F_{ys} = 485 \text{ MPa}$		Flanges $F_{yf} = 690 \text{ MPa}$	
True strain (mm/mm)	True stress (MPa)	True strain (mm/mm)	True stress (MPa)
0	0.00	0	0.00
0.0024138	485.00	0.0034483	690.00
0.0045895	485.95	0.0045895	691.35
0.05	597.93	0.05	850.66
0.1	651.32	0.1	926.62
0.15	651.32	0.15	926.62

3.2.4. Residual Stresses and Geometric Imperfections

3.2.4.1 Residual Stresses

Residual stresses are not considered in this work. A number of prior studies have shown that residual stresses have a small effect on the shear strength behavior of I-girders (e.g., Horne and Grayson (1983); Stanway et al. (1993); White et al. (2001); Aydemir (2001)). Horne and Grayson (1983) specifically observe that the effect of residual stresses on the behavior of intermediate transverse stiffeners is small.

3.2.4.2 Geometric Imperfection Patterns, Straight I-Girders

Geometric imperfections are specified within the finite element analysis models based in large part on the findings by Rahal and Harding (1991). These investigators studied a large variety of geometric imperfection patterns in nominally flat webs with single-sided plate stiffeners and found that for $d_o/D = 1, 1.5$ and 2.0 , the pattern shown in Figure 3.5 gives the largest magnitude of stress within the critical stiffener and the largest reduction in the maximum shear strength. This geometric imperfection pattern includes an out-of-straightness of the critical stiffener in the direction of its outstand (the tip of the transverse stiffener), and an out-of-flatness of the web panels in a single “wave” in the opposite direction from the stiffener out-of-straightness². For $d_o/D = 0.5$, Rahal and Harding (1991) determined that the geometric imperfection pattern shown in Figure 3.6 is the most critical. Stanway et al. (1993) used similar geometric imperfections in their studies with double-sided transverse stiffeners.

² The stiffener out-of-straightness in this imperfection pattern is in the same direction as the out-of-straightness that would tend to be induced due to welding distortion.

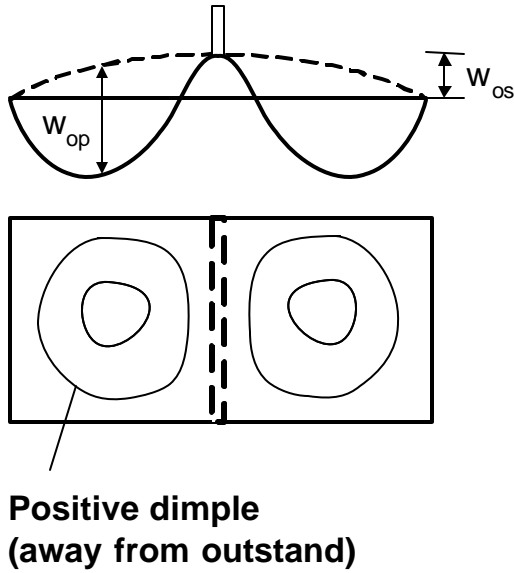


Figure 3.5. Critical geometric imperfection pattern for nominally-flat webs with $d_o/D = 1, 1.5$ and 2.0 (Rahal and Harding 1991).

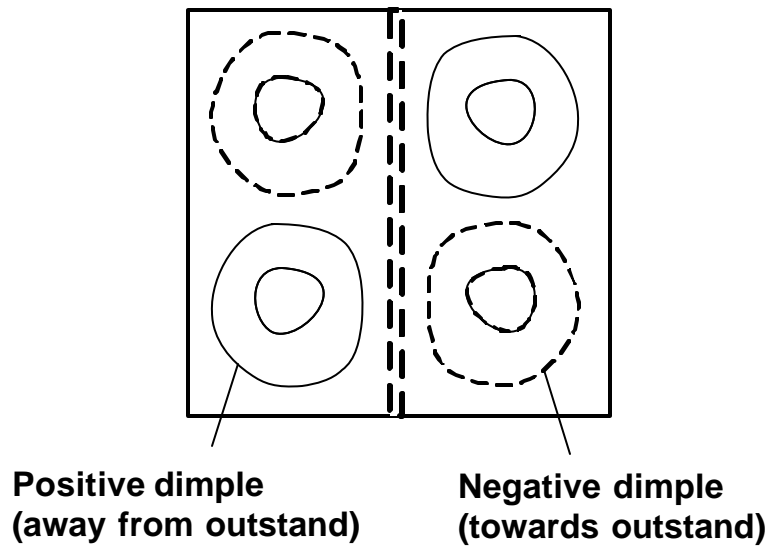


Figure 3.6. Critical geometric imperfection pattern for nominally-flat webs with $d_o/D = 0.5$ (Rahal and Harding 1991).

One of the most common approaches to the modeling of geometric imperfections is the use of a combination of scaled buckling mode shapes. As discussed by Stanway et al. (1993), this approach typically is not appropriate for modeling of the geometric imperfections within a transversely stiffened web plate. Although it is important that the geometric imperfections should have some affinity with the buckling modes of the web-stiffener assembly, it is desirable to define both a stiffener out-of-straightness and a web panel out-of-flatness at values representative of fabrication tolerances. The magnitude of the lateral deflections of the stiffener and of the web panel obtained from a buckling analysis generally are a function of the relative stiffener and web panel rigidities. If the stiffener rigidity is relatively large within the buckling analysis, its corresponding lateral deflections will be quite small. Furthermore, due to the spread of yielding within the web plate and/or the critical transverse stiffener during the progress of the full nonlinear finite element analysis, the fundamental buckling modes of the stiffened web may change as the maximum shear strength is approached.

Based on the above considerations, geometric imperfections similar to the critical pattern identified by Rahal and Harding (1991) for $d_o/D = 1, 1.5$ and 2 are utilized for analysis of straight I-girders in this research. Furthermore, this type of geometric imperfection pattern is selected also for $d_o/D = 0.5$ and 3.0 . The rationale for this decision is the expectation that the out-of-straightness of the transverse stiffeners and the out-of-flatness of the web panels due to fabrication typically will be predominantly a single “wave” over the depth of the stiffeners and the width and depth of the web panels. Also, Rahal and Harding (1990a) show that for a web panel with $d_o/D = 0.5$ and $D/t_w = 180$ and the imperfection pattern shown in Figure 3.6, negating the amplitudes of the

dimples in one of the panels (such that the geometric imperfections are symmetric about the line of the transverse stiffener) has essentially zero effect on the maximum shear strength.

The specifics of the geometric imperfection pattern are slightly different than that specified by Rahal and Harding (1991) corresponding to Figure 3.5. Rahal and Harding defined the panel out-of-flatness as a single sine wave within each panel. This gives a kink in the panel geometry at the location of the transverse stiffener. In this research, the geometric imperfections are generated by performing a “pre-analysis” in which the critical transverse stiffener is subjected to a specified sinusoidal lateral displacement with a magnitude equal to the desired out-of-straightness. In this pre-analysis, the displacements along the other edges of the adjacent web panels are constrained to have zero lateral displacement and these panels are subjected to a uniform lateral pressure. The magnitude of the uniform lateral pressure is specified such that the desired maximum web panel out-of-flatness is obtained relative to the deflected panel geometry associated with the transverse stiffener out-of-straightness. The deflections from the pre-analysis are then imported as the initial imperfections in the subsequent full nonlinear analysis of the girders.

One other attribute of the geometric imperfection patterns utilized in the present study pertains to the imperfections specified for the limiting cases where the critical transverse stiffener is removed (i.e., I_s equal to zero). In this limiting case, a single wave geometric imperfection is specified over the full length between the bearing stiffeners within the middle test length in Figure 3.1. Geometric imperfection patterns intermediate between this imperfection and the one shown in Figure 3.5 are not considered. For cases where

the critical transverse stiffener has some finite bending rigidity, the stiffener is assumed to have an out-of-straightness consistent with the specific tolerance discussed in the next section.

3.2.4.3 Magnitude of the Geometric Imperfections

As noted previously, an important attribute of the specified geometric imperfections is that they should represent typical imperfections within fabrication tolerances in physical girders. In this regard, a stiffener out-of-straightness $w_{os} = D/750$ is selected. This value is equal to the stiffener imperfection used by Stanway et al. (1993 and 1996) and results in a maximum out-of-straightness of the stiffeners equal to 3.25 mm (0.128 in) for all of the girders studied in this research, since $D = 2438$ mm (96 in) (Rahal and Harding (1990a and b, 1991) used $w_{os} = b/750$). The maximum web panel out-of-flatness relative to the panel deflected geometry associated with the stiffener geometric imperfection is taken as $w_{op} = D/120$. This value is the same as that selected for the amplitude of the web panel geometric imperfections by Lee et al. (2003) in their FEA studies, and it results in a maximum web out-of-flatness relative to the deformed geometry associated with the stiffener out-of-straightness of 20.32 mm (0.80 in) for all of the girders studied in this research. The web panel out-of-flatness is somewhat larger than the value of $w_{op} = b (F_{yw}/355)^{0.5} / 165$ used by Rahal and Harding (1990a and b, 1991) and by Stanway et al. (1993 and 1996), which is based on fabrication tolerances within the British Standard at the time of their research.

It is interesting to compare the above imperfection magnitudes to geometric tolerances specified within AWS (2000). The AWS Standard specifies that the out-of-straightness variation of intermediate transverse stiffeners shall not exceed 13 mm (0.5

in) for girders up to 1.8 m (6 ft) deep, and 19 mm (0.75 in) for girders over 1.8 m deep, with due regard for members with frame into them. This corresponds to a stiffener out-of-straightness of $D/96$, a value substantially larger than the imperfection of $D/750$ used by Stanway et al. (1993 and 1996) and specified in this research. Nevertheless, the value of $D/750$ is selected for the stiffener out-of-straightness in this research since this value is already double the value accepted as appropriate for determination of column strength curves (Galambos 1998), and since it is expected that typical fabricated I-girders will not deviate from the ideal geometry to the extent allowed by the above AWS tolerance. Also, given that the transverse stiffener behavior is dominated by bending rather than axial loading, the strength behavior is insensitive to the stiffener geometric imperfections.

The AWS (2000) tolerances for the web out-of-flatness vary significantly depending on the web slenderness, whether intermediate stiffeners are placed on one or both sides of the web, and whether the members are interior or fascia girders. The most liberal tolerance is $b/67$ for interior girders with $D/t_w \geq 100$ and intermediate stiffeners only on one side of the web, whereas the most restrictive tolerance for transversely-stiffened girders is $b/130$ for fascia girders with $D/t_w < 150$ and intermediate stiffeners on both sides of the web. The web out-of-flatness tolerance is $b/150$ for girders with no intermediate stiffeners. These tolerances are to be compared to the “offset from the actual web centerline to a straight edge whose length is greater than the least panel dimension and placed on a plane parallel to the nominal web plane,” and the measurements are to be taken prior to erection. Based on these definitions, one can conclude that the out-of-flatness w_{op} may be significantly different from the above values

within an erected bridge structure. The out-of-flatness $w_{op} = D/120$ is selected in this research as a reasonable representative magnitude for the web geometric imperfection.

3.2.4.4 Geometric Imperfection Patterns and Inside versus Outside Location of One-Sided Transverse Stiffeners in Curved I-Girders

In curved I-girders, the web panels have an inherent out-of-flatness due to the nominal horizontal curvature. This out-of-flatness is similar to the web out-of-flatness induced by the stiffener out-of-straightness shown in Figure 3.5, except that the horizontally curved web is nominally flat in the vertical direction (i.e., a straight edge placed vertically between the flanges would be in contact with the web along its entire height). Therefore, one would expect that if the geometric imperfections shown in Fig. 3.5 are most critical for straight girders, the same imperfection (with the one-sided transverse stiffeners located on the outside of the web and the out-of-flatness oriented in the direction toward the center of the horizontal curvature) would produce the largest stiffener stresses and the largest reduction in the shear strength in curved girders.

This expectation is confirmed with respect to the web out-of-flatness in the studies by Jung and White (2003), where these researchers found that curved I-girder maximum shear strengths were reduced the most when the web out-of-flatness was specified in the direction toward the center of the horizontal curvature. However, Jung and White did not consider transverse stiffener geometric imperfections or location (inside or outside relative to the web) in their work. Jung and White (2003) modeled the transverse stiffeners on the same side of the web as selected in the physical tests conducted by Zureick et al. (2002), the inside of the web.

In order to check the above expectation with respect to the transverse stiffener out-of-straightness and location, studies are conducted in this research in which the initial geometric imperfection pattern of Figure 3.5 is specified, but in which one-sided transverse stiffeners are placed on the outside of the web in one case and on the inside of the web in the other case. Both straight and curved I-girders are considered, with the inside direction for the straight I-girders defined as the direction of the web panel out-of-flatness. In the straight I-girders, the pattern shown in Figure 3.5 is confirmed to be the most critical, but the difference between the maximum shear strengths with the transverse stiffener located on the inside or the outside of the web is small in all cases. The largest difference in the maximum shear strengths is 3.0 percent. This occurs for $D/t_w = 300$ and $d_o/D = 1$ and for a transverse stiffener size that is significantly smaller than required by AASHTO (2004) as well as by the final recommendations proposed in this work.

Conversely, when the above expectation is checked for curved I-girders, the maximum shear strengths are either identical for all practical purposes or are somewhat smaller when the transverse stiffener is located on the inside. The maximum effect of the inside or outside location of the transverse stiffener in this case is 11.3 percent relative to the shear strength for the geometry shown in Figure 3.5. However, again this difference corresponds to a web slenderness equal to the largest value allowed by AASHTO (2004) for longitudinally stiffened I-girders ($D/t_w = 300$), $d_o/D = 1$, and a transverse stiffener size that is significantly smaller than required by AASHTO (2004) as well as by the final recommendations proposed in this work.

In all the cases studied and for transverse stiffeners that meet the final recommendations proposed in this work, the largest difference between the maximum

shear strengths determined for the curved I-girders with one-sided transverse stiffeners on the inside of the web is approximately four percent relative to the strength for the geometry shown in Figure 3.5. It is only 2.4 percent for transverse stiffeners that satisfy the AASHTO (2004) provisions. These differences again correspond to I-girders with $D/t_w = 300$ and $d_o/D = 1$. For smaller D/t_w and for other panel aspect ratios, the differences are smaller except for some cases with stiffeners sized by the AASHTO (2004) provisions, where the AASHTO (2004) provisions are found to be inadequate. For girders with $D/t_w = 150$ and $d_o/D = 1$ and in which the stiffeners satisfy the final recommendations proposed in this work, the largest difference between the maximum shear strengths determined for the curved girders with the intermediate transverse stiffeners on the inside of the web is approximately three percent relative to the strength determined for the geometry shown in Figure 3.5.

For the curved I-girders, the above behavior appears to be related to a radial loading applied to the transverse stiffeners from the web tension field. For the cases with the most slender webs ($D/t_w = 300$), this radial loading induces a significant tensile stress at the tip of the outstand when the transverse stiffener is located on the inside of the web. Conversely, it induces axial compression at the tip of the outstand when the transverse stiffener is located on the outside. Furthermore, the axial loading effect on the stiffener from the tension field action of the web panels causes additional bending due to the eccentricity of the stiffener relative to the mid-thickness of the web plate, although this effect tends to be more minor than the lateral loading effect caused by the tendency of the web plate to move laterally. When the transverse stiffener is located on the inside of the web, the above two effects are additive, both causing tension at the tip of the outstand.

Given the above behavior for curved I-girders, the imperfection shown in Figure 3.7 is considered for these girder types with $D/t_w = 300$ and $d_o/D = 1$, since this geometric imperfection causes an additional tension at the tip of the outstand due to the effect of the stiffener axial compression acting through the out-of-straightness of the stiffener, when the stiffener is located on the inside of the web. The largest reduction in the maximum shear strength is 11.7 percent for this geometry relative to the geometry illustrated by Figure 3.5; the largest reduction is 6.0 percent relative to the strength predicted for the imperfection shown in Figure 3.5 but with the stiffener placed on the inside of the web. However, these reductions in strength again occur for stiffener sizes that neither satisfy the AASHTO (2004) requirements nor the final recommendations from this research. For a stiffener that satisfies the final recommendations of this research, the reduction in the maximum shear strength is 4.7 percent relative to the strength obtained using the imperfection shown in Figure 3.5 (with the one-sided stiffener placed on the outside). Furthermore, the FEA prediction of the web shear strength is 96.7 percent of the nominal strength calculated by the AASHTO (2004) shear strength equations in this case. For a one-sided transverse stiffener that satisfies the corresponding AASHTO (2004) requirements, the maximum reduction in the shear strength is 2.4 percent for the geometry shown in Figure 3.7 relative to that for the geometry shown in Figure 3.5.

Based on the above results, the solutions reported in Chapter IV for curved girders with one-sided transverse stiffeners are based on the imperfection shown in Figure 3.5, but with the stiffener located on the inside of the web, unless noted otherwise. Detailed results pertaining to the imperfection sensitivity are presented for the most critical I-girders in Chapter IV. In general, it is important to recognize that the specific and

detailed demands placed on the intermediate transverse stiffeners are influenced in very complex ways by the pattern of the assumed geometric imperfections and by other characteristics of the I-girder geometry (i.e., one-sided stiffener inside or outside orientation relative to the horizontal curvature or relative to the web out-of-flatness, D/t_w , d_o/D , etc.). However, as observed by Horne and Grayson (1983), the geometric imperfection pattern generally has a discernable but only a small effect on the maximum capacity in shear (for girders in which the stiffeners are adequately sized).

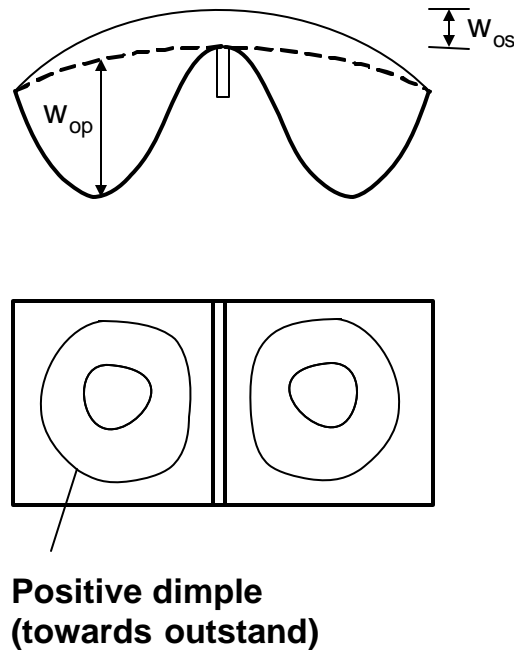


Figure 3.7. Critical geometric imperfection pattern for curved I-girders.

3.2.5. Comparison of FEA Predictions to Experimental Test Results

To demonstrate the effectiveness of the finite element modeling approach used in this study, analyses are conducted of two girders tested experimentally by Rockey et al.

(1981). These tests are labeled by Rockey et al. as TGV7-2 and TGV8-1. In test TGV7-2, the transverse stiffener performed its intended function. However, in test TGV8-1, significant transverse stiffener lateral deflections occurred, leading to a reduction in the maximum shear strength and a significant negative slope in the post-peak applied load-vertical deflection response. The geometric configuration for both of these tests is illustrated in Figure 3.8. The test girders are simply-supported straight I-girders with one-sided intermediate transverse stiffeners. A concentrated load of $P = 2V$ is applied at the mid-span of the girders. The webs are subdivided into equal width panels on each side of their mid-span. Table 3.3 summarizes the girder dimensions while Table 3.4 gives the yield strengths of the webs, flanges and stiffeners for these tests. Rockey et al. (1981) do not specify any additional details of the material stress-strain response. For simplicity, the true stress-strain curve shown in Figure 3.3 is scaled to match the yield strengths of the different plates. Also, initial geometric imperfections are not reported by Rockey et al. (1981). Therefore, the initial imperfections described in Section 3.2.4 and Figure 3.5 are assumed for the finite element analyses of these test girders.

Rockey et al. (1981) conducted two tests on each of the above girders. For each girder, a shear failure occurred within the right-hand side panels in Figure 3.8 – the panels subdivided by stiffener SA – in the first test. These panels were then reinforced and a second test was conducted in which the panels subdivided by stiffener SB governed the maximum shear strength. The finite element analyses conducted in this study correspond to the second test of girder TGV7 (test TGV7-2) and the first test of girder TGV8 (test TGV8-1). In the analysis of test TGV7-2, geometric imperfections are specified only in stiffener SB and its panels. The initial geometry is modeled as perfectly

straight and perfectly flat in stiffener SA and its panels. The prior test to failure of stiffener SA and its panels and the subsequent reinforcing of these panels is not modeled.

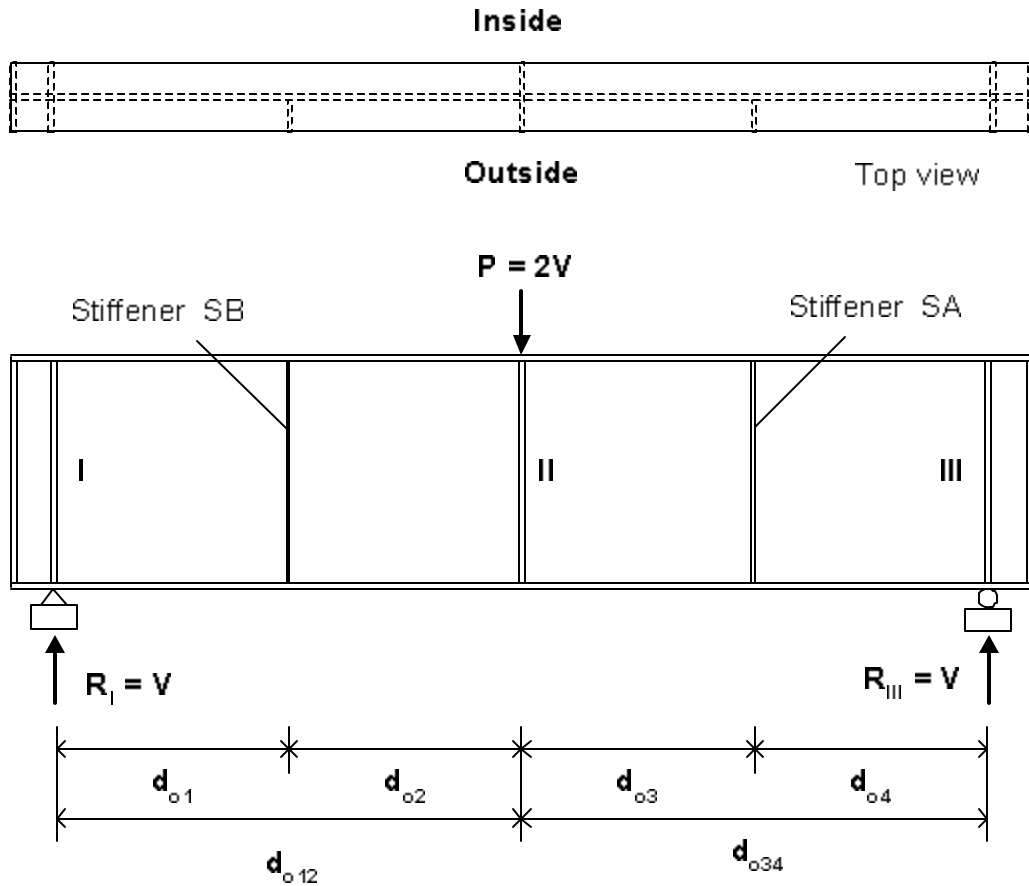


Figure 3.8. Geometric configuration of tests TGV7 and TGV8 (Rockey et al. 1981)
 $(d_{o1} = d_{o2} = d_{o12}/2, d_{o3} = d_{o4} = d_{o34}/2)$.

Table 3.3 Dimensions of the test girders TGV7 and TGV8 (Rockey et al. 1981)

Girder	Web				Flanges				Stiffener - SA		Stiffener - SB	
	D	t _w	d _{o12}	d _{o34}	b _{fc}	b _{ft}	t _{fc}	t _{ft}	b _s	t _s	b _s	t _s
	(mm)	(mm)	(mm)	(mm)	(mm)	(mm)	(mm)	(mm)	(mm)	(mm)	(mm)	(mm)
TGV7	599.0	1.98	1181	1191	200.6	200.7	10.10	10.08	12.4	5.75	25.21	5.10
TGV8	598.7	1.92	1191	1191	200.4	200.4	10.08	10.08	20.5	3.22	15.95	5.71

Table 3.4. Material properties for test girders TGV7 and TGV8 (Rockey et al. 1981)

Girder	Yield Stress			
	Web	Flanges	Stiffener - SA	Stiffener - SB
	(MPa)	(MPa)	(MPa)	(MPa)
TGV7	221.2	250.3	284.2	283.4
TGV8	218.3	201.4	247.6	212.4

Table 3.5 summarizes several key parameters pertinent to the design of the intermediate transverse stiffeners in girders TGV7 and TGV8. The web slenderness is nominally $D/t_w = 300$ and the panel aspect ratio is nominally $d_o/D = 1$ in all of the tests conducted by Rockey et al. (1981). In all, eleven girders (22 shear tests) were studied by these investigators. The transverse stiffeners in girders TGV7 and TGV8 are all rather stocky relative to the maximum limit of $b_s/t_s = 16$ allowed by AASHTO (2004). All of the stiffeners considered in these tests have a moment of inertia I_s larger than the AASHTO (2004) required value for development of the web shear buckling strength, I_{scr} , given by Equation (2.2). The ratio I_s/I_{scr} ranges from 1.49 in test TGV7-1 (girder TGV7 with stiffener SA) to 10.38 in test TGV7-2 (girder TGV7 with stiffener SB). However, all of the stiffeners violate the AASHTO (2004) transverse stiffener area requirement given by Equation (2.28). The ratio of the stiffener area to the required area, labeled as $A_s/A_{s,reqd}$ in Table 3.5, ranges from 0.26 for test TGV8-1 to 0.54 for test TGV7-2. Also,

the ratio of the stiffener moments of inertia to the corresponding values based on the final recommendations of this study are labeled as I_s/I_{sR} and are listed in the last column of the table. This ratio ranges from 0.06 for test TGV7-1 to 0.43 for test TGV7-2. The reader should note that for a given stiffener width-to-thickness ratio, the ratio of the actual to the required stiffener dimensions ($b_s/b_{s,reqd}$ or $t_s/t_{s,reqd}$) varies with the $1/4$ power of I_s .

Therefore, the stiffener with $I_s/I_{sR} = 0.43$ corresponds to $b_s/b_{s,reqd} = 0.81$, or in other words, the stiffener is under-sized by 19 percent.

Table 3.5. Key parameters pertinent to the design of the intermediate transverse stiffeners in girders TGV7 and TGV8

Girder	D/t _w	d _o /D	b _s /t _s	I _s (mm ⁴)	A _s (mm ²)	I _s /I _{scr} AASHTO	A _s /A _{s,reqd} AASHTO	I _s /I _{sR} ⁽¹⁾
TGV7-1	303	0.994	2.16	3654	71	1.49	0.30	0.06
TGV7-2	303	0.986	4.94	27238	129	10.38	0.54	0.43
TGV8-1	312	0.995	6.37	9247	66	4.16	0.26	0.16
TGV8-2	312	0.995	2.79	7723	91	3.48	0.30	0.13

⁽¹⁾ Based on the final recommendations of this study.

The load versus mid-span vertical displacement curves from the finite element analyses of tests TGV7-2 and TGV8-1 are compared with the corresponding curves presented by Rockey et al. (1981) for tests TGV7-2 and TGV8-1 in Figures 3.9 and 3.10. Unfortunately, the experimental load-deflection curve and other detailed results for test TGV8-1 are not provided by Rockey et al. (1981). Only the static and dynamic failure loads are provided along with a statement that the stiffeners deflected laterally and the post-peak load-vertical displacement curve exhibited significant unloading, i.e., a negative slope in TGV8-1. The experimental load-deflection curve in Figure 3.10 is for test TGV 8-2. The reported experimental static load levels corresponding to tests TGV7-1 and TGV8-1 are shown in the plots.

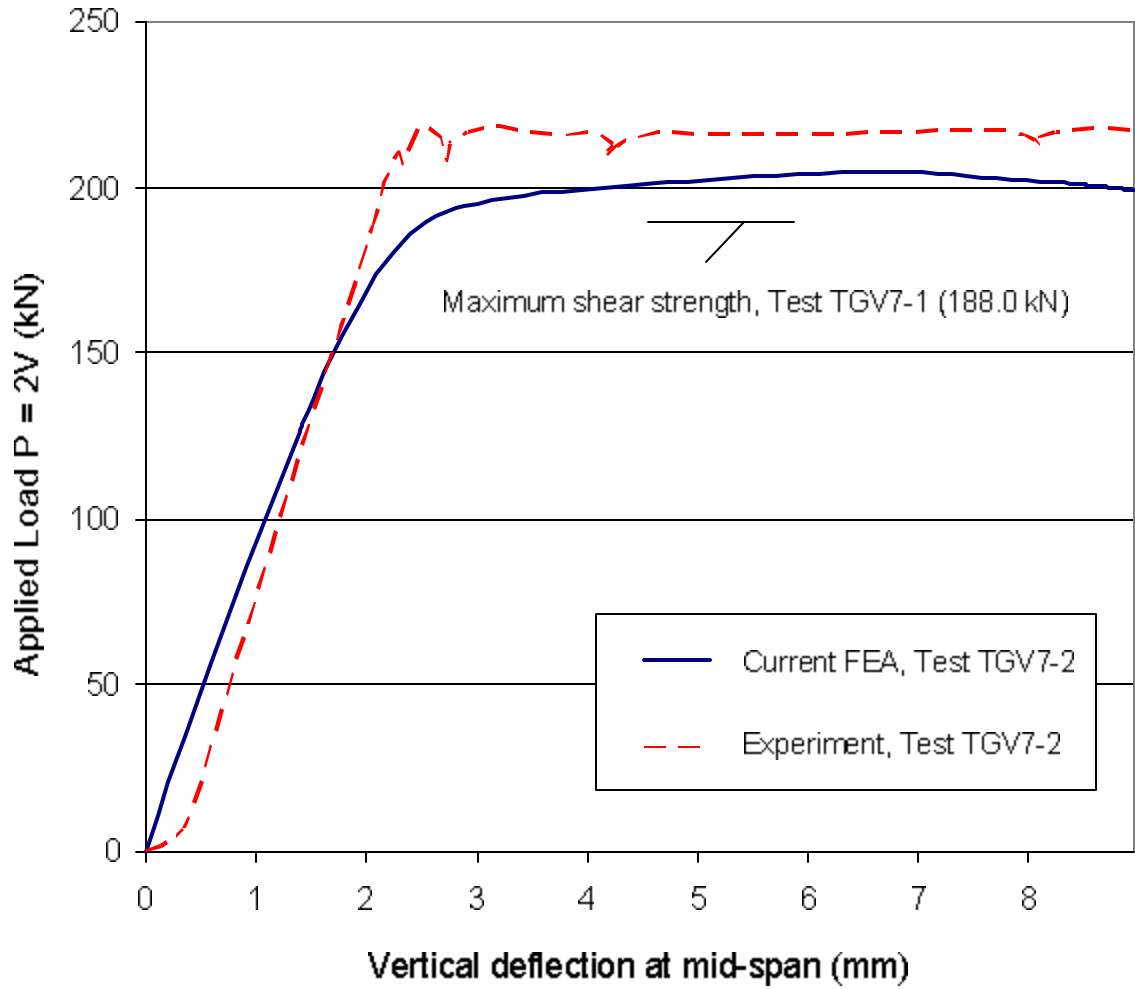


Figure 3.9 Load-deflection curves from finite element analysis of girder TGV7-2 and from experimental testing of girder TGV7-2 (Rockey et al. 1981).

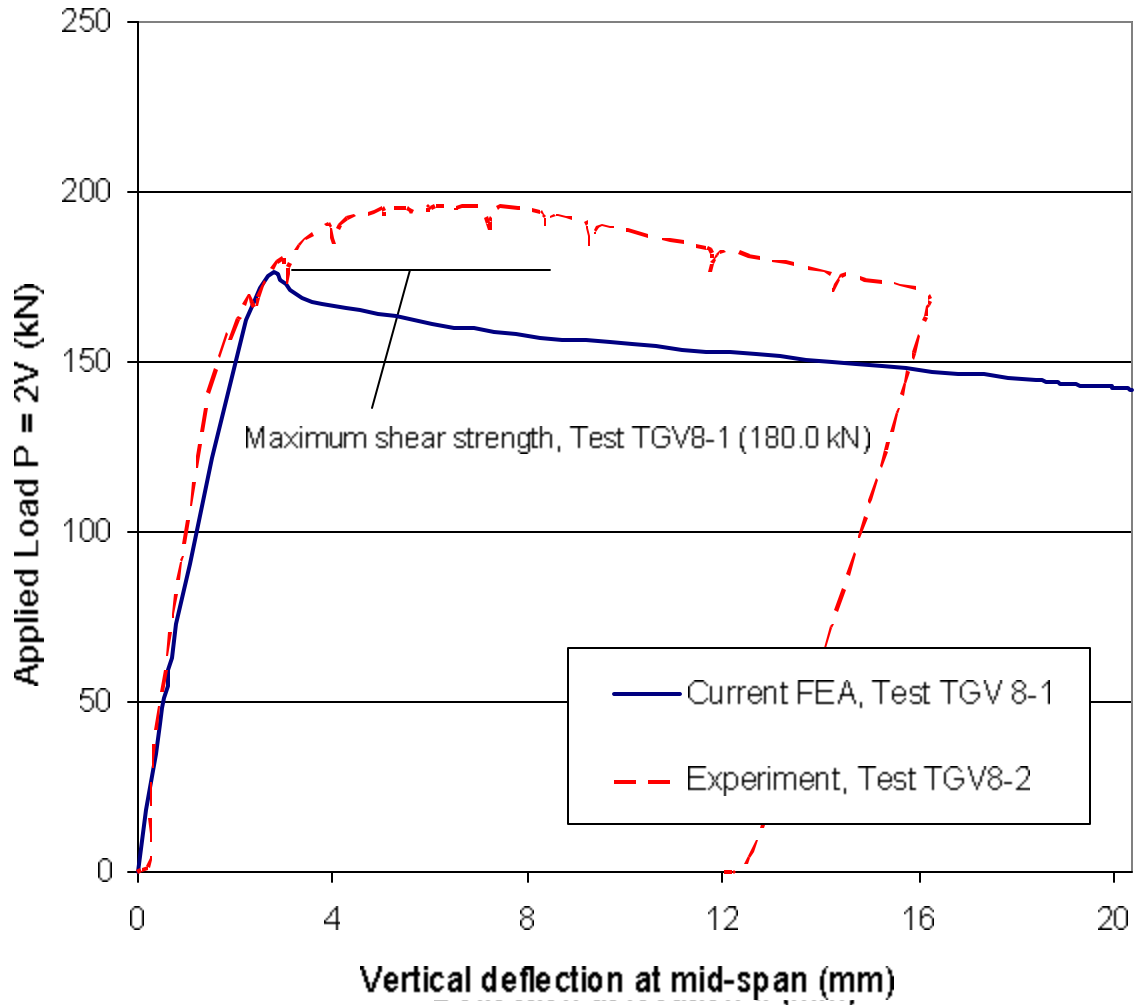
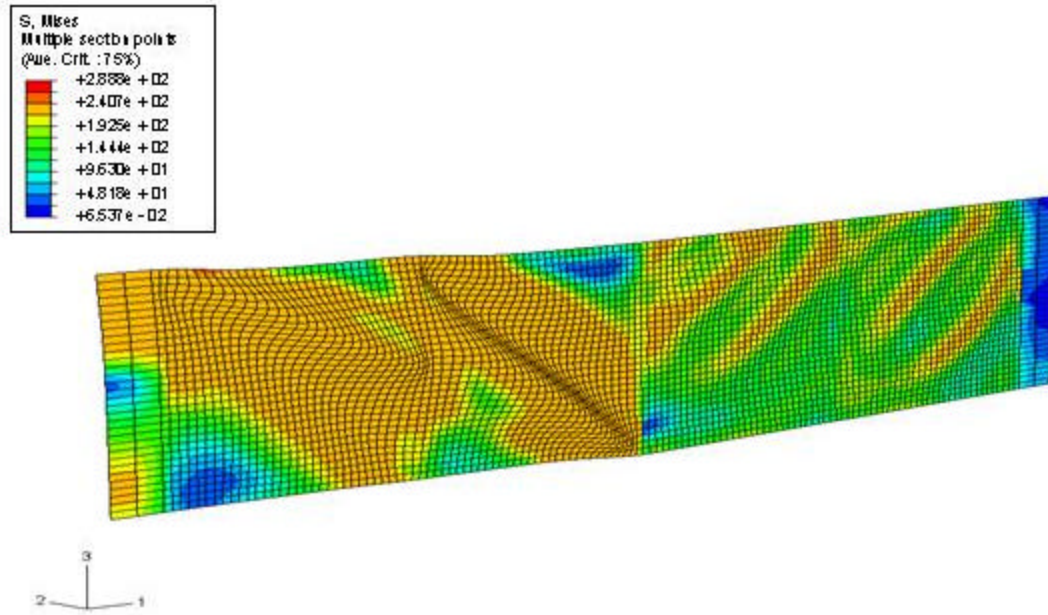


Figure 3.10. Load-deflection curves from finite element analysis of girder TGV8-1 and from experimental testing of girder TGV8-2 (Rockey et al. 1981).

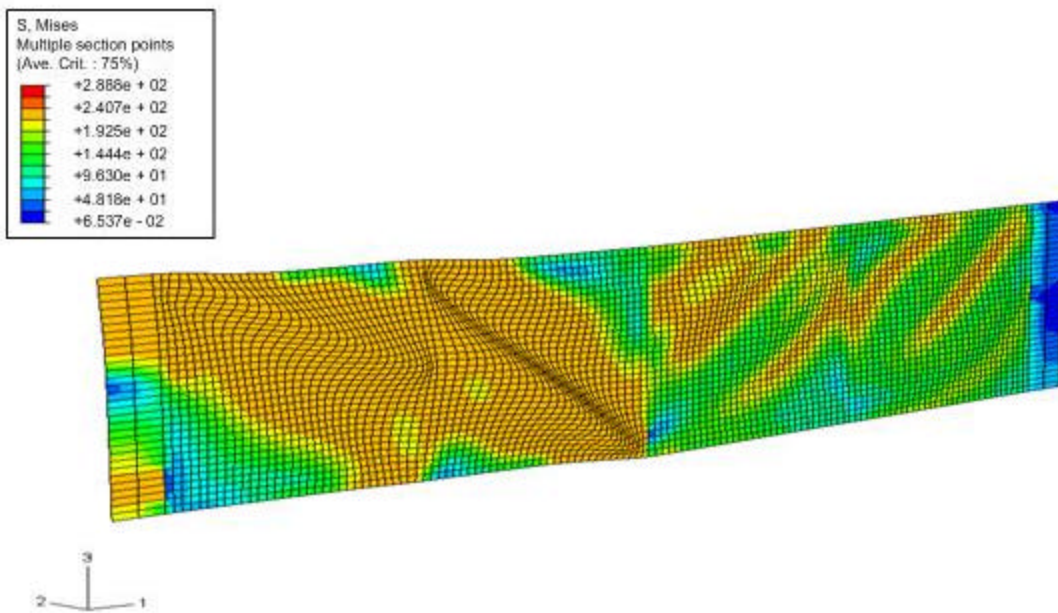
For girder TGV7-2, the limit load in the finite element analysis is 204.4 kN. This is 3.1 percent smaller than the static failure load of 211.0 kN reported by Rockey et al. for this test. Rockey et al. (1981) also report that the transverse stiffener remained effectively straight and the post-peak load-deflection curve was satisfactory in this test. The FEA solution also exhibits these characteristics. For girder TGV8-1, the FEA limit load is 176.1 kN versus 180.0 kN for the static failure load within the physical test, i.e., the predicted FEA limit load is 2.2 percent smaller than the physical test result. Rockey et al. (1981) report significant lateral deflections in the transverse stiffener and a post-peak load-deflection curve that is “falling away” in TVG8-1. The stiffener lateral deflection and the characteristics of the load-deflection curve are similar in the FEA model.

Rockey et al. (1981) obtain a static failure load as high as 225.0 kN in other tests with relatively large two-sided transverse stiffeners, even though the web yield strength was five percent smaller than in girder TGV7. Given that the initial geometric imperfections within the physical tests are not known, and as discussed in the previous section, the maximum shear strength can be somewhat sensitive to the geometric imperfection pattern for $D/t_w = 300$ and $d_o/D = 1$, the above finite element predictions are believed to be quite acceptable.

The von Mises stresses predicted on the inside and outside surfaces of the web at the predicted limit load are shown on the corresponding deformed geometry for test TGV7-2 in Figure 3.11. As discussed in Section 3.2.2.4, the inside direction is the direction in which the web panels are bowed due to the initial out-of-flatness. The stiffeners are attached to the outside surface of the web. The view of the geometry in Figure 3.11 is



(a) von Mises stress contours of the inside surface



(b) von Mises stress contours on the outside surface

Figure 3.11. von Mises stress contours on the deformed geometry at the limit load in test TGV7-2 (view from the outside direction, deformation scale factor = 5).

from the outside direction, i.e., the same direction as the view in Figure 3.8. The flanges and the transverse stiffeners are not shown in Figure 3.11. Only the deformed geometry of the web panels is shown. The software utilized in viewing the analysis results shows the beam finite element responses only on a line representation of the flange and stiffener components. The panels subdivided by stiffener SB are located toward the left-hand side in this figure. One can observe that the predominant failure occurs on the side corresponding to this stiffener.

The von Mises stress contours show a pattern of yielding in the web indicating that the tension field may not be fully developed within the individual web panels. The yield bands in the panels on the left side of the figure are oriented more along the diagonal of the two web panels than between the corners of the individual panels.

Figure 3.12 shows a contour of the web lateral deflections when the vertical deflection at mid-span is 8 mm, again with the view of the geometry taken from the outside direction. One can observe that the dominant waves within the web panels are oriented more along the diagonal of the two web panels. Also, one can observe from the deflection contours that stiffener SB is deflected by about 15 mm ($D/40$) at the maximum load limit whereas the web is deflected by 25 mm ($D/24$). The displacements of the web and the stiffeners due to the initial geometric imperfections are not included within these displacement contours. The web deformations are drawn to scale in Figure 3.12, i.e., the deformation scale factor is equal to 1.0. In Figure 3.11, the displacements are magnified five times. The stiffener lateral displacements can be discerned from the deformed geometry in Figure 3.11.

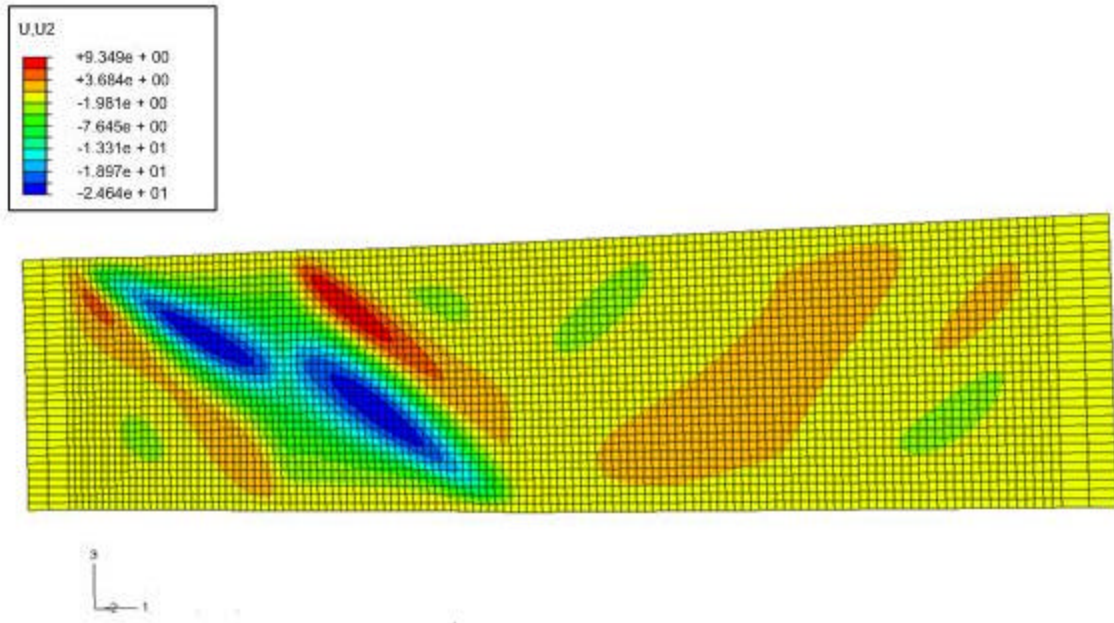
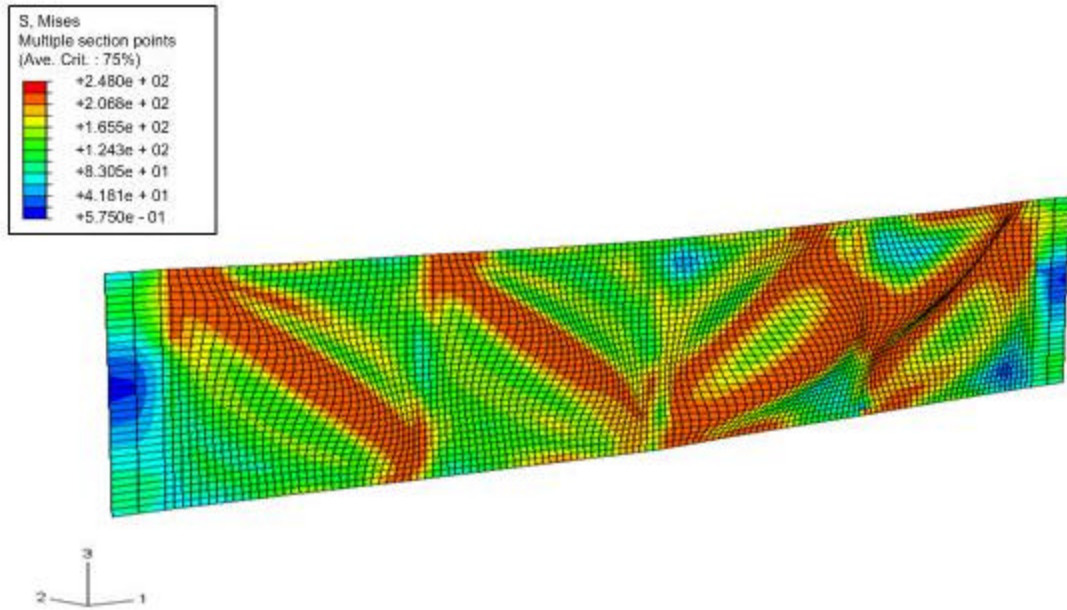


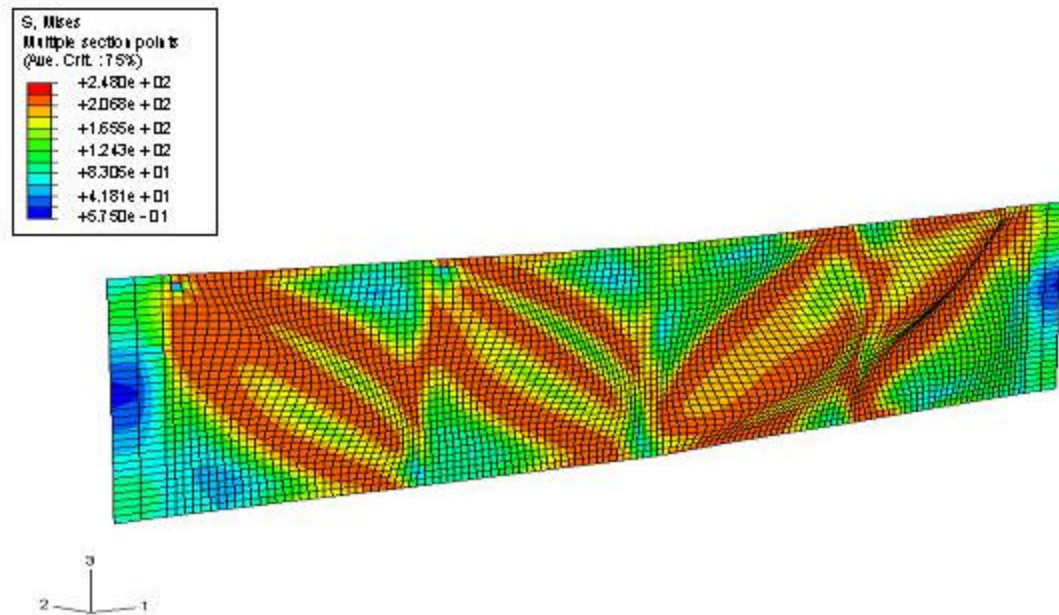
Figure 3.12 Lateral deflection contours on the deformed geometry when the vertical deflection at mid-span is 8 mm in test TGV7-2 (view from the outside direction, deformation scale factor = 1.0).

Rockey et al. (1981) provide a photograph of stiffener SB and its panels after completion of test TGV7-2. The orientation of the residual buckles within these web panels is approximately the same as the direction of the buckles shown in Figures 3.11 and 3.12. However, there is essentially no residual lateral deformation of the transverse stiffener, i.e., the stiffener appears to have responded elastically in this test.

Figures 3.13 and 3.14 show the results for test TGV8-1. In these figures, the view is again from the outside of the web, and stiffener SA and the failed web panels are located on the right-hand side. The vertical displacements are smaller at the limit load in this test, since this girder unloads abruptly with little inelastic deformation at its predicted maximum shear strength (see Figure 3.10). Therefore, the deformations are scaled 10 times in Figure 3.13. There is only one predominant yield band within the failed panels corresponding to stiffener SA on the right-hand side in this figure. However, one can



(a) von Mises stress contours on the inside surface



(b) von Mises stress contours on the outside surface

Figure 3.13 von Mises stress contours on the deformed geometry at the limit load in test TGV8-1 (view from the outside direction, deformation scale factor = 10).

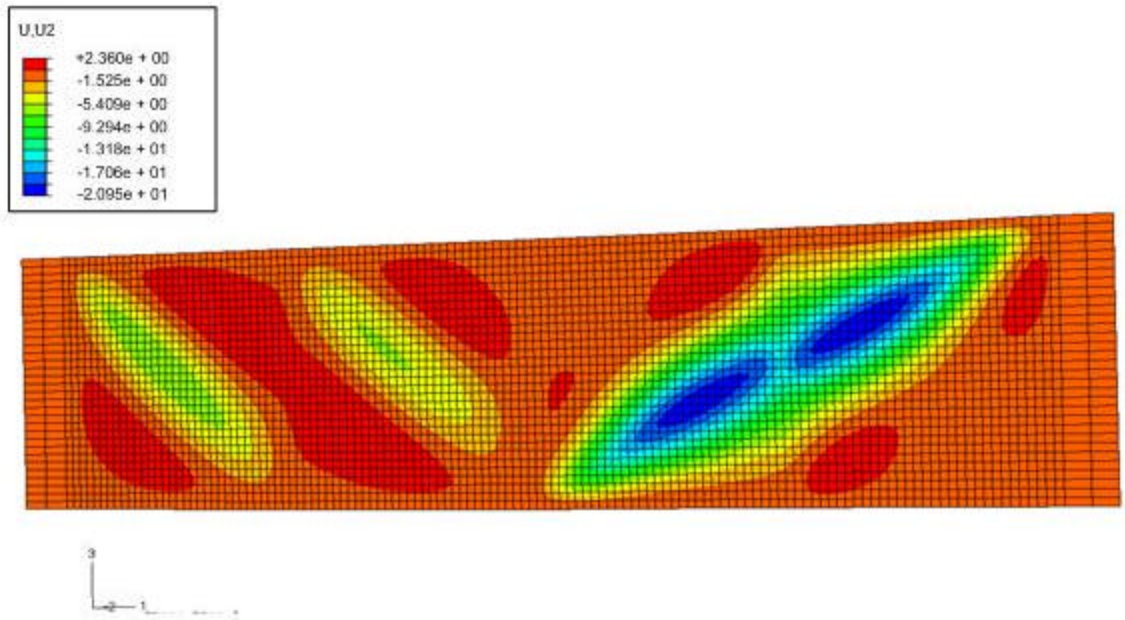


Figure 3.14 Lateral deflection contours on the deformed geometry when the vertical deflection at mid-span is 4 mm in test TGV8-1 (view from the outside direction, deformation scale factor = 1.0).

observe that significant tension field action is starting to develop in the panels corresponding to stiffener SB on the left-hand side. Stiffener SB appears to be subdividing the panels on the left-hand side reasonably well at the maximum load level.

Figure 3.14 shows that the transverse stiffener SA is significantly deformed relative to its corresponding panel deflections. The view in this figure is also from the outside and therefore stiffener SA and its panels are on the right-hand side of the geometry. The stiffener in this plot again has a maximum lateral displacement of about 15 mm ($D/40$), but the web panels in this case have a maximum lateral displacement of only 21 mm ($D/30$). Rockey et al. (1981) do not show photos of girder TGV8 after the completion of test TGV8-1.

CHAPTER IV

PARAMETRIC STUDY RESULTS

4.1. Overview

This chapter presents the results of the FEA parametric studies conducted in this research, provides a synthesis of these solutions along with key results from prior research studies, and concludes with recommendations for the design of intermediate transverse stiffeners in straight and curved bridge I-girders. First, Section 4.2 summarizes the results from the current parametric study in terms of web maximum shear strengths versus normalized stiffener bending rigidities. Sections 4.3 through 4.5 then focus on important attributes of the underlying strength behavior. Section 4.3 follows with a detailed discussion of stiffener axial and bending strains. Section 4.4 discusses the sensitivity of the shear strengths to the geometric imperfection patterns specified in the finite element analysis. Lastly, Section 4.5 gives examples of the web strength behavior both for I-girders in which the intermediate transverse stiffeners do not adequately subdivide the web panels as well as for I-girders in which the stiffeners adequately perform their intended function and are a “near optimum” size.

Section 4.6 presents a synthesis of the results from this work as well as key results from prior research. This section first summarizes a suggested minor change to the AASHTO (2004) stiffener moment of inertia requirement to develop the web shear buckling strengths, discussed previously in Chapter II: the use of $b = \min(d_o, D)$ instead of d_o in Equation (2.2). This change has no effect on the result obtained relative to AASHTO (2004) for $d_o/D \leq 1$, but provides stiffener sizes for $d_o/D > 1$ that are more

consistent with the the physical behavior. That is, this minor change removes some of the conservatism of the AASHTO (2004) provisions for $d_o/D > 1$.

Section 4.6 then presents the stiffener size requirements in a normalized fashion that, to the knowledge of the author, has not been considered in prior studies. For a given web panel aspect ratio d_o/D and yield strength F_{yw} , the required stiffener sizes for different D/t_w plot in a particularly simple way when they are normalized by the stiffener size required for a web proportioned at the largest D/t_w such that $C = 1$. Interestingly, the stiffener size required for a web having this D/t_w ($= 1.12\sqrt{Ek/F_{yw}}$) works well for all other web slenderness values.

Sections 4.7 through 4.9 address several additional considerations necessary for the development of comprehensive design provisions for transverse stiffeners in bridge I-girders. These sections address the application of the concepts developed in this study to general stiffener cross-section geometries, the influence of stiffener yield strengths that are smaller than the yield strength of the web plate ($F_{ys} < F_{yw}$), and reduction of the required stiffener sizes when the applied shear force is smaller than the web shear strength, i.e., $V_u < V_n$.

Section 4.10 concludes the chapter by summarizing the final recommendations from this work.

4.2. I-Girder Shear Strength versus Stiffener Rigidity

Figures 4.1 through 4.7 show the effect of varying the stiffener bending rigidity on the maximum shear strengths for the different panel aspect ratios d_o/D and web slenderness values D/t_w considered in the author's studies. The abscissa in each of these plots is the ratio of the stiffener moment of inertia to the moment of inertia required by

AASHTO (2004) for development of the shear buckling load, I_s/I_{scr} . The ordinate of the plots is the ratio of the FEA shear limit load to the nominal web shear capacity given by the AASHTO (2004) shear strength equations including tension field action,

$$V_{max}/V_{n(AASHTO)}.$$

In each of these figures, the normalized moment of inertia that satisfies the AASHTO (2004) area requirement for single-plate transverse stiffeners, denoted by I_{sA1}/I_{scr} , is used as the maximum value for the abscissa (with the exception of one case where this moment of inertia requirement is zero). A width-to-thickness ratio for the transverse stiffeners of $b_s/t_s = 10$ is used throughout these solutions. The influence of b_s/t_s is addressed in Section 4.7. The normalized rigidity requirement I_{sA1}/I_{scr} is labeled in each of the plots. Also, the normalized moment of inertia corresponding to satisfaction of the AASHTO (2004) area requirement for two-sided transverse stiffeners (a pair of plates), denoted by I_{sA2}/I_{scr} , is shown in all of the plots. In all cases, I_{sA2}/I_{scr} is either zero or quite small relative to I_{sA1}/I_{scr} . Finally, the normalized moment of inertia requirement based on the final recommendations presented at the end of this chapter, I_{sR}/I_{scr} , is marked in each of the figures.

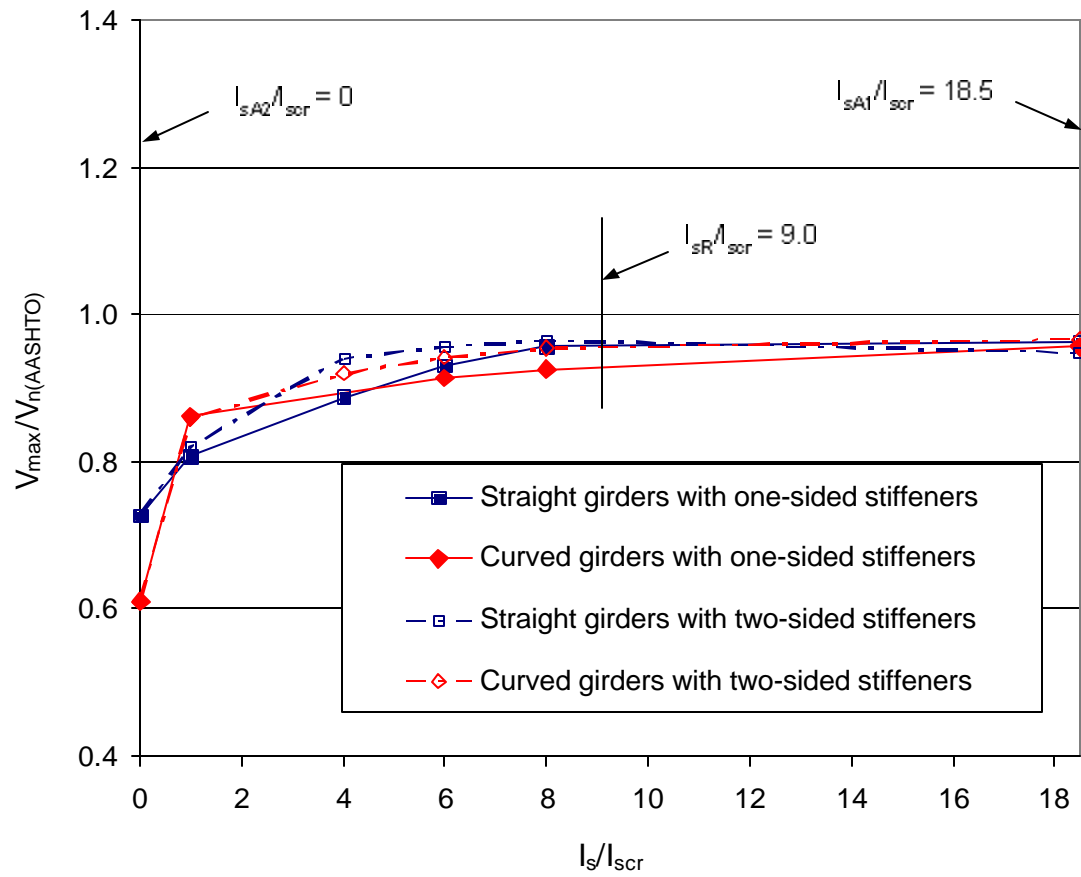


Figure 4.1. Strength versus stiffener rigidity for $d_o/D = 1$ and $D/t_w = 150$.

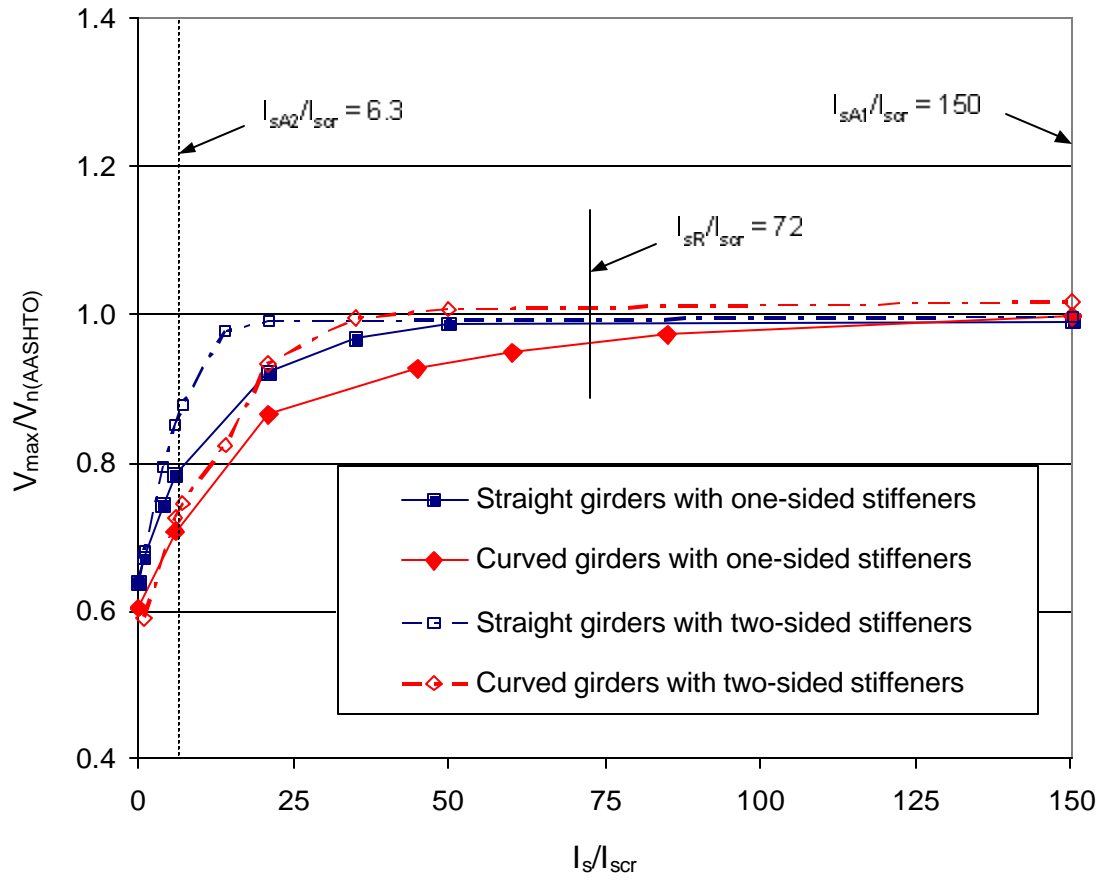


Figure 4.2. Strength versus stiffener rigidity for $d_o/D = 1$ and $D/t_w = 300$.

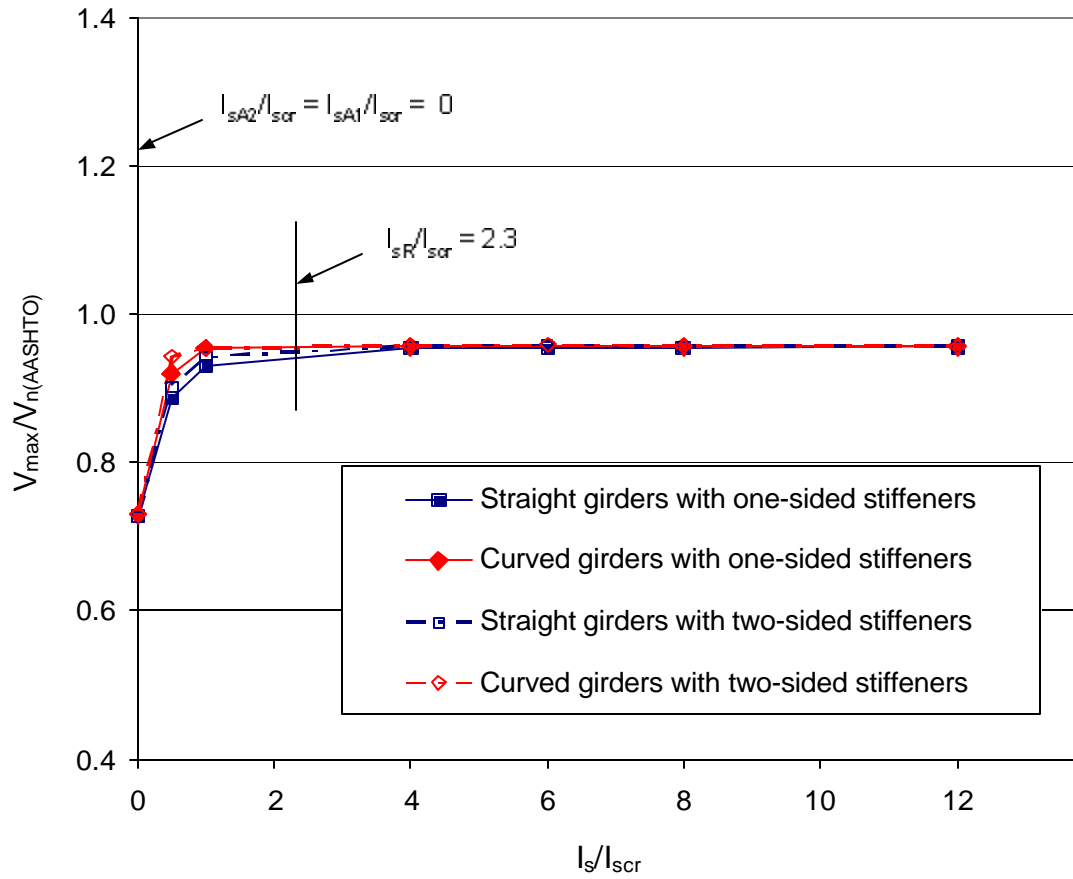


Figure 4.3. Strength versus stiffener rigidity for $d_o/D = 0.5$ and $D/t_w = 150$.

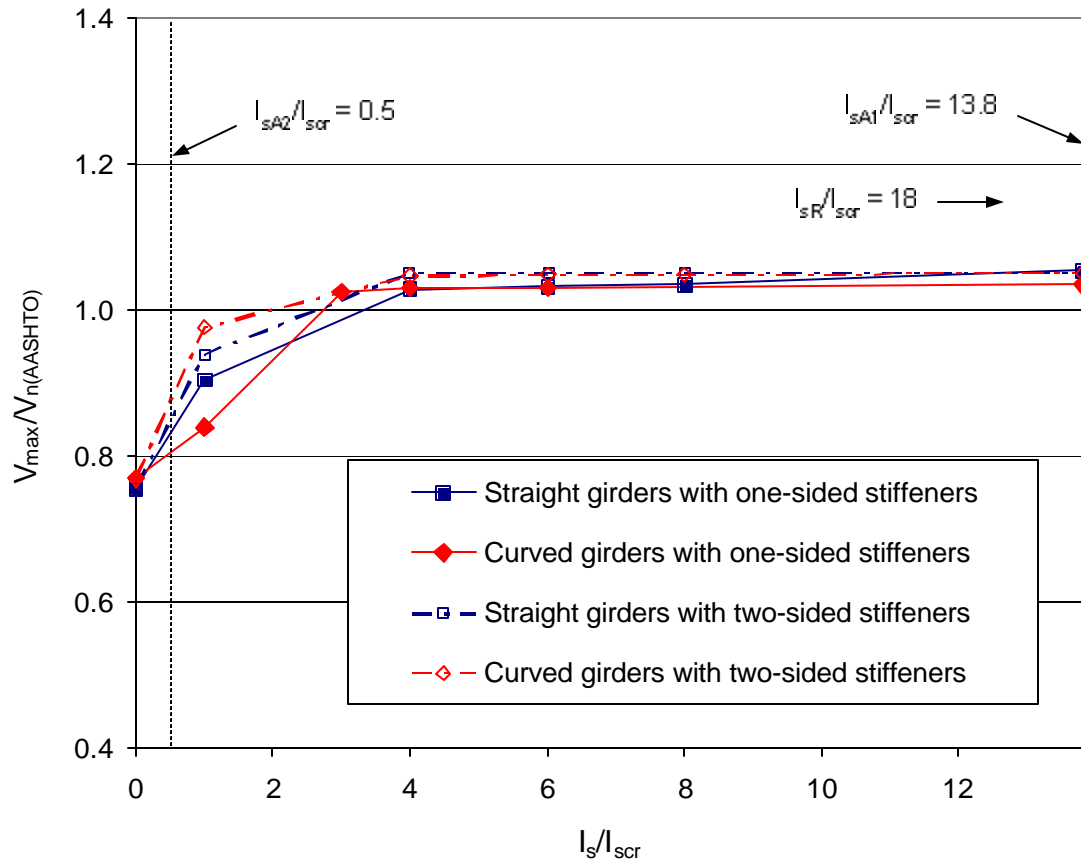


Figure 4.4. Strength versus stiffener rigidity for $d_o/D = 0.5$ and $D/t_w = 300$.

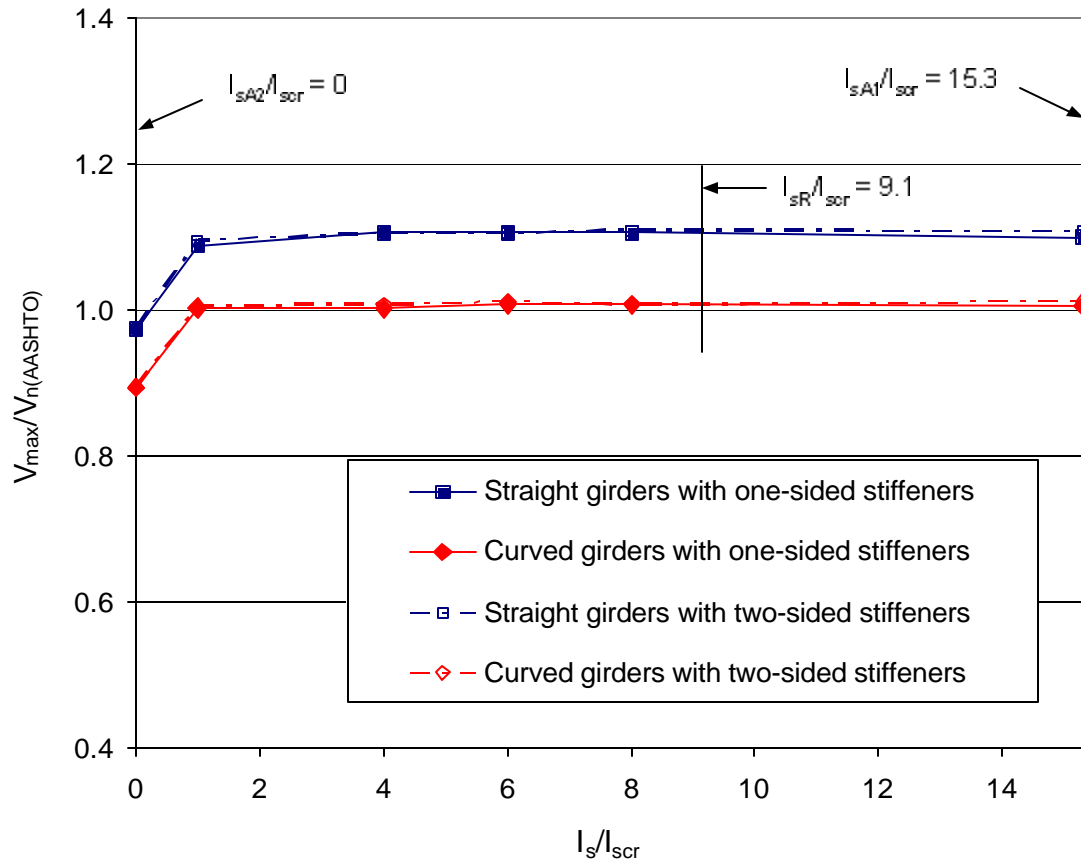


Figure 4.5. Strength versus stiffener rigidity for $d_o/D = 2$ and $D/t_w = 150$.

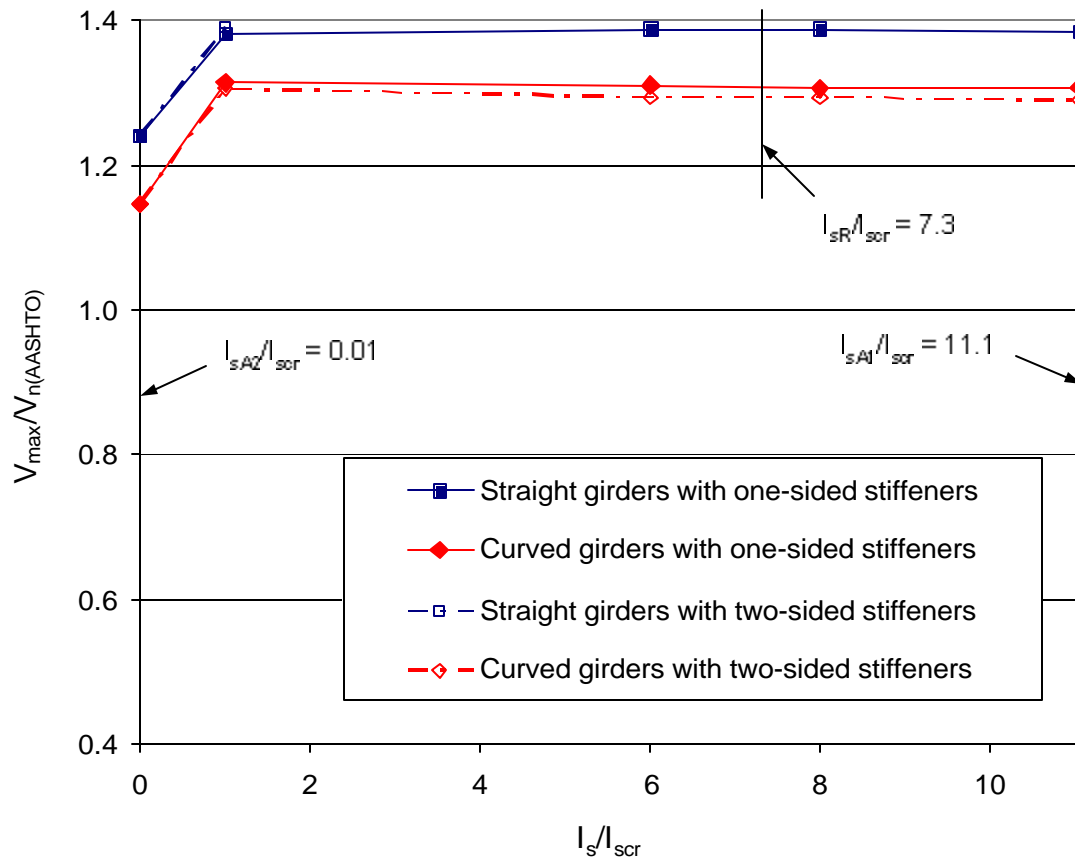


Figure 4.6. Strength versus stiffener rigidity for $d_o/D = 3$ and $D/t_w = 150$.

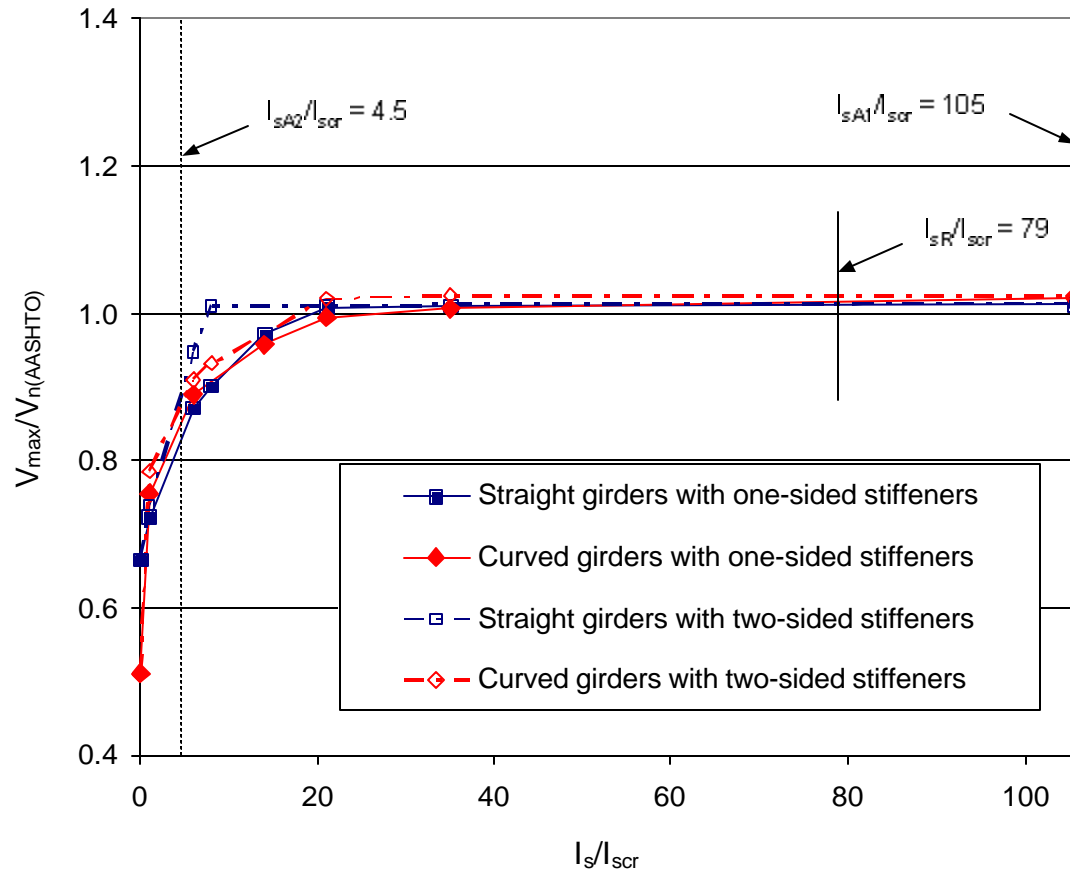


Figure 4.7. Strength versus stiffener rigidity for $d_o/D = 1.5$ and $D/t_w = 300$.

Four curves are shown for the shear strength versus the stiffener bending rigidity in each of Figures 4.1 through 4.7. These curves correspond to straight I-girders with one- and two-sided plate stiffeners, and curved I-girders with both one- and two-sided stiffeners. These curves may be compared to assess the influence of stiffener type and/or horizontal curvature on the variation of $V_{\max}/V_{n(\text{AASHTO})}$ as a function of I_s/I_{scr} .

In general, V_{\max} first increases rather abruptly as I_s is increased from zero. However, for I_s larger than a particular value (e.g., larger than approximately $I_s = 8I_{\text{scr}}$ in Figure 4.1), further increases in the stiffener bending rigidity have a negligible effect on the maximum shear strength. Horne and Grayson (1983) refer to the stiffener moment of inertia in the vicinity of this transition or bend in the V_{\max} versus I_s curve, as the maximum shear strength approaches a plateau, as the “knuckle value.” Horne and Grayson (1983), Rahal and Harding (1990a and b), Stanway et al. (1996) and Xie (2000) all consider the bending rigidity within this region as the “optimum.” All of these prior research studies show that stiffeners with I_s values to the left of the knuckle value tend to exhibit relatively large bending strains and lateral deflections prior to the web reaching its maximum shear strength. This characteristic strength behavior is observed also in the current study.

The following key observations can be gleaned from Figures 4.1 through 4.7:

- For a given d_o/D and D/t_w combination, the $V_{\max} - I_s$ curves are all sufficiently similar such that it appears that one set of stiffener design provisions could be used for one- or two-sided stiffeners in straight or curved I-girders without any major penalty.

That is, it appears that the influence of the stiffener eccentricity and/or the member horizontal curvature can be neglected in the consideration of stiffener design rules.

- The largest differences between the four curves in the plots, and also the largest demands on the transverse stiffeners in terms of the I_s/I_{scr} needed to reach the “plateau” of the $V_{max} - I_s$ curves, occur for the girders with $d_o/D = 1$ and $D/t_w = 300$ (Figure 4.2).
- In all of Figures 4.1 to 4.7, the shear strengths along the $V_{max} - I_s$ curves for the girders with two-sided stiffeners are either practically the same as or slightly larger than the shear strengths along the curves for the girders with one-sided stiffeners. For the girders with $d_o/D = 1$ and $D/t_w = 300$ (Figure 4.2), the straight girders with two-sided stiffeners show shear strengths as much as eight percent larger than the straight members with one-sided stiffeners. Also, for the curved girders in Figure 4.2, the strengths using two-sided stiffeners are as much as nine percent larger than those for one-sided stiffeners. However, all of the $V_{max} - I_s$ curves in Figure 4.2 reach approximately the same “plateau strengths” with increasing I_s .
- In the plots for $d_o/D = 1$, the strength gain with increasing I_s is noticeably more gradual and the value of I_s/I_{scr} needed to reach the strength plateau is noticeably larger for the curved girders (see Figures 4.1 and 4.2). The strength gain in the $V_{max} - I_s$ curve for curved girders with one-sided stiffeners is particularly more gradual. However, as noted above, the variations between the different curves are small enough such that it would appear that they can be ignored. Based on the consideration of imperfection sensitivities for the worst-case girders with $d_o/D = 1$ and $D/t_w = 300$, discussed subsequently in Section 4.4, it appears that similar differences in the $V_{max} - I_s$ curves can be created by changing the geometric imperfection patterns.

- In general, the value of I_s/I_{scr} necessary for the girders to reach their plateau strengths is affected the most by the parameters d_o/D and D/t_w . That is, the knuckle values for I_s/I_{scr} vary most significantly between each of Figures 4.1 through 4.7. For the I-girders with $D/t_w = 150$ and $d_o/D = 2$ or 3 (Figures 4.5 and 4.6), the knuckle value of I_s/I_{scr} is approximately at $I_s/I_{scr} = 1$, whereas for $d_o/D = 1$ and $D/t_w = 300$ (Figure 4.2), the curved girders with one-sided stiffeners do not reach the plateau strength until around $I_s/I_{scr} \cong 85$. Therefore, it appears that the recommendation of $I_s/I_{scr} = 6$ for development of the full shear postbuckling strength by Lee et al. (2003) is in general ill founded. This recommendation is close to the value needed to reach the plateau on the V_{max} - I_s curves in all cases for $D/t_w = 150$; however, it is too small for larger D/t_w values.
- In all of the cases studied except for $d_o/D = 0.5$ and $D/t_w = 150$ (Figure 4.3), single-sided transverse stiffeners with $b_s/t_s = 10$, sized according to the AASHTO (2004) area requirement, have more than enough bending rigidity for the I-girders to reach the plateau of the V_{max} - I_s curves. In other words, I_{sA1}/I_{scr} is larger than the knuckle value for the normalized bending rigidity. For large d_o/D , I_{sA1}/I_{scr} is an order of magnitude larger than the knuckle value (see Figures 4.5 through 4.7).
- For the girders with $d_o/D = 0.5$ and $D/t_w = 150$, I_{sA1} is equal to zero. That is, the AASHTO (2004) equation for A_s (Equation 2.28) gives a negative value for the required stiffener area. In this case the appropriate interpretation described in AASHTO (2004) is that the web area assumed to act with the transverses stiffener is adequate by itself to transmit the vertical strut forces associated with Basler's (1961) tension field theory. Negative values for A_s are not intended to mean that no

stiffener is required. Rather, AASHTO (2004) implicitly asserts that a transverse stiffener with $I_s = I_{scr}$ is sufficient to hold the web such that the shear postbuckling strength can be developed in these cases. One can observe that this assertion is essentially true in Figure 4.3, i.e., I_{scr} is effectively the knuckle value for the stiffener bending rigidity in this plot. Therefore, the AASHTO (2004) provisions generally result in adequate to conservative transverse stiffener sizes in all of the specific cases studied in this research¹.

- In all cases (Figures 4.1 through 4.7), the AASHTO (2004) provisions produce under-sized two-sided stiffeners. As noted above, I_{sA2} is zero or quite small relative to I_{sA1} in all of the figures. Furthermore, in general, $I_s = I_{scr}$ is far to the left of the corresponding knuckle value for I_s . Therefore, for two-sided stiffeners, it is not sufficient in general to default to the rigidity requirement for development of only the shear buckling load (Equation (2.1)) when the area equation (Equation (2.28)) does not control. In Figure 4.2, the area requirement governs the stiffener size, but I_{sA2}/I_{cr} is only 6.3 while the largest knuckle value of I_s/I_{scr} for straight and curved girders with two-sided stiffeners is approximately 50 (eight times larger). The shear strength V_{max} is reduced by as much as 30 percent relative to the corresponding plateau value at $I_{sA2}/I_{scr} = 6.3$.
- For the girders with $d_o/D = 2$ and $d_o/D = 3$ ($D/t_w = 150$) (see Figures 4.5 and 4.6), the plateau shear strengths are noticeably smaller for the curved girders. However, these maximum shear strengths exceed the AASHTO (2004) nominal shear capacities, i.e., $V_{max}/V_{n(AASHTO)}$ is greater than one. For the widest stiffener spacing, $V_{max}/V_{n(AASHTO)}$

¹ Section 4.6.2.2 shows FEA solutions from prior research which indicate that for some I-girders with one-sided stiffeners and $D/t_w < 150$, the knuckle value for I_s is greater than the I_s that satisfies the AASHTO (2004) provisions.

> 1 even for $I_s = 0$. These results are consistent with the observations by White et al. (2001), Zureick et al. (2002), Jung and White (2003) and White and Barker (2004).

Table 4.1 summarizes the approximate maximum knuckle values in I_s/I_{scr} for each of the cases in Figures 4.1 through 4.7. These values are utilized in Section 4.6 as the required stiffener sizes from the FEA studies of this research. The final recommended values, I_{sR}/I_{scr} , are generally somewhat larger than these values, with the exception of $d_o/D = 1$ and $D/t_w = 300$, where I_{sR}/I_{scr} is slightly smaller than the approximate maximum knuckle value in Figure 4.2. In this case, the knuckle value of $I_s/I_{scr} = 85$ is based on the results for the curved girders with one-sided stiffeners, where the strength gain with increasing stiffener bending rigidity is very gradual. One can observe that for the other cases with $d_o/D = 1$ and $D/t_w = 300$ in Figure 4.2, the maximum knuckle value is less than or equal to about $I_s/I_{scr} = 50$, which is smaller than the final recommended I_{sR}/I_{scr} .

Table 4.1. Summary of the approximate maximum knuckle values for I_s/I_{scr} .

D/t _w	150				300		
d _o /D	0.5	1	2	3	0.5	1	1.5
I _s /I _{scr}	1	8	1	1	4	85	21

4.3. Stiffener Strains

To gain a better understanding of the behavior underlying the strength versus stiffener bending rigidity curves presented in Figures 4.1 to 4.7, it is helpful to consider the strains due to the axial loads and/or bending moments induced within the stiffeners. Figure 4.8a and b show the variation of the normal strains across the width of the critical stiffener at the maximum FEA shear capacity for the girders with $d_o/D = 1$, $D/t_w = 150$ and $I_s/I_{scr} = 8$. This I_s/I_{scr} is the approximate maximum knuckle value for the curves in Figure 4.1. The

thickness of the web t_w is neglected in these plots such that the total width of the two-sided stiffeners is taken as $2b_s$. The web is located at $x/b_s = 0$. The stiffener strains in Figures 4.8 are normalized by the yield strain ($e_y = F_{ys}/E$, where $F_{ys} = 485$ MPa (70 ksi) and $E = 200$ GPa (29000 ksi)).

Plots are shown in Figures 4.8a and b corresponding to each of the curves in Figure 4.1. Also, a fifth curve is shown that illustrates the stiffener strains if a one-sided stiffener is located on the outside rather than on the inside surface of the web in a curved I-girder. As discussed in Section 3.2.4.4, a one-sided stiffener on the inside generally is more critical with respect to the maximum strength of the curved girders. However, a one-sided stiffener on the outside is found to be more critical with respect to the straight I-girder maximum strengths. All the results for the curved girders with one-sided stiffeners in Figures 4.1 through 4.7 are for one-sided stiffeners on the inside, whereas all the results for the straight girders with one-sided stiffeners are for one-sided stiffeners on the outside.

Figure 4.8a shows the strains at the mid-height of the critical stiffener whereas Figure 4.8b shows the strains at the stiffener end having the largest total strain value of the two ends. These normal strains are taken at the mid-thickness of the transverse stiffeners, to avoid the consideration of additional strains due to the biaxial bending of the stiffeners associated with their three-dimensional physical behavior. The following attributes can be observed from Figures 4.8:

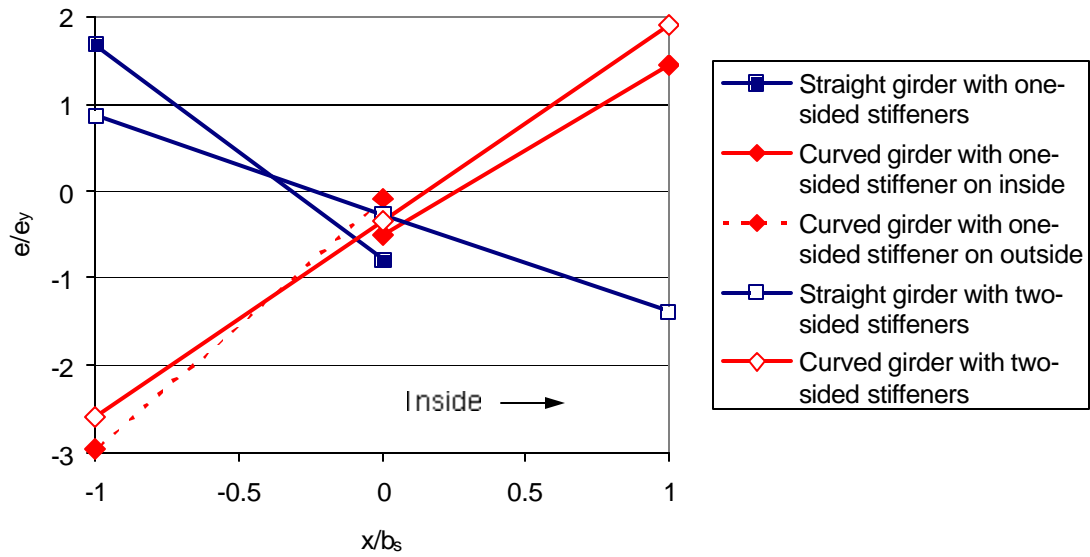


Figure 4.8a. Variation of stiffener mid-height strains at maximum shear strength for $d_o/D = 1.0$, $D/t_w = 150$ and $I_s/I_{scr} = 8$.

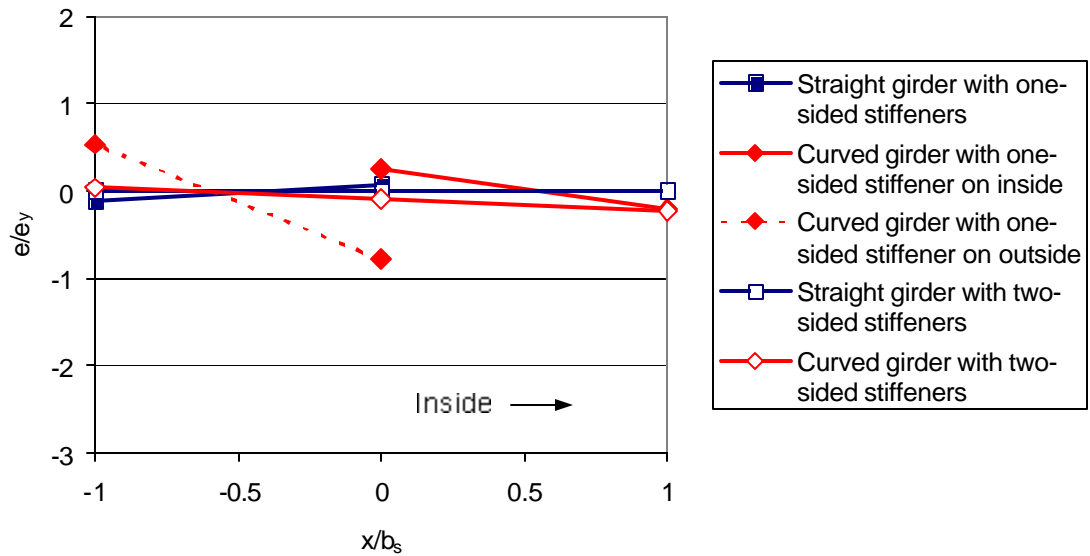


Figure 4.8b. Variation of stiffener end strains at maximum shear strength for $d_o/D = 1.0$, $D/t_w = 150$ and $I_s/I_{scr} = 8$.

- In general, the critical stiffener is partially yielded at its mid-height when the I-girders reach their maximum shear strengths.
- The stiffener actions at the mid-height are dominated by bending in each of the five cases shown in these figures. This confirms the observations by multiple prior independent research studies (Horne and Grayson 1983; Rahal and Harding 1990a and b, 1991; Stanway et al. 1993 and 1996; Xie 2000; Lee et al. 2002 and 2003) that the most important web panel influence on the transverse stiffeners is lateral loading, not axial loading. There is some compressive axial strain at the web-stiffener juncture in all cases. However, this axial strain is relatively small compared to the strain gradient across the width of the stiffener.
- The axial and bending strains at the stiffener ends are generally much smaller than at the mid-height. The axial strain at the web-stiffener juncture is tensile at the stiffener ends in some cases. Also, the bending strains at the stiffener ends (Figure 4.8b) are always opposite to the bending strains at the stiffener mid-height (Figure 4.8a) in this example, indicating the presence of some restraint to the lateral bending of the stiffeners from the torsional rigidity of the flanges. This is not always the case in general however. In some situations (not shown in Figures 4.8), the bending strains at one or more of the stiffener ends and at the mid-height are in the same direction. This behavior, as well as the fact that the stiffener strains are tensile (but small) at the web-stiffener juncture in Figure 4.8b and in some other cases not shown, are due to complex interactions between the stiffeners and the general three-dimensional girder actions. In general, it is difficult to synthesize these complex interactions down to simple engineering design descriptions.

- The curved I-girder stiffeners are bent predominantly toward the inside direction whereas the straight I-girder stiffeners are bent predominantly toward the outside. The precise reasons for this behavior are again difficult to synthesize. Obviously, if the horizontal curvature is varied, there must be some value of the curvature where the curved girder stiffeners would be loaded in the same direction as those in the straight girders.
- The largest mid-height strains occur for the curved girder with two-sided stiffeners and for the curved girder with one-sided stiffeners on the outside. However, the magnitude of the gradient in the strain across the stiffener width in the case of the straight girder with a one-sided stiffener is essentially the same as that for the curved girder cases. The mid-height strain pattern for all three of the curved I-girder cases implies that the pattern and magnitude of the loading from the web must be similar regardless of whether the stiffener is two-sided, one-sided and on the outside, or one-sided and on the inside. However, the bending restraint at the ends of the stiffener for the one-sided curved case with the stiffeners on the outside is larger (see Figure 4.8b). Also, the strain variation across the stiffener width is significantly different for the one- and two-sided stiffeners within the straight I-girders. In general, the detailed stiffener behavior is complex. The detailed differences in the strain patterns for the different cases are not easily explained.

Figures 4.9a and b show similar results for the I-girders with $d_o/D = 1$ and $D/t_w = 300$ (previously considered in Figure 4.2). However, in these figures, the strain curves do not necessarily correspond to the same I_s/I_{scr} values. This is because the knuckle values for I_s/I_{scr} are noticeably different for the different I-girders in Figure 4.2. The general

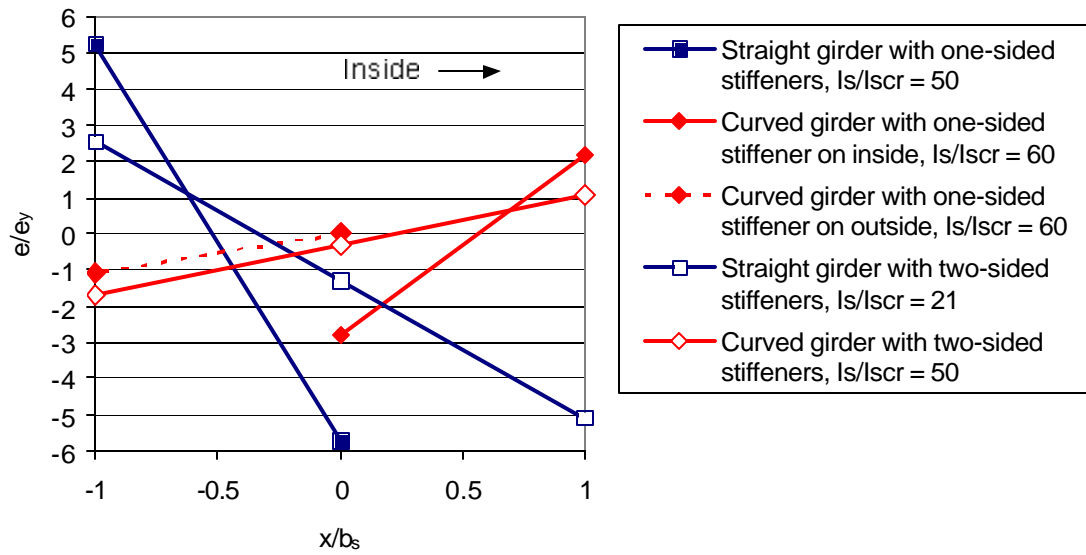


Figure 4.9a. Variation of stiffener mid-height strains at maximum shear strength for $d_o/D = 1.0$ and $D/t_w = 300$.

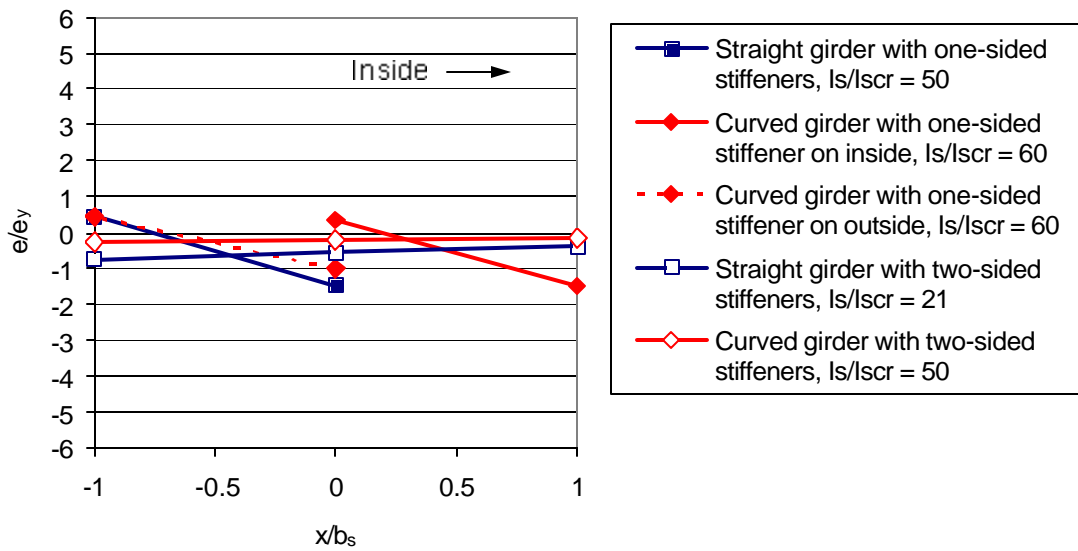


Figure 4.9b. Variation of stiffener end strains at maximum shear strength for $d_o/D = 1.0$ and $D/t_w = 300$ (at stiffener end having the largest strain).

comments on Figures 4.8 also apply to the plots in Figures 4.9. However, the strain gradient across the stiffener width in the straight girder with one-sided stiffeners is substantially larger than that associated with the other cases. This is in spite of the fact that the knuckle value for the straight one-sided case is approximately $I_s/I_{scr} = 50$, whereas the corresponding value for the straight two-sided case is approximately $I_s/I_{scr} = 21$.

Figures 4.10 through 4.13 provide additional insight into the stiffener responses by illustrating the variation of the mid-height stiffener strains at the edges and middle of the stiffeners as a function of the applied shear load for several cases from Figures 4.8 and 4.9. Figure 4.10 shows the stiffener strains versus the normalized load $V/V_{n(AASHTO)}$ for the curved girder with $d_o/D = 1$, $D/t_w = 150$, $I_s/I_{scr} = 8$ and two-sided stiffeners. One can observe that the axial and bending strains are the same order of magnitude for small $V/V_{n(AASHTO)}$. However, as the shear load is increased beyond about $V/V_{n(AASHTO)} = 0.83$, the direction of bending reverses in the critical stiffener, and the stiffener response is dominated by bending toward the inside (i.e., toward the center of the horizontal curvature).

Figure 4.11 shows the comparable stiffener responses for the straight I-girder with $d_o/D = 1$, $D/t_w = 300$, $I_s/I_{scr} = 50$ and one-sided stiffeners. The one-sided stiffeners are always on the outside and the web out-of-flatness is directed toward the inside for the straight I-girder results presented in this work. In this case, the stiffener responses are relatively large at the shear limit load, which corresponds to the shear strength plateau in Figure 4.2. The reader should note that the load-strain plot in Figure 4.11 is clipped at $e/e_y = \pm 3$; the strains at the stiffener edges are larger than these values as V approaches

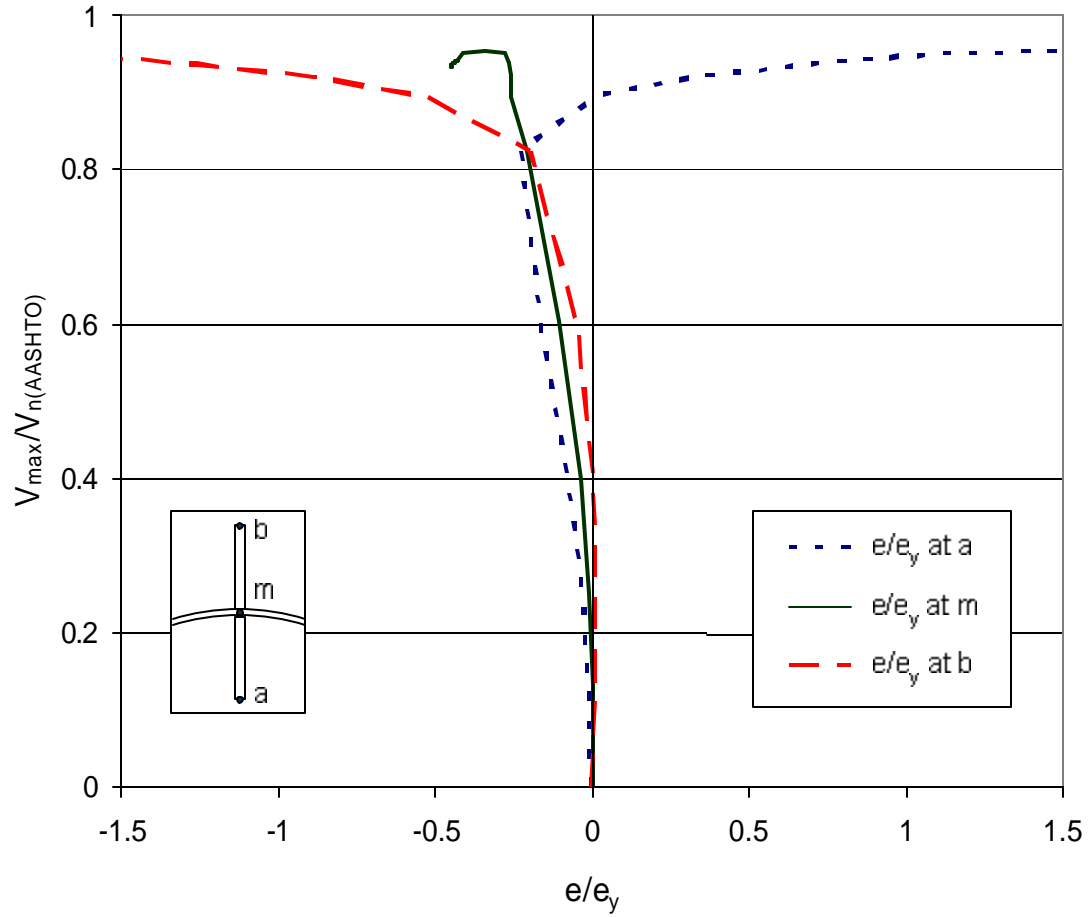


Figure 4.10. Stiffener mid-height strains versus shear force, curved girder with two-sided stiffeners, $d_o/D = 1$, $D/t_w = 150$ and $I_s/I_{scr} = 8$.

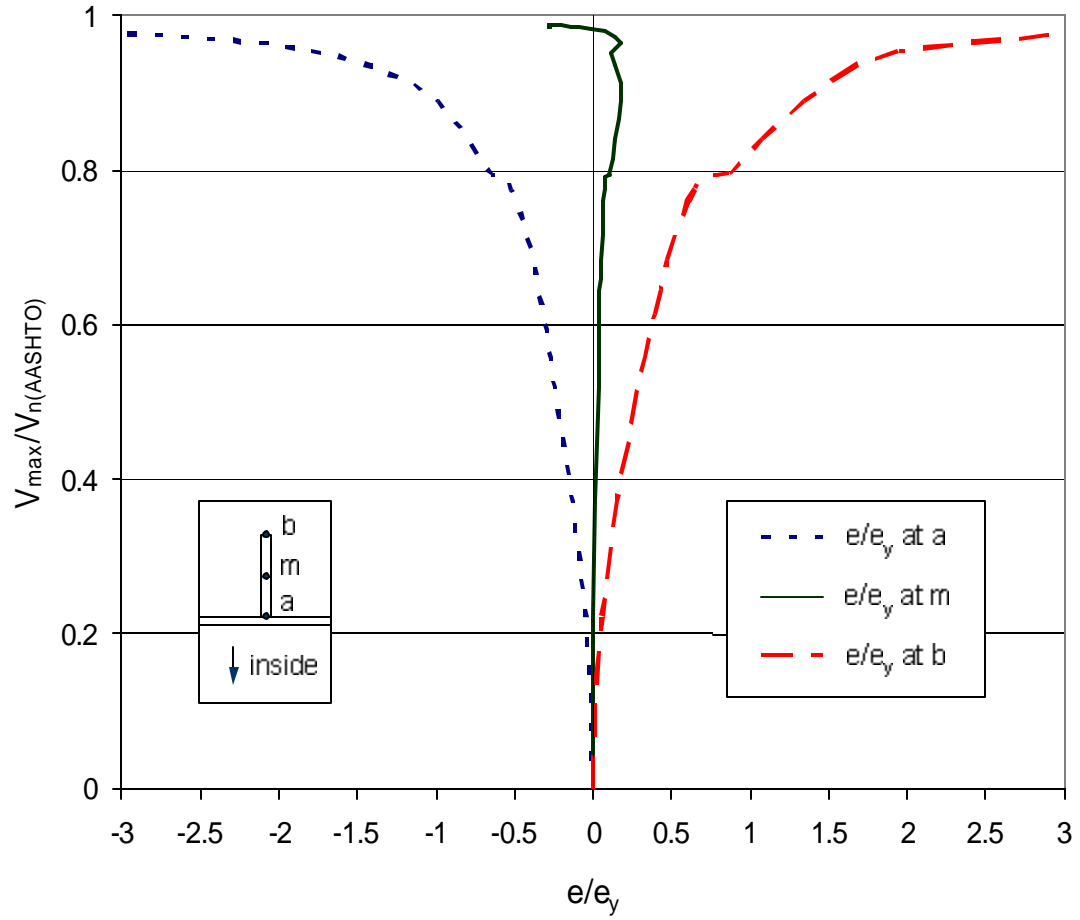


Figure 4.11. Stiffener mid-height strains versus shear force, straight girder with one-sided stiffeners on outside, $d_o/D = 1$, $D/t_w = 300$ and $I_s/I_{scr} = 50$.

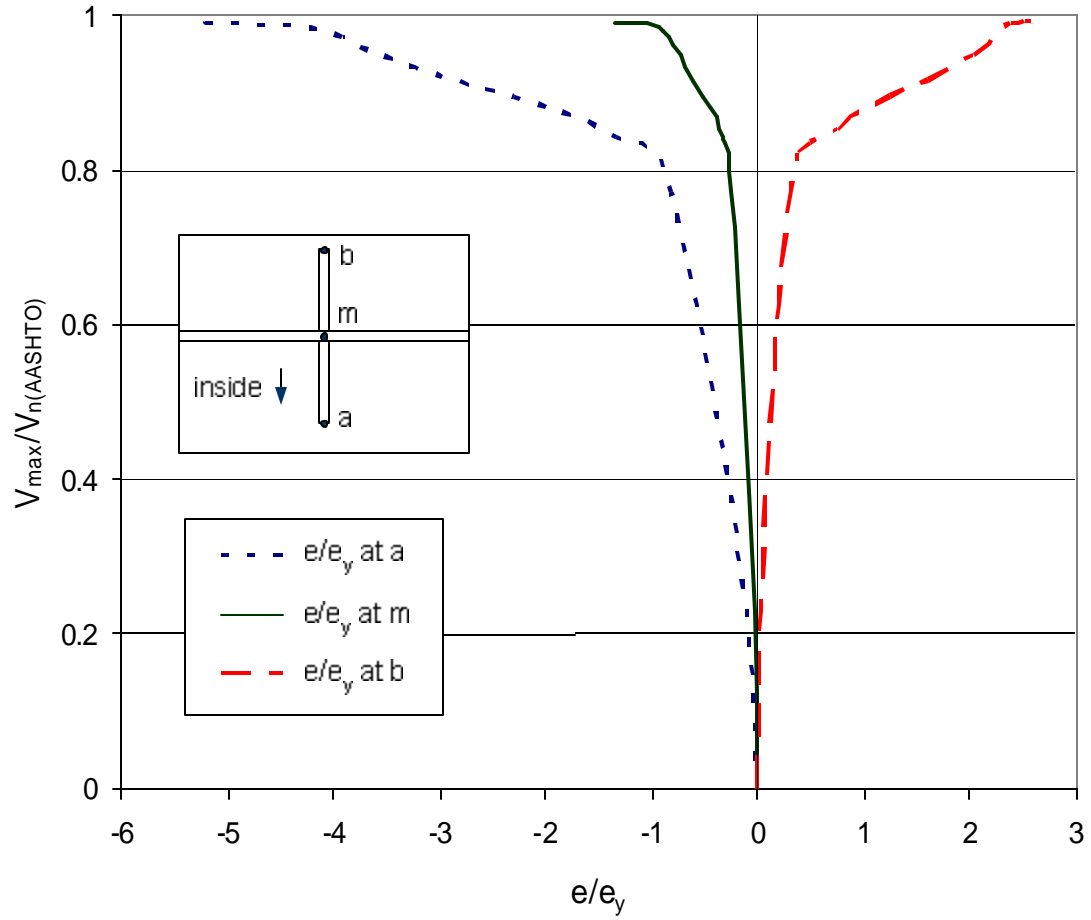


Figure 4.12. Stiffener mid-height strains versus shear force, straight girder with two-sided stiffeners, $d_o/D = 1$, $D/t_w = 300$ and $I_s/I_{scr} = 21$.

V_{\max} . The stiffener axial strain in Figure 4.11 is relatively small. Much of the axial force within the corresponding tension field vertical strut is transmitted directly by the web.

Lastly, Figure 4.12 shows the above responses for the straight I-girder with two-sided stiffeners, $d_o/D = 1$, $D/t_w = 300$ and $I_s/I_{scr} = 21$. This I_s/I_{scr} is the approximate knuckle value for this girder type as shown in Figure 4.2. Again, the stiffener response is dominated by bending at all levels of $V/V_{n(AASHTO)}$. The stiffener bending strains exceed the yield strain significantly starting at approximately $V/V_{n(AASHTO)} = 0.83$. Nevertheless, the girder is able to develop the plateau shear strength in Figure 4.2.

One should note that the stiffener strains corresponding to the stiffener bending rigidities recommended at the end of this chapter are generally smaller than the values illustrated in the above figures. However, the recommended bending rigidities in general do not ensure that the stiffeners will not yield prior to girders reaching their maximum shear strength.

4.4. Sensitivity of the Shear Strength to the Geometric Imperfection Pattern

Figure 4.13 shows several results for the girders having the largest sensitivity to the selected geometric imperfection pattern of the cases studied in this research – curved I-girders with $d_o/D = 1$, $D/t_w = 300$ and one-sided stiffeners. The curves shown in this figure illustrate the normalized strength $V_{\max}/V_{n(AASHTO)}$ versus I_s/I_{scr} for one-sided stiffeners located on: (1) the outside of the web (away from the center of curvature), (2) the inside of the web with the stiffener initial out-of-straightness directed away from the center of curvature, and (3) the inside of the web with the stiffener initial out-of-straightness such that the stiffener is bowed toward the center of curvature. As discussed

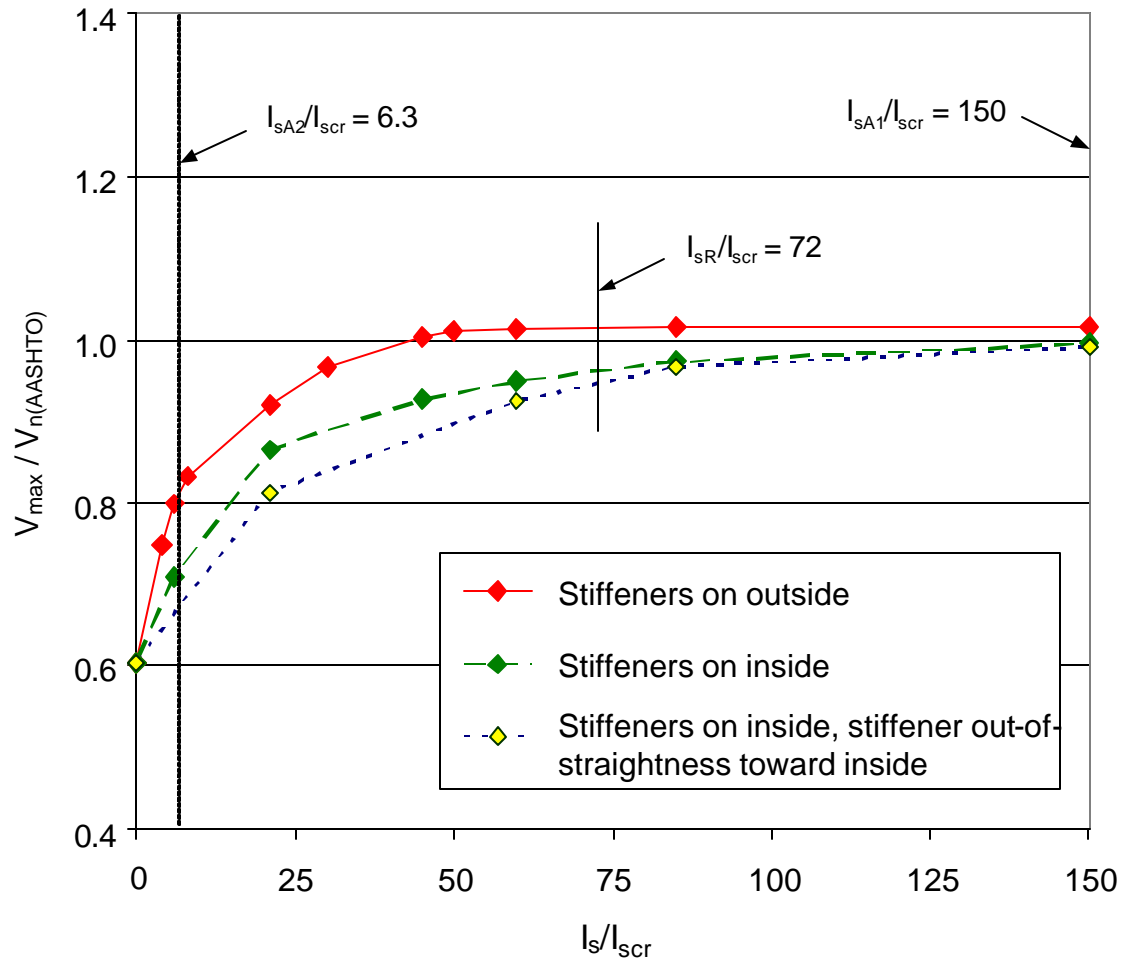


Figure 4.13. Effect of geometric imperfection pattern for curved girders with $d_o/D = 1$, $D/t_w = 300$ and one-sided stiffeners.

in Section 3.2.4.4, the FEA results for the curved girders with one-sided stiffeners always correspond to the second of these options unless noted otherwise.

For the curved girders with one-sided transverse stiffeners, the largest strengths are obtained generally when the stiffeners are placed on the outside. This is opposite to the behavior observed for the straight girders. The largest increase in strength relative to the results for the above option (2) is approximately 13 percent, and corresponds to $I_s/I_{scr} = 6$. The largest decrease relative to the results for the above option (2) is six percent and corresponds to $I_s/I_{scr} = 21$. It is important to note that the sensitivity of V_{max} to the geometric imperfection pattern is reduced substantially for girders that satisfy the final recommendations of this research ($I_{sR}/I_{scr} = 72$ for the girders in Figure 4.13). For girders that satisfy these recommendations, the maximum shear strengths are essentially the same for either of the above options (2) or (3), and the reduction in the shear strength relative to option (1) is approximately five percent. For all the other d_o/D and D/t_w values studied in this research, the sensitivity to the geometric imperfection pattern is significantly smaller. Therefore, the geometric imperfection patterns discussed in Section 3.2.4.4 are believed to provide an acceptable representation of the influence of geometric imperfections on the stiffener responses and the maximum I-girder shear strengths.

4.5. Web Behavior

Figures 4.14 through 4.16 show example web responses at the maximum shear strength for an I-girder where the transverse stiffeners do not fulfill their intended function. Conversely, Figures 4.17 through 4.19 show example responses where the transverse stiffeners subdivide the panels and the I-girder develops the plateau shear strength within the corresponding $V_{max} - I_s$ plot. Figures 4.14 through 4.16 correspond to

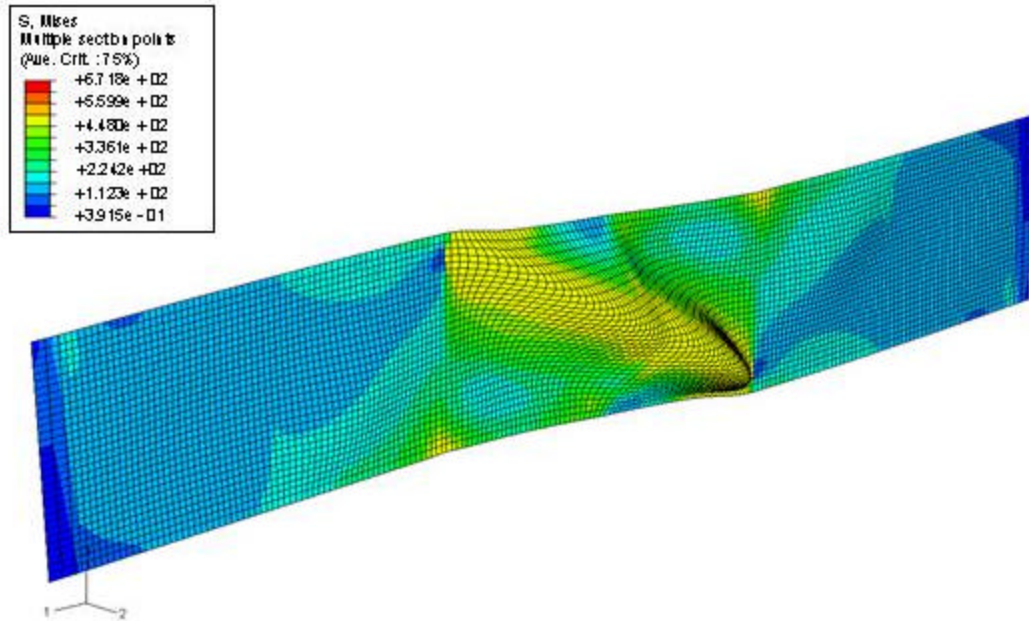


Figure 4.14. von Mises stress at web mid-thickness for $V = V_{\max}$, straight girder with one-sided stiffener on outside, $d_o/D = 1$, $D/t_w = 150$ and $I_s/I_{scr} = 1$ (deformation scale factor = 10).

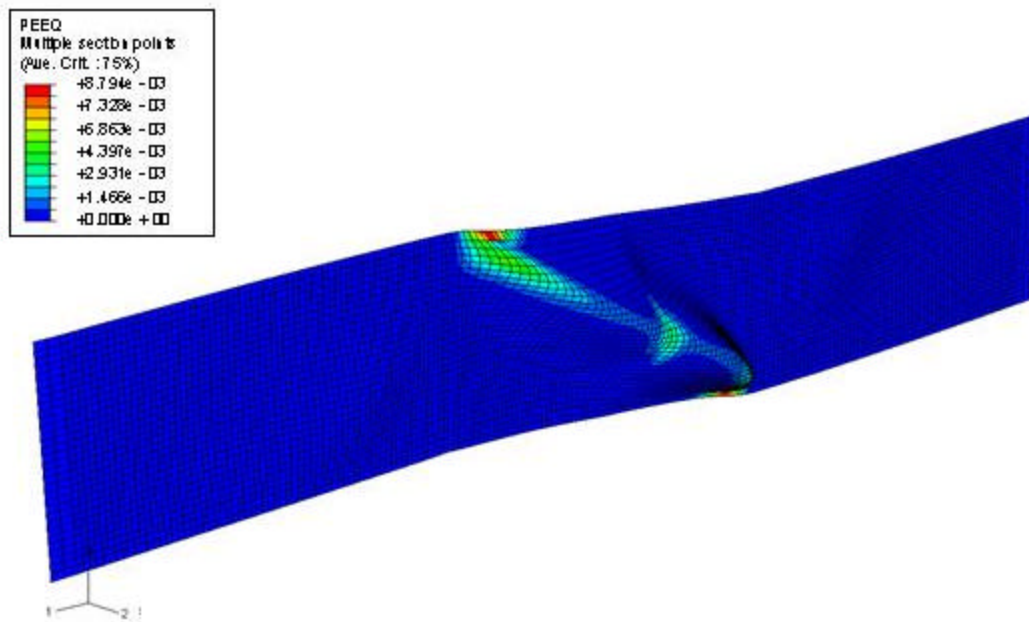


Figure 4.15. Equivalent plastic strain at web mid-thickness for $V = V_{\max}$, straight girder with one-sided stiffener on outside, $d_o/D = 1$, $D/t_w = 150$ and $I_s/I_{scr} = 1$ (deformation scale factor = 10).

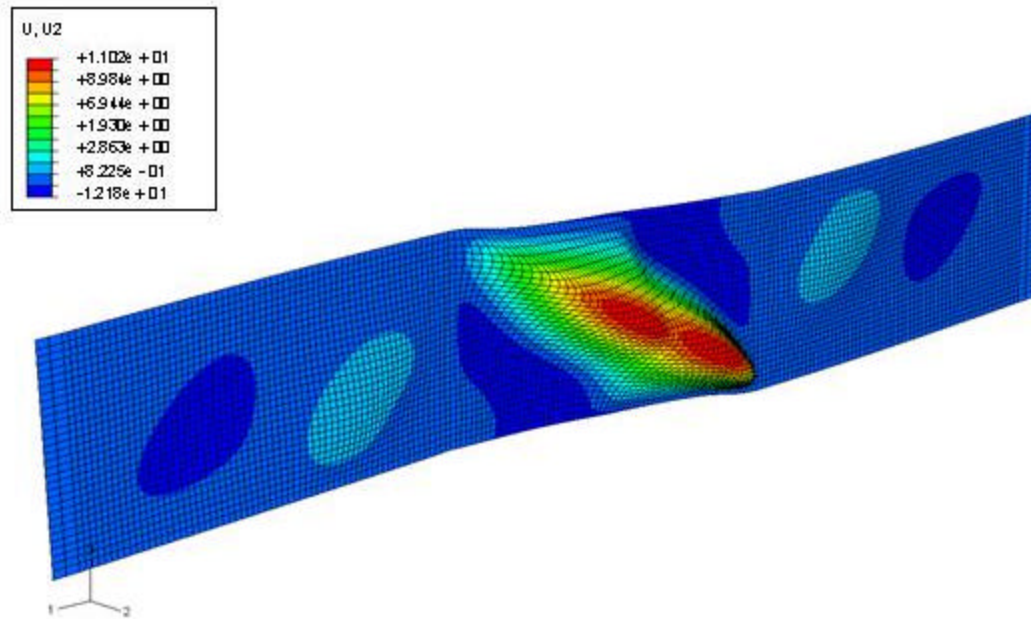
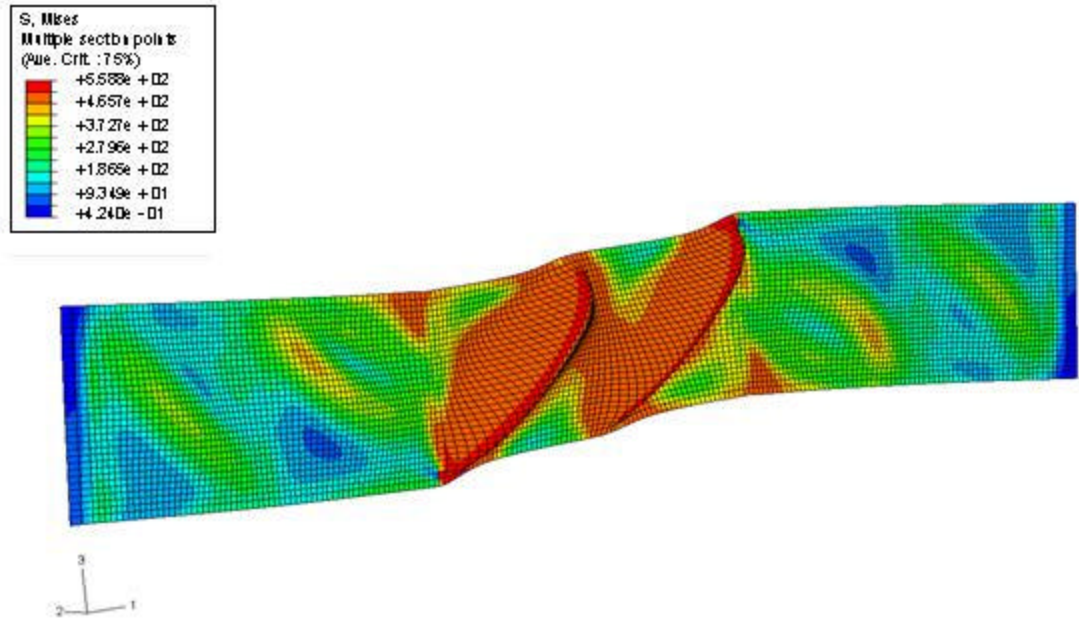


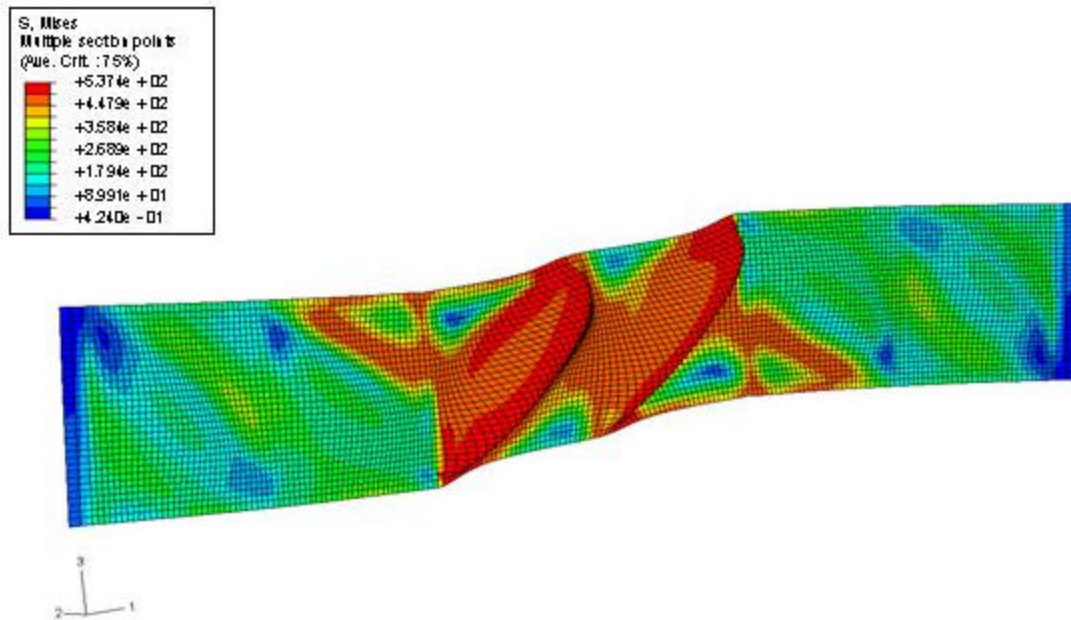
Figure 4.16. Lateral deflection contours at $V = V_{\max}$, straight girder with one-sided stiffener on outside, $d_o/D = 1$, $D/t_w = 150$ and $I_s/I_{scr} = 1$ (deformation scale factor = 10).

a straight girder with a one-sided stiffener, $d_o/D = 1$, $D/t_w = 150$ and $I_s/I_{scr} = 1$. As can be observed from Figure 4.1, this girder's maximum shear strength is substantially below the plateau value. Figures 4.14 and 4.15 show contours of the von Mises stress and the equivalent plastic strain on the deformed geometry of the member. Figure 4.16 shows contours of the lateral deflections within the web panels. The web lateral displacements are substantial at the critical transverse stiffener in the center of the test segment. Correspondingly, the von Mises stress and equivalent plastic strain contours indicate that the tension field forms between the bearing stiffeners at the ends of the test section. The critical transverse stiffener has only a minor effect on the maximum strength behavior in Figures 4.14 through 4.16, although it does increase the maximum strength to some extent as shown in Figure 4.1.

Figures 4.17 through 4.19 are for a curved I-girder with one-sided transverse

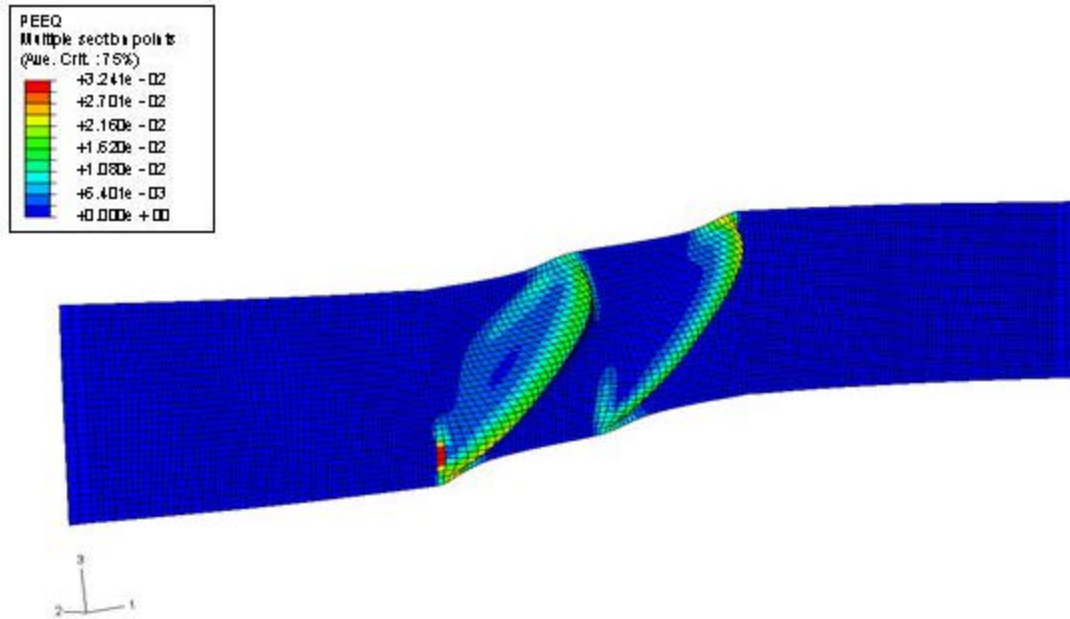


(a) von Mises stress at web outside surface

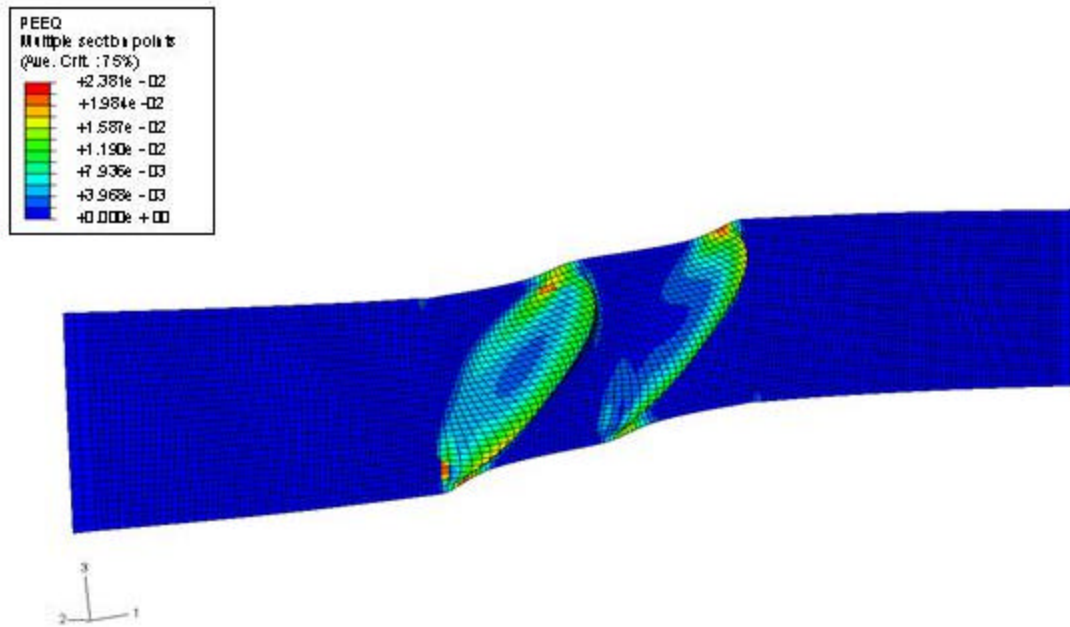


(b) von Mises stress at web inside surface

Figure 4.17. von Mises stress contours for $V = V_{\max}$, curved girder with one-sided stiffener, $d_o/D = 1$, $D/t_w = 150$ and $I_s/I_{scr} = 8$ (deformation scale factor = 10).



(a) Equivalent plastic strain at web outside surface



(b) Equivalent plastic strain at web inside surface

Figure 4.18. Equivalent plastic strain contours for $V = V_{max}$, curved girder with one-sided stiffener, $d_o/D = 1$, $D/t_w = 150$ and $I_s/I_{scr} = 8$ (deformation scale factor = 10).

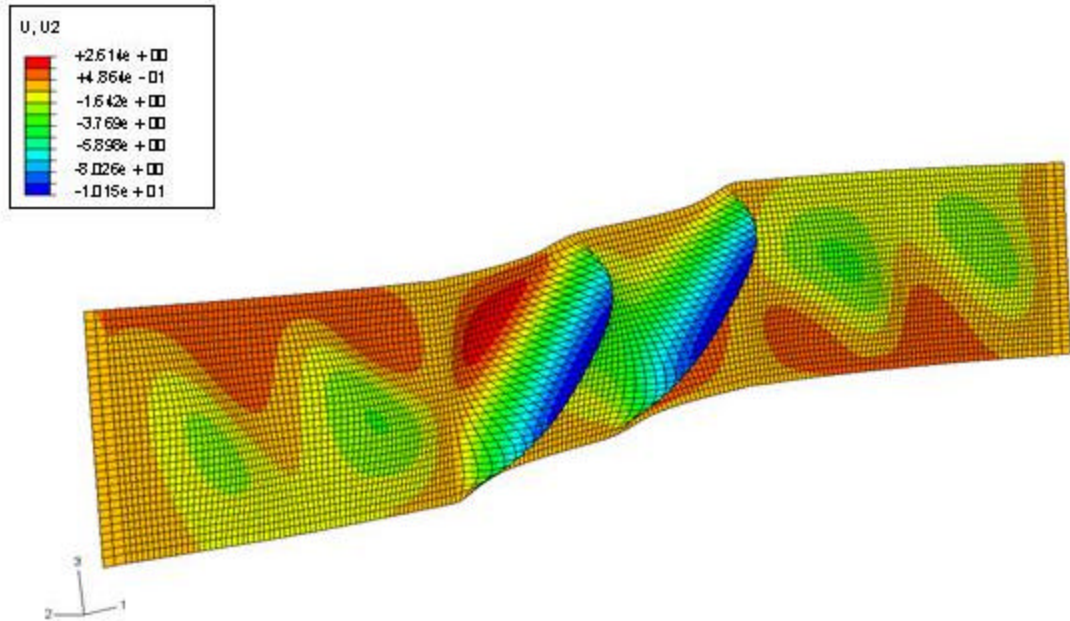


Figure 4.19. Lateral deflection contours at $V = V_{\max}$, curved girder with one-sided stiffener, $d_o/D = 1$, $D/t_w = 150$ and $I_s/I_{scr} = 8$ (deformation scale factor = 10).

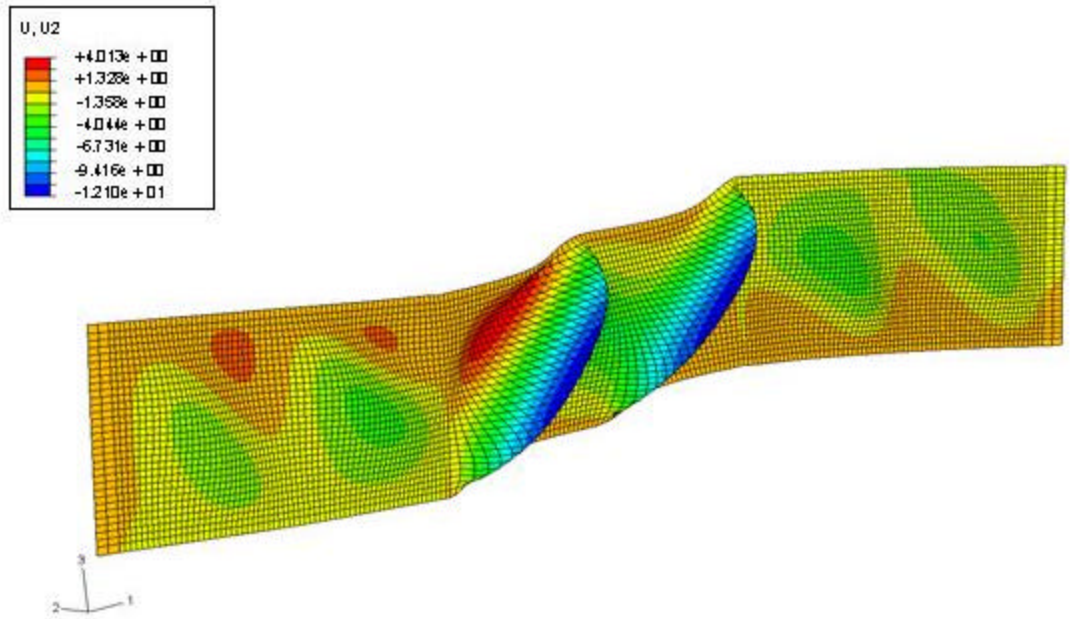


Figure 4.20. Lateral deflection contours at $V = V_{\max}$, curved girder with two-sided stiffener, $d_o/D = 1$, $D/t_w = 150$ and $I_s/I_{scr} = 8$ (deformation scale factor = 10).

stiffeners (located on the inside), $d_o/D = 1$, $D/t_w = 150$ and $I_s/I_{scr} = 8$. One can observe from Figure 4.1 that the plateau shear strength is nearly developed for this curved member (the strength gain with increasing I_s/I_{scr} is very gradual in this case). Figure 4.17 shows the von Mises contours on the inside and outside surface of the deformed web for this girder at $V = V_{max}$, whereas Figure 4.18 shows the equivalent plastic strain on these surfaces at the maximum shear capacity. Figure 4.19 shows contours of the lateral deflections on the deformed geometry. One can observe that the lateral deflections at the critical transverse stiffener are relatively small for this case, and that a tension field extends diagonally across each of the web panels. The von Mises stress and equivalent plastic strain contours show that the web is yielded through its entire thickness along the tension field bands in each of the panels.

Figure 4.20 shows one other example lateral deflection contour corresponding to a curved I-girder with two-sided stiffeners, $d_o/D = 1$, $D/t_w = 150$ and $I_s/I_{scr} = 8$. By comparison of this figure to Figure 4.19, it can be seen that the largest web transverse displacements at the peak shear capacity are somewhat larger within this girder than in the corresponding curved girder with one-sided stiffeners.

4.6. Synthesis of Results

4.6.1. Stiffener Requirements for Development of the Shear Buckling Strength

As discussed in Sections 2.1.3 and 2.2.1, the AASHTO (2004) shear buckling strengths are developed accurately to conservatively in general transversely-stiffened I-section members when the transverse stiffeners satisfy the requirement

$$I_s \geq I'_{scr} \quad (4.1)$$

where

$$I'_{scr} = \min(d_o, D) t_w^3 J' = b t_w^3 J' \quad (4.2)$$

and

$$J' = \frac{2.5}{\left(\frac{d_o}{D}\right)^2} - 2.0 \geq 0.5 \quad (4.3)$$

This set of equations is modified only slightly from the corresponding transverse stiffener rigidity requirement in AASHTO (2004) in that the term $b = \min(d_o, D)$ is used in Equation (4.2) rather than the term d_o in AASHTO (2004). Equations (4.1) through (4.3) are identical to the equations in AASHTO (2004) for $d_o/D \leq 1$, but account for the smaller demands placed on the transverse stiffeners for $d_o/D > 1$.

4.6.2. Stiffener Requirements for Development of Shear Postbuckling Strength

4.6.2.1. The $I'_{scr(C=1)}$ Concept – Required Stiffener Size at the Largest Web Slenderness Corresponding to $C = 1$

Section 4.2 shows that the stiffener moment of inertia needed to develop I-girder postbuckling shear strengths varies significantly relative to I_{scr} , where I_{scr} is the value required by AASHTO (2004) to prevent web buckling prior to reaching the shear force corresponding to shear buckling of a simply-supported panel with the same d_o/D and D/t_w . Since I'_{scr} given by Equations (4.1) to (4.3) is closely related to I_{scr} , it is simple to see that the requirements also vary significantly relative to I'_{scr} .

As discussed by Lee et al. (2003), it is important to recognize that if the web slenderness D/t_w is sufficiently small, the transverse stiffener moment of inertia needed to develop the shear buckling strength always should be sufficient. Given that the AASHTO (2004) shear strength equations are a reasonably accurate representation of general I-girder shear capacities (White and Barker 2004), and given that Equations (4.1)

to (4.3) are an accurate representation of the stiffener requirements to develop the shear buckling strengths, the requirement $I_s \geq I'_{scr}$ must be acceptable at

$$\frac{D}{t_w} = 1.12 \sqrt{\frac{Ek}{F_{yw}}} \quad (4.4)$$

where k is the AASHTO (2004) shear buckling coefficient given by Equation (2.7). The rationale behind this statement is the fact that Equation (4.4) is the web slenderness at which the AASHTO (2004) inelastic shear buckling strength V_{cr} is equal to the web plastic shear resistance V_p , or at which the shear buckling parameter $C = V_{cr}/V_p = 1$. Therefore, at the web slenderness defined by Equation (4.4), the fully-plastic shear resistance is developed without any consideration of postbuckling or tension field action.

The stiffener moment of inertia requirement corresponding to Equation (4.4) is obtained by solving Equation (4.4) for t_w , and substituting into Equation (4.2):

$$I'_{scr(C=1)} = \frac{bD^3J}{1.4 \left(\frac{Ek}{F_{yw}} \right)^{1.5}} \quad (4.5)$$

where $b = \min(d_o, D)$. If the stiffener bending rigidities from Section 4.1 needed to develop the web postbuckling strengths (i.e., the maximum knuckle values from Figures 4.1 through 4.7, summarized in Table 4.1) are expressed for different d_o/D and D/t_w values relative to the normalized parameter $I_s/I'_{scr(C=1)}$, an interesting simplification is apparent in the stiffener requirements. Section 4.6.2.2 presents these results.

Furthermore, it is easier to understand the physical stiffener requirements if they are expressed in terms of the required width for a given I_s and stiffener width-to-thickness ratio b_s/t_s rather than as the stiffener moment of inertia itself. The stiffener width

corresponding to $I'_{scr(C=1)}$ in Equation (4.5) may be determined by equating the approximation

$$I_s = \frac{nb_s^3 t_s}{3} = \frac{nb_s^4}{3(b_s/t_s)} \quad (4.6)$$

where $n = 1$ for a single-sided stiffener and $n = 2$ for a double-sided stiffener, to Equation (4.5) and solving for the resulting stiffener width, denoted by $b'_{scr(C=1)}$:

$$b'_{scr(C=1)} = \left[\frac{3}{n} \left(\frac{b_s}{t_s} \right) I'_{scr(C=1)} \right]^{1/4} \quad (4.7a)$$

Also, the stiffener width corresponding to any general required moment of inertia I_s is

$$b_s = \left[\frac{3}{n} \left(\frac{b_s}{t_s} \right) I_s \right]^{1/4} \quad (4.7b)$$

Furthermore, the normalized stiffener width associated with a given required $I_s/I'_{scr(C=1)}$ is simply

$$\frac{b_s}{b'_{scr(C=1)}} = \left(\frac{I_s}{I'_{scr(C=1)}} \right)^{1/4} \quad (4.8)$$

It is emphasized that for $d_o/D \leq 1$, $I'_{scr} = I_{scr}$ and thus $I'_{scr(C=1)} = I_{scr(C=1)}$ and $b'_{scr(C=1)} = b_{scr(C=1)}$, where $I_{scr(C=1)}$ is the AASHTO (2004) stiffener moment of inertia required at $D/t_w = 1.12 \sqrt{Ek/F_{yw}}$ (Equation (4.4)) and $b_{scr(C=1)}$ is the corresponding stiffener width for a given stiffener type and width-to-thickness ratio.

Lastly, in interpreting the implications of the AASHTO (2004) area requirement equations, it is useful to convert them to a corresponding moment of inertia requirement (note that the AASHTO (2004) area requirement is converted to and presented in terms of

the moment of inertia in the previous Figures 4.1 through 4.7). The conversion equation is

$$I_{sA} = \frac{A_s^2 (b_s/t_s)}{3n} \quad (4.9)$$

where $n = 1$ for one-sided stiffeners and $n = 2$ for two-sided stiffeners.

4.6.2.2. Required Stiffener Sizes Relative to the Size Corresponding to $I'_{scr(C=1)}$

4.6.2.2.1. Comparisons to the Parametric Study Results from This Research

Figures 4.21 through 4.25 summarize the normalized stiffener size requirements, expressed as $b_s/b'_{scr(C=1)}$, from five sources for each of the d_o/D values considered in this research:

1. The combined AASHTO (2004) moment of inertia and area requirements, given by Equations (2.1) and (2.28).
2. The stiffener moment of inertia requirement developed by Horne and Grayson (1983), given by Equation (2.1) with J specified by Equation (2.15).
3. The combined stiffness and strength criteria developed by Stanway et al. (1996), given by Equations (2.13) and (2.14), and Equatons (2.30) through (2.33) respectively.
4. The approximate maximum knuckle values determined from the FEA parametric studies conducted in this research (Figures 4.1 through 4.7 and Table 4.1).
5. The point $(b'_{scr(C=1)}, 1.12\sqrt{Ek/F_{yw}})$, where the abscissa is obtained by setting Equation (4.8) equal to 1.0.

For the cases with $d_o/D = 1$, the symbol $b_{scr(C=1)}$ is used in the figures to emphasize the fact that $b'_{scr(C=1)} = b_{scr(C=1)}$. The results for $d_o/D = 1$ are presented first, since the demands on the transverse stiffeners are generally the greatest for this aspect ratio (see the

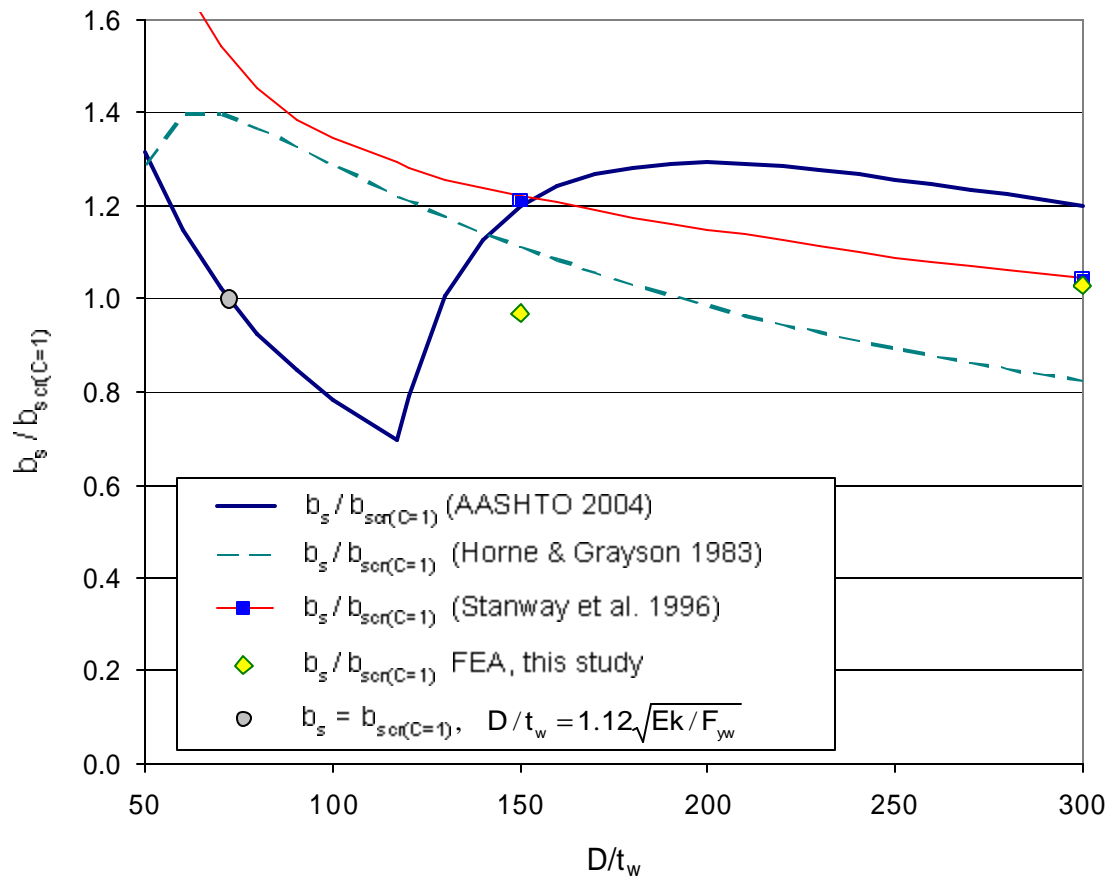


Figure 4.21a. Required stiffener sizes, girders with one-sided stiffeners, $d_o/D = 1$, $F_{yw} = 485$ MPa (70 ksi).

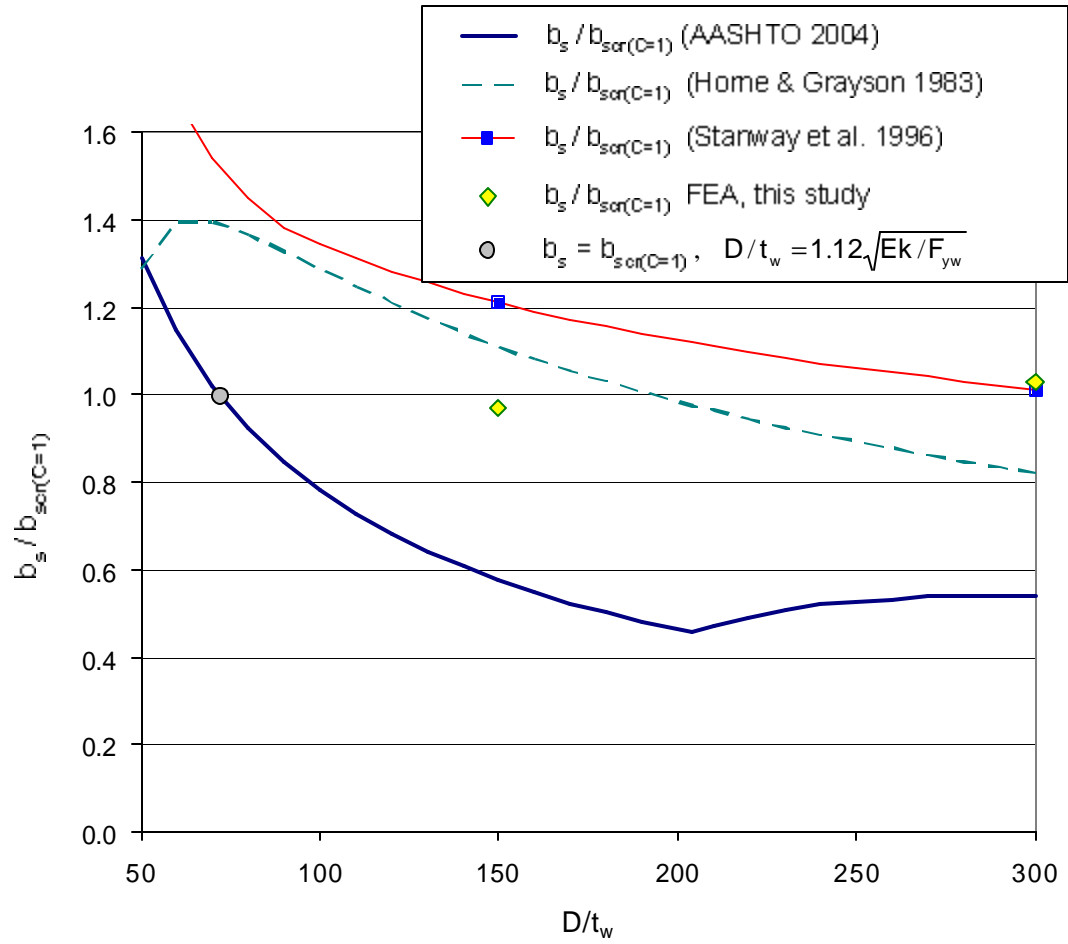


Figure 4.21b. Required stiffener sizes, girders with two-sided stiffeners, $d_o/D = 1$, $F_{yw} = 485 \text{ MPa}$ (70 ksi).

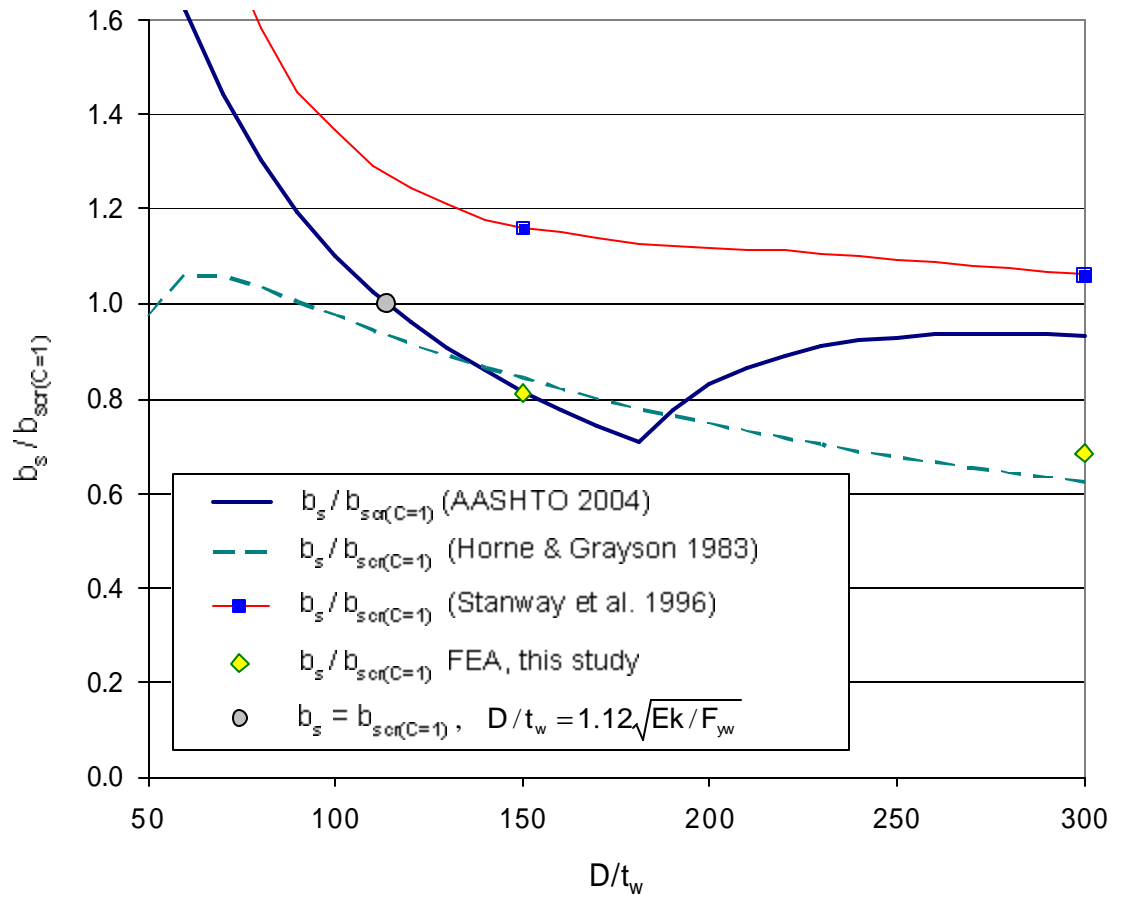


Figure 4.22a. Required stiffener sizes, girders with one-sided stiffeners, $d_o/D = 0.5$, $F_{yw} = 485 \text{ MPa}$ (70 ksi).

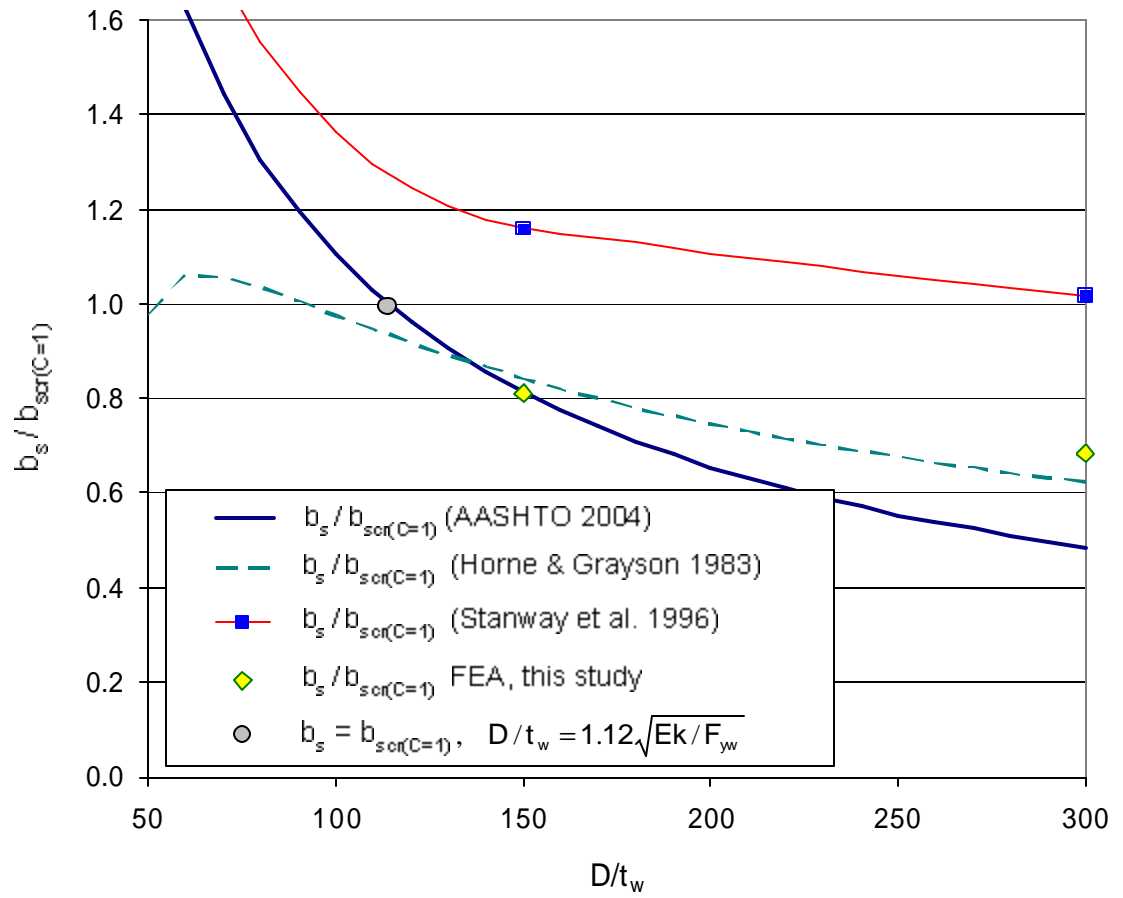


Figure 4.22b. Required stiffener sizes, girders with two-sided stiffeners, $d_o/D = 0.5$, $F_{yw} = 485 \text{ MPa}$ (70 ksi).

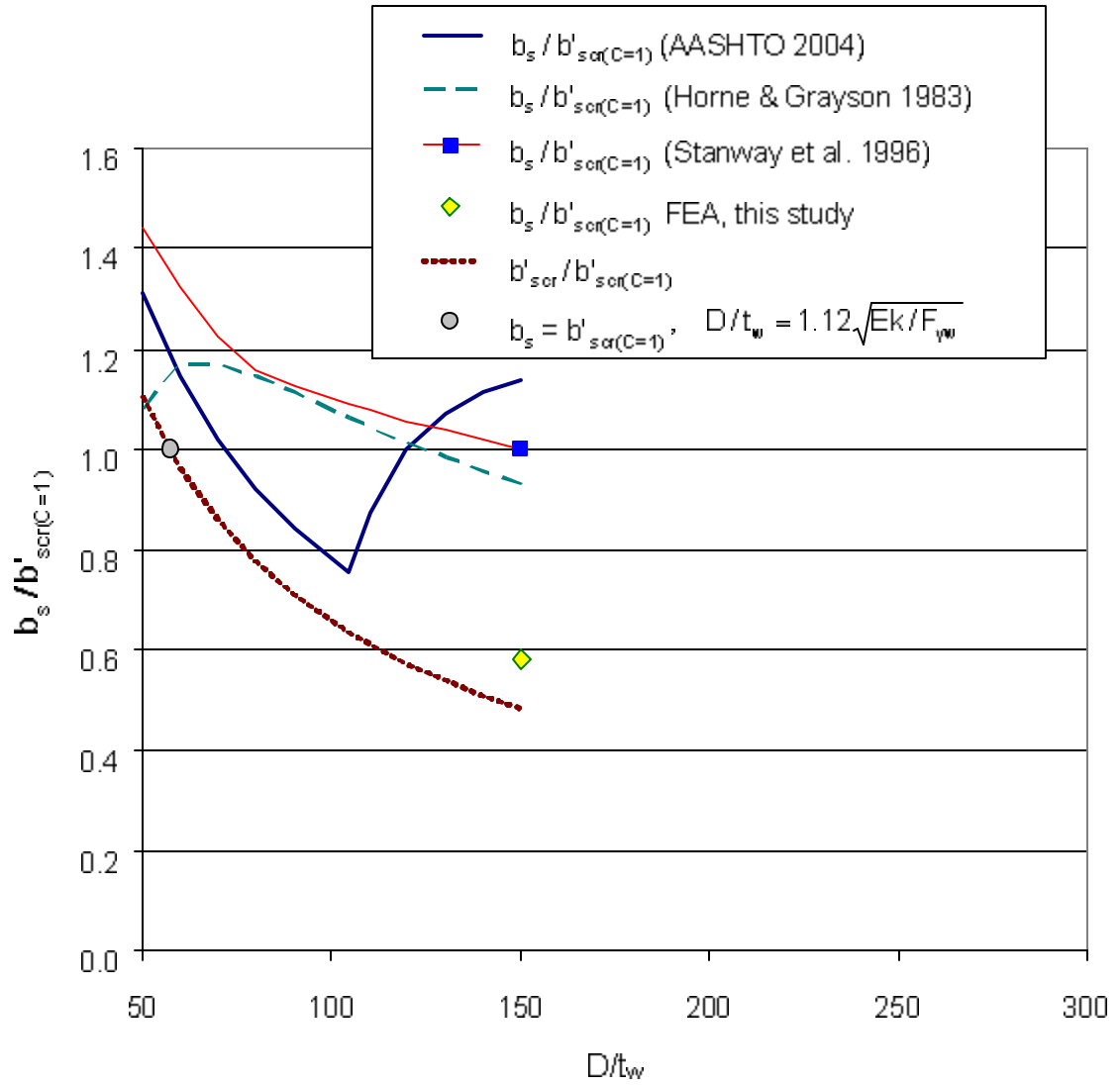


Figure 4.23a. Required stiffener sizes, girders with one-sided stiffeners, $d_o/D = 2$, $F_{yw} = 485 \text{ MPa}$ (70 ksi).

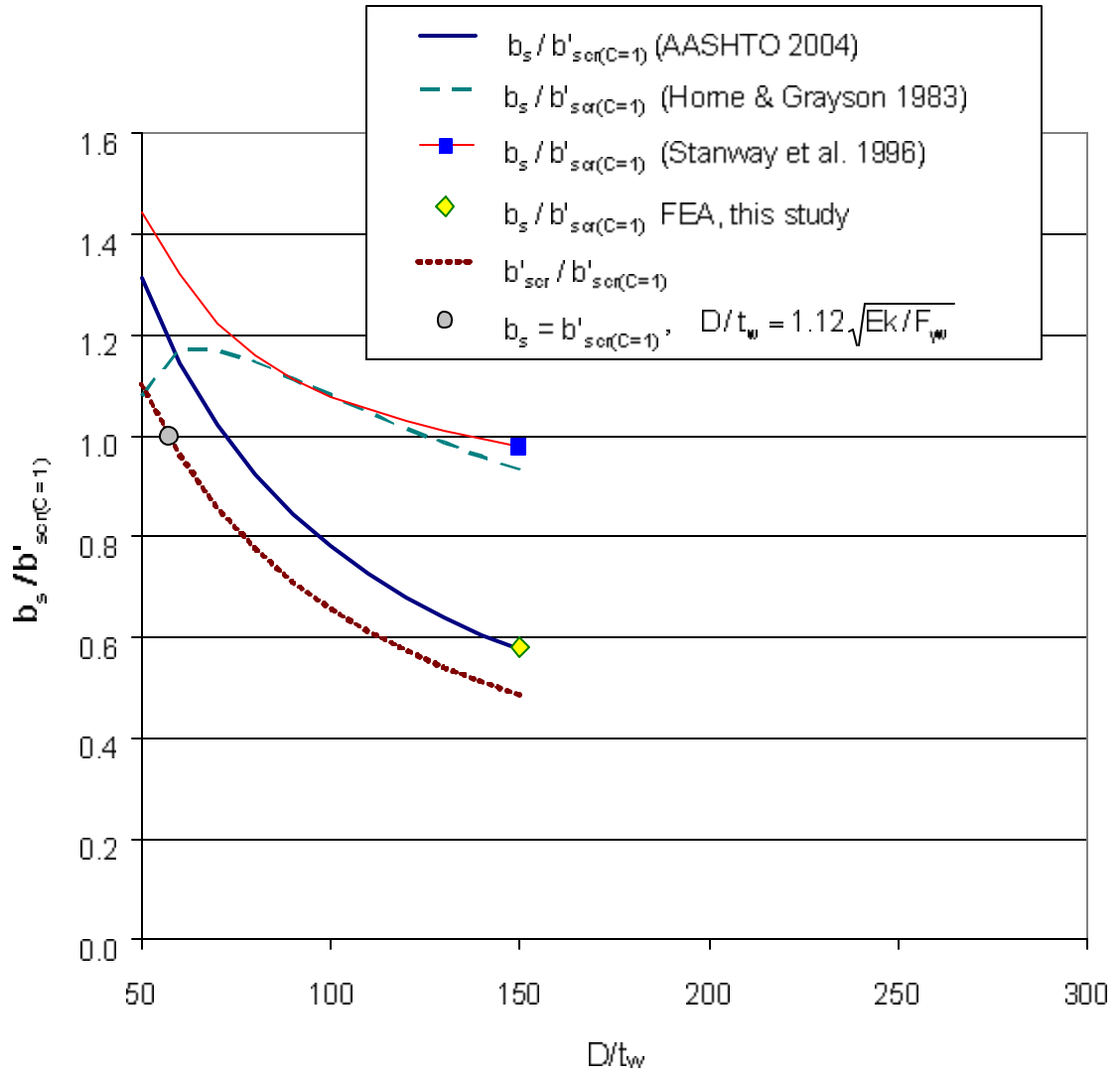


Figure 4.23b. Required stiffener sizes, girders with two-sided stiffeners, $d_o/D = 2$, $F_{yw} = 485 \text{ MPa}$ (70 ksi).

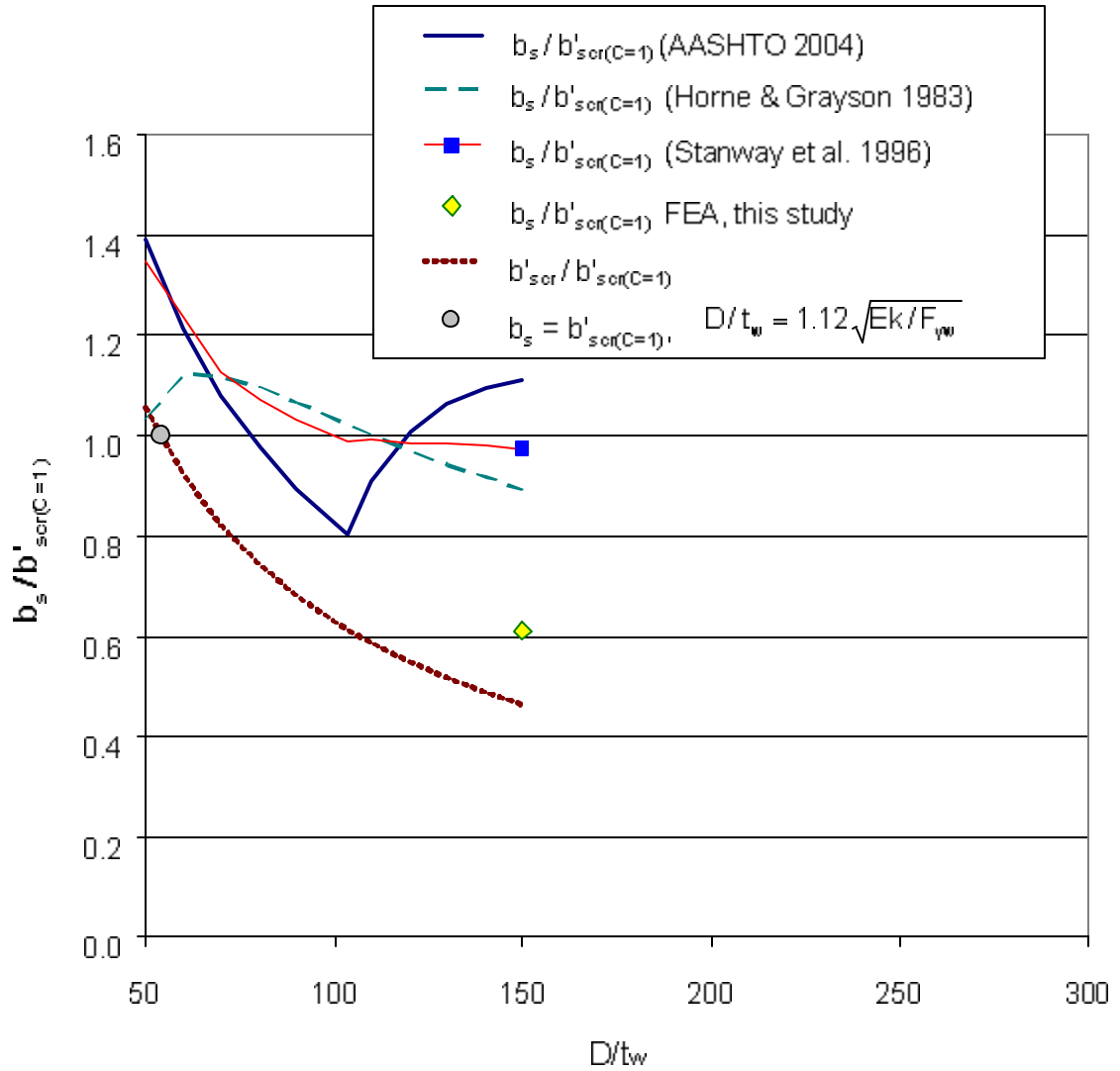


Figure 4.24a. Required stiffener sizes, girders with one-sided stiffeners, $d_o/D = 3$, $F_{yw} = 485 \text{ MPa}$ (70 ksi).

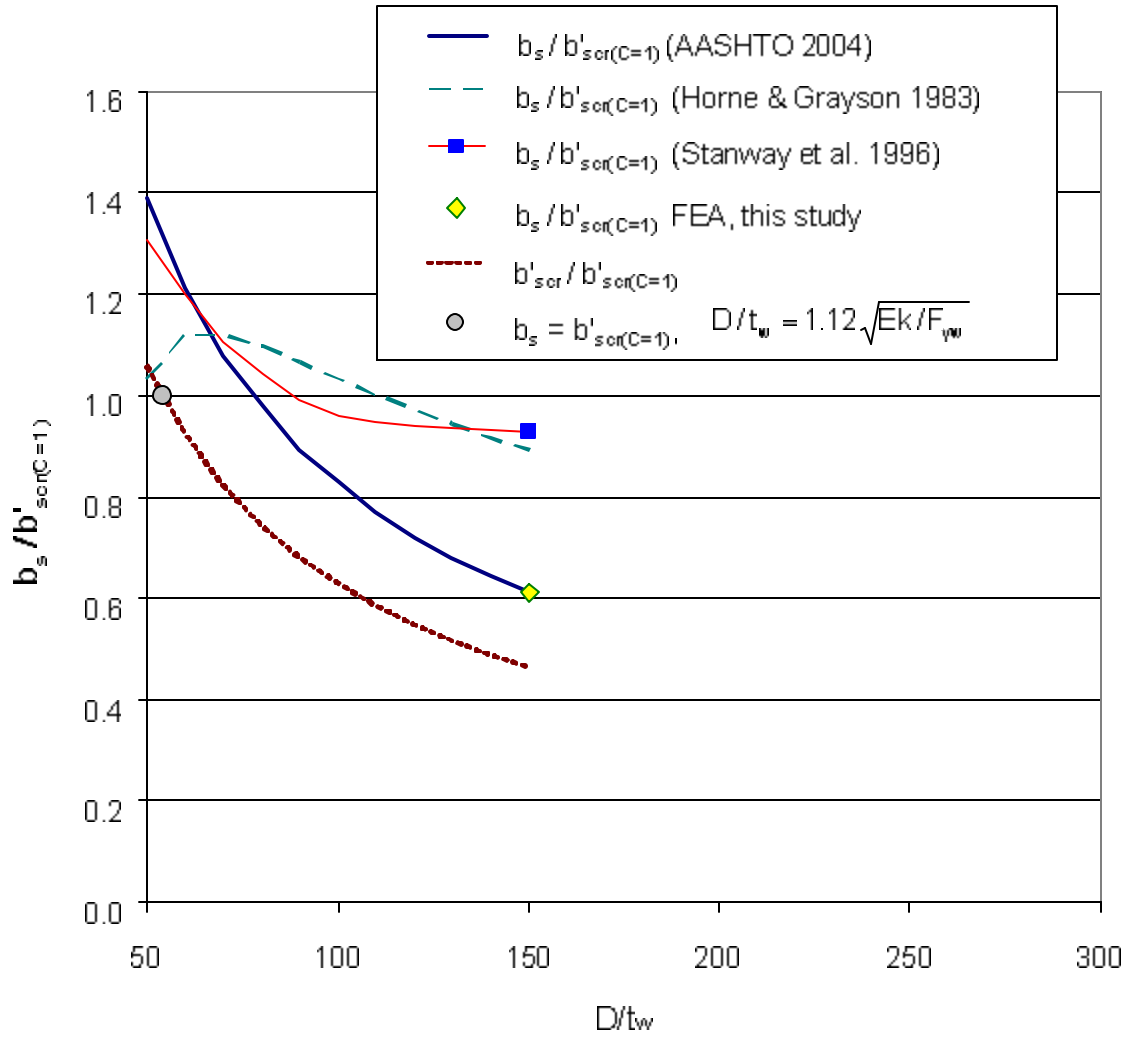


Figure 4.24b. Required stiffener sizes, girders with two-sided stiffeners, $d_o/D = 3$, $F_{yw} = 485 \text{ MPa}$ (70 ksi).

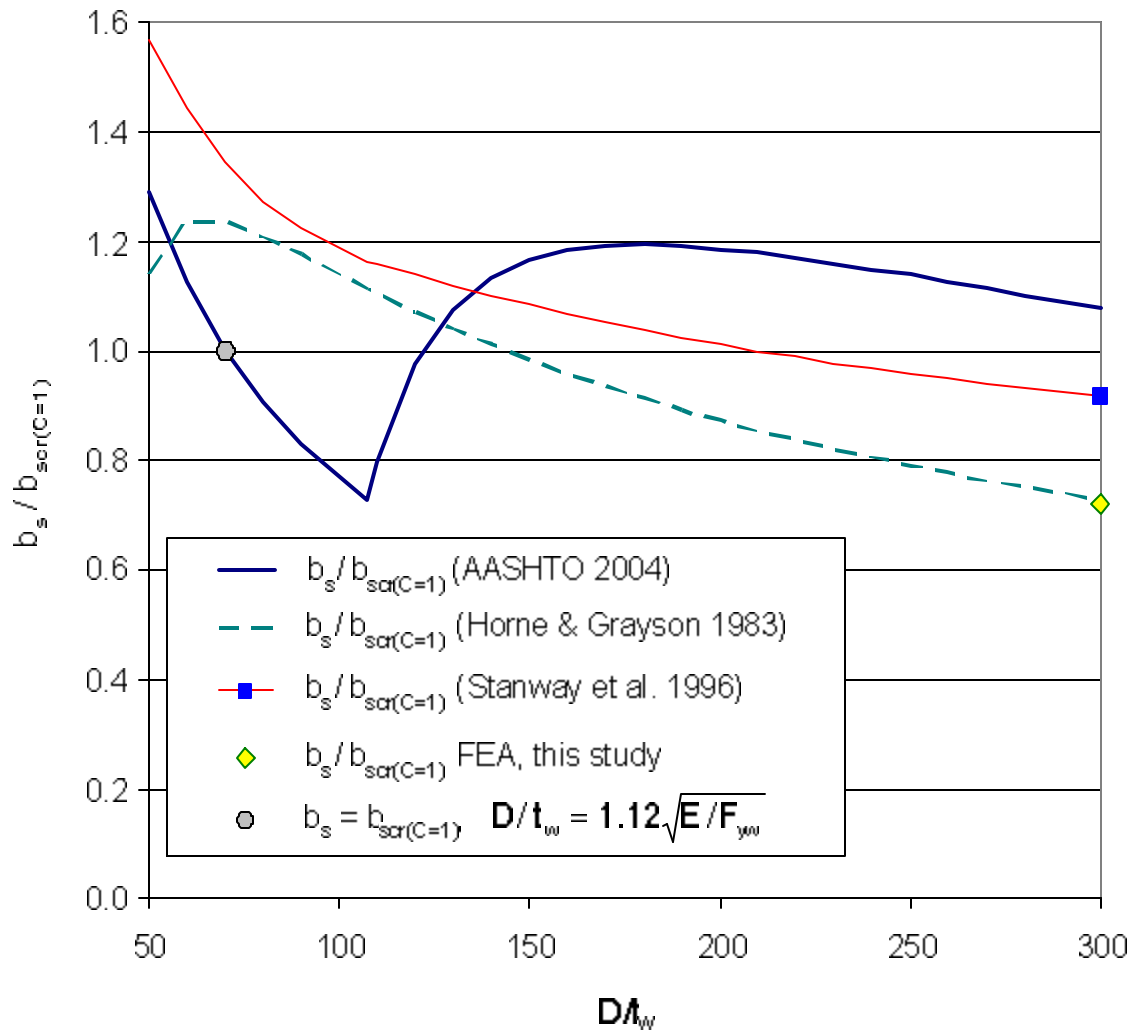


Figure 4.25a. Required stiffener sizes, girders with one-sided stiffeners, $d_o/D = 1.5$, $F_{yw} = 485 \text{ MPa}$ (70 ksi).

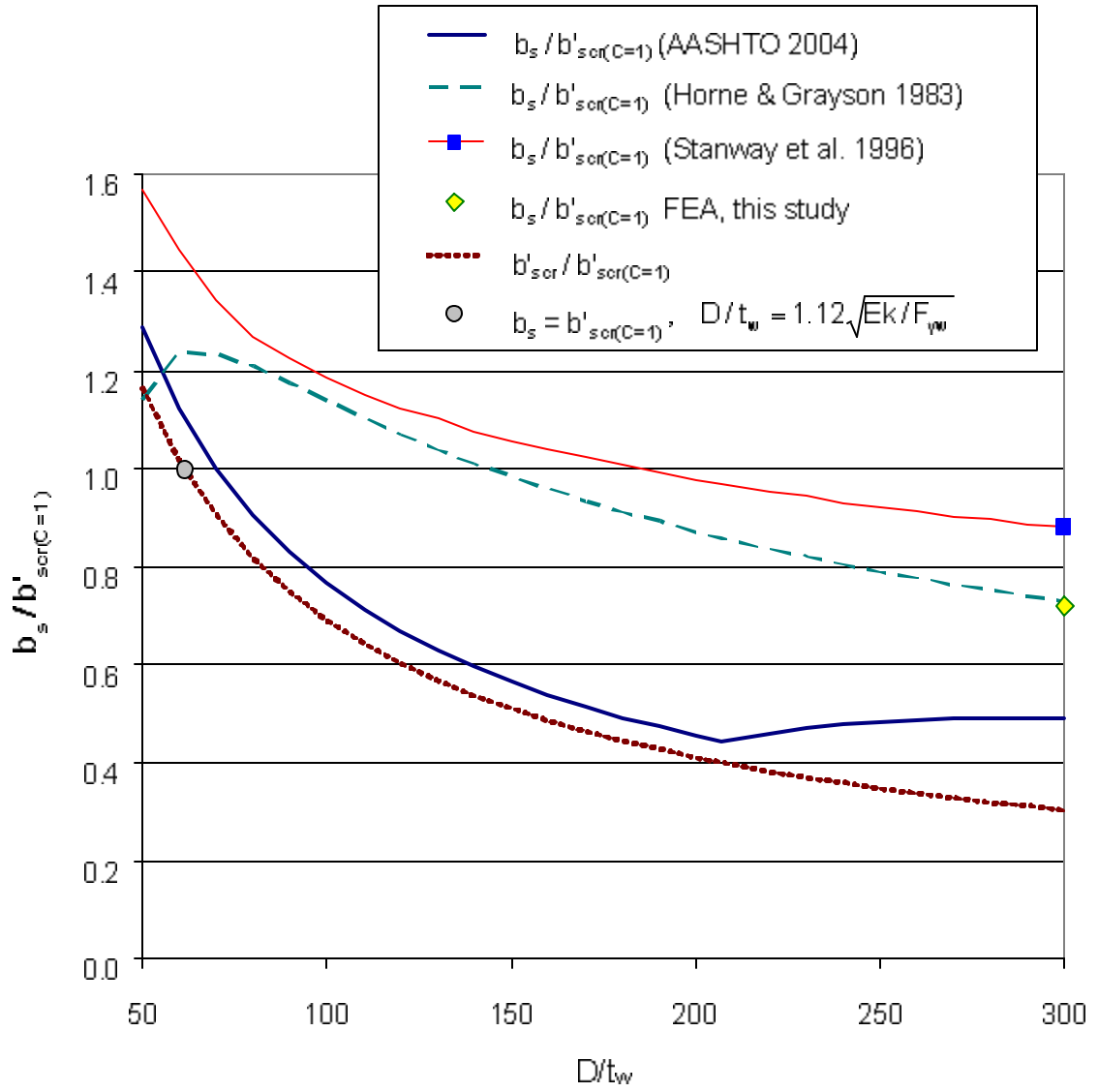


Figure 4.25b. Required stiffener sizes, girders with two-sided stiffeners, $d_o/D = 1.5$, $F_{yw} = 485 \text{ MPa}$ (70 ksi).

discussions in Section 4.2). This is followed by the results for $d_o/D = 0.5, 2, 3$ and 1.5 . The reader is reminded that the FEA parametric studies in this research are conducted both for $D/t_w = 150$ and 300 at $d_o/D = 1$ and 0.5 . Only $D/t_w = 150$ is considered for $d_o/D = 2$ and 3 though, since this is the largest web slenderness ratio allowed for transversely stiffened I-girders in AASHTO (2004), and longitudinally stiffened I-girders are restricted to a maximum of $d_o/D = 1.5$. For each of Figures 4.21 to 4.25, two plots are provided. The first plot (plot (a)) shows the results for single-sided transverse stiffeners while the second plot (plot (b)) shows the results for double-sided transverse stiffeners.

It is important to note that the moment of inertia requirements determined from the knuckle values in Figures 4.1 through 4.7 are for all practical purposes independent of the stiffener type, i.e., one-sided or two-sided. Also, with the exception of AASHTO (2004), all of the solutions plotted in Figures 4.21 to 4.25 are independent of the stiffener type. However, the AASHTO (2004) solutions for one- and two-sided stiffeners differ substantially in general depending on whether or not the AASHTO area requirement governs. All of the solutions shown in parts (a) and (b) of the above figures are identical with the exception of the AASHTO (2004) solutions.

The results shown in Figures 4.21 to 4.25 can be understood by first focusing on Figures 4.21a and b (corresponding to $d_o/D = 1$). It can be observed that a constant $b_s / b_{scr(C=1)} = b_s / b'_{scr(C=1)} = 1$ fits the requirements determined from the FEA studies in this research along with the obvious data point at $(b_s, D/t_w) = (b_{scr(C=1)}, 1.12 \sqrt{Ek / F_{yw}})$ amazingly well. That is, if one selects the stiffener size needed to develop the web shear buckling strength corresponding to $D/t_w = 1.12 \sqrt{Ek / F_{yw}}$ and $C = 1$, then based on the FEA solutions for the critical $d_o/D = 1$ case conducted in this research, this stiffener is the

appropriate size for the other D/t_w values greater than $1.12 \sqrt{Ek / F_{yw}}$. This is a key result that ultimately leads to the final recommendations of this research.

Important characteristics of the other solutions shown in Figure 4.21a are as follows:

- The AASHTO (2004) solution is governed by the moment of inertia requirement (Equation (2.1)) for small D/t_w . Since Equation (2.1) does not account for the additional demands on the transverse stiffeners due to the postbuckling response of the web, the AASHTO (2004) solution dips below the constant requirement of $b_s = b_{scr(C=1)} = b'_{scr(C=1)}$ for $D/t_w > 1.12 \sqrt{Ek / F_{yw}} = 72$ until the area requirement begins to control. The area requirement begins to govern at the lowest point along the AASHTO (2004) curve. Once the area requirement begins to control, the corresponding $b_s/b_{scr(C=1)}$ requirement rapidly increases to a value greater than one as D/t_w increases. For $D/t_w > 130$, the AASHTO (2004) area requirement requires a larger stiffener than that based on $b_s = b_{scr(C=1)}$ and based on the refined FEA solutions. The reader should note that the results in Figures 4.21 through 4.25 are based on the stiffeners with $b_s/t_s = 10$. If stockier stiffeners are used, then the AASHTO (2004) area requirement would be smaller than in these figures. For example, when the one-sided stiffeners with $b_s/t_s = 5$ are used in the girders with $d_o/D = 1.0$ and $F_{yw} = 485$ MPa (70 ksi), the AASHTO (2004) area requirement starts to govern at the point, $D/t_w = 121$ and the largest stiffener width required is $1.09 b'_{scr(C=1)}$. In Figure 4.21a, the largest stiffener width required is $1.29 b'_{scr(C=1)}$.
- The solutions from both Horne and Grayson (1983) and Stanway et al. (1996) require a stiffener size substantially larger than that required by AASHTO (2004) when the web slenderness is in the vicinity of $D/t_w = 1.12 \sqrt{Ek / F_{yw}} = 72$. However, it is well

established and accepted that the stiffener size $b_s = b_{scr(C=1)}$ is sufficient at this value of D/t_w . It is believed that the conservatism of the solution by Stanway et al. (1996) for small D/t_w is related in part to the use of first-yield as the strength criterion for the stiffeners in their work. FEA solutions from Stanway et al. (1993) presented in the next section indicate that the data point $(b_s, D/t_w) = (b'_{scr(C=1)}, 1.12 \sqrt{Ek / F_{yw}})$ corresponds approximately to $\mu_u = 0.9$ from Equation (2.13) (also see Tables 2.1 through 2.3).

- For large D/t_w , the solution from Horne and Grayson (1983) is slightly more liberal than that based on $b_s = b_{scr(C=1)}$ ($= b'_{scr(C=1)}$ for $d_o/D = 1$) and based on the refined FEA studies in this research. However, the requirement from Stanway et al. (1996) is essentially the same as the latter two of these three solutions at $D/t_w = 300$.

As noted above, all the normalized solutions in Figures 4.21 through 4.25 are the same for the girders with one- or two-sided stiffeners with the exception of the AASHTO (2004) results. Figure 4.21b shows the corresponding plot for $d_o/D = 1$ and girders with two-sided stiffeners. One can observe that in this case, the area requirement does not control the size of the stiffener until $D/t_w \geq 204$. As a result, the stiffener size b_s permitted by AASHTO (2004) is substantially smaller than that required by the refined FEA solutions and by the rule $b_s = b_{scr(C=1)}$. The two-sided stiffener width allowed by AASHTO (2004) is as small as $0.46b_{scr(C=1)}$. In terms of the moment of inertia, this corresponds to I_s values as small as $(0.46)^4 I_{scr(C=1)} = 0.045 I_{scr(C=1)}$.

The solutions for other d_o/D values, shown in Figures 4.22 through 4.25, are similar to the above with the exception that the required $b_s/b'_{scr(C=1)}$ values obtained from the refined FEA solutions tend to be less than one, particularly for larger D/t_w . Also, for the

plots corresponding to $d_o/D > 1$, one additional curve is shown. This curve shows $b'_{scr}/b'_{scr(C=1)}$ based on Equation (4.8) with $I_s = I'_{scr}$. By comparing this curve to the portion of the AASHTO (2004) curve governed by the moment of inertia requirement, one can ascertain the reduction in the stiffener sizes permitted by the recommended Equations (4.1) to (4.3) relative to the AASHTO (2004) requirements for stiffener spacings d_o greater than D .

4.6.2.2.2. Comparisons to the Parametric Study Results from Prior Research

Figures 4.26 through 4.28 compare the normalized stiffener size requirements from AASHTO (2004), Horne and Grayson (1983) and Stanway et al. (1996) to the FEA solutions generated by Stanway et al. (1993 and 1996) corresponding to $\mu_u = 0.9$ (see Equation (2.13)). Stanway et al. (1993 and 1996) assumed $F_{yw} = F_{ys} = 245$ MPa (36 ksi) in all of their solutions. Therefore, Figures 4.26 through 4.28 serve the important purpose of illustrating the stiffener size requirements for significantly different web and stiffener yield strengths than those considered in the current research. All of the FEA studies conducted in the author's studies focus on $F_{yw} = F_{ys} = 345$ MPa (70 ksi). The plots in Figures 4.26 to 4.28 are the same format as those in Figures 4.21 to 4.25, but the results from the different approaches to sizing of the stiffeners are compared to the FEA results from Stanway et al. (1993 and 1996) for $F_{yw} = F_{ys} = 245$ MPa (36 ksi). Stanway et al. studied girders with $d_o/D = 0.5, 1$ and 2 . As in Section 4.6.2.2.1, the results for $d_o/D = 1$ are presented first (see Figures 4.26a and b) since the demands on the transverse stiffeners are the largest for this panel aspect ratio.

One can observe from Figures 4.26a and b that once again, the simple rule $b_s = b_{scr(C=1)}$ gives an accurate fit to the required stiffener size obtained from the

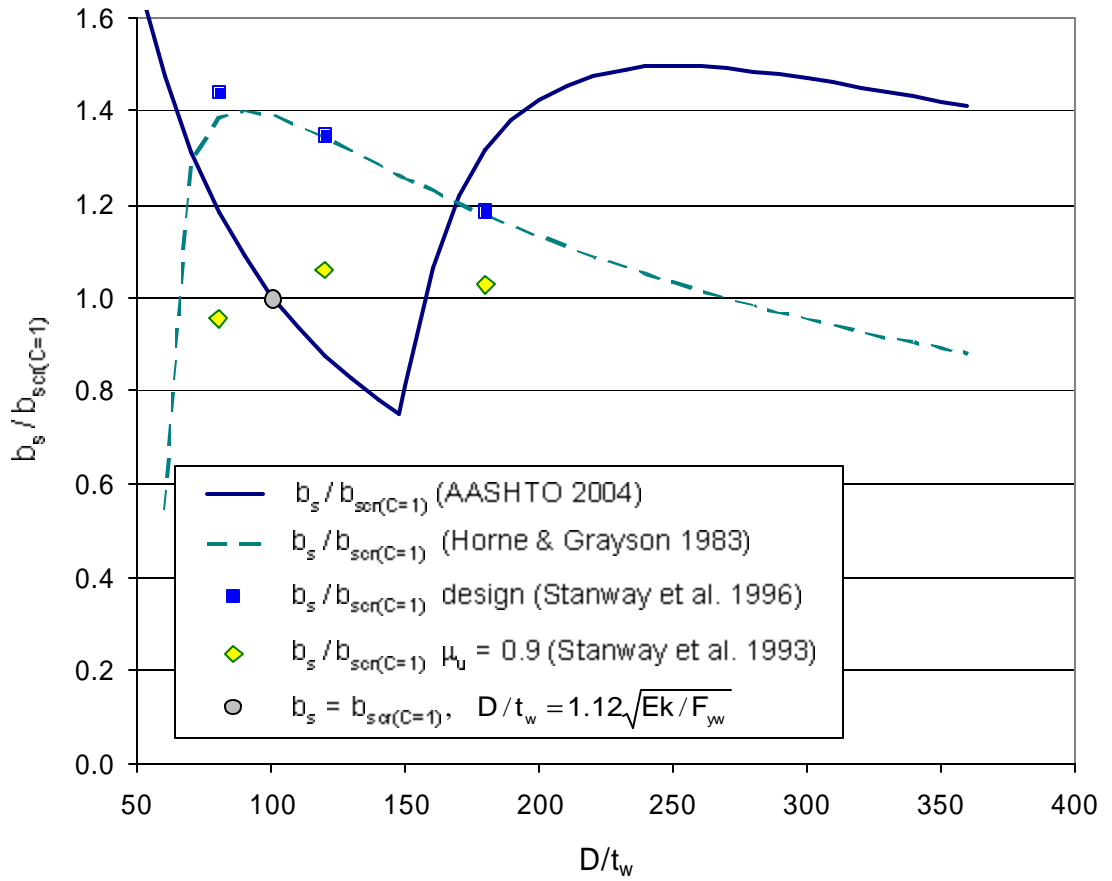


Figure 4.26a. Required stiffener sizes, girders with one-sided stiffeners, $d_o/D = 1$, $F_{yw} = 245 \text{ MPa}$ (36 ksi).

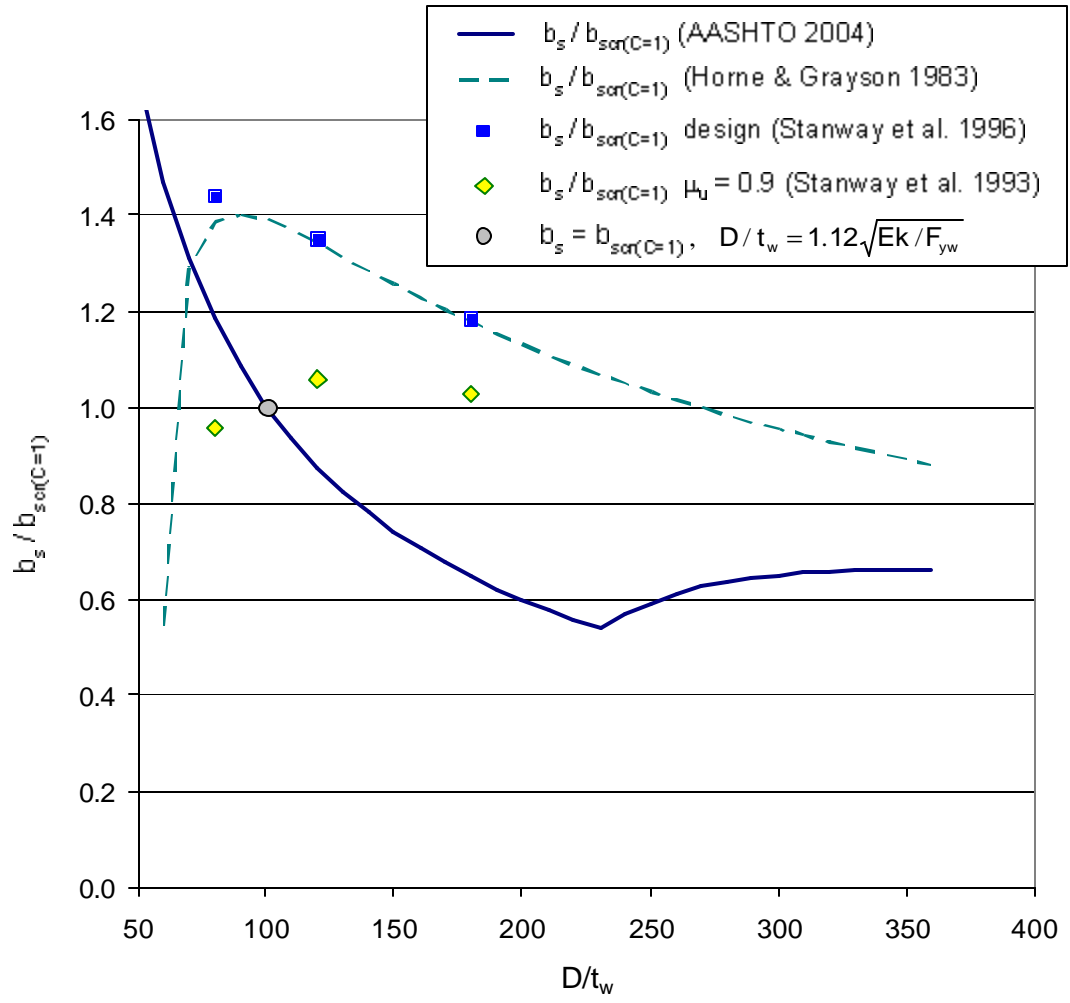


Figure 4.26b. Required stiffener sizes, girders with two-sided stiffeners, $d_o/D = 1$, $F_{yw} = 245 \text{ MPa}$ (36 ksi).

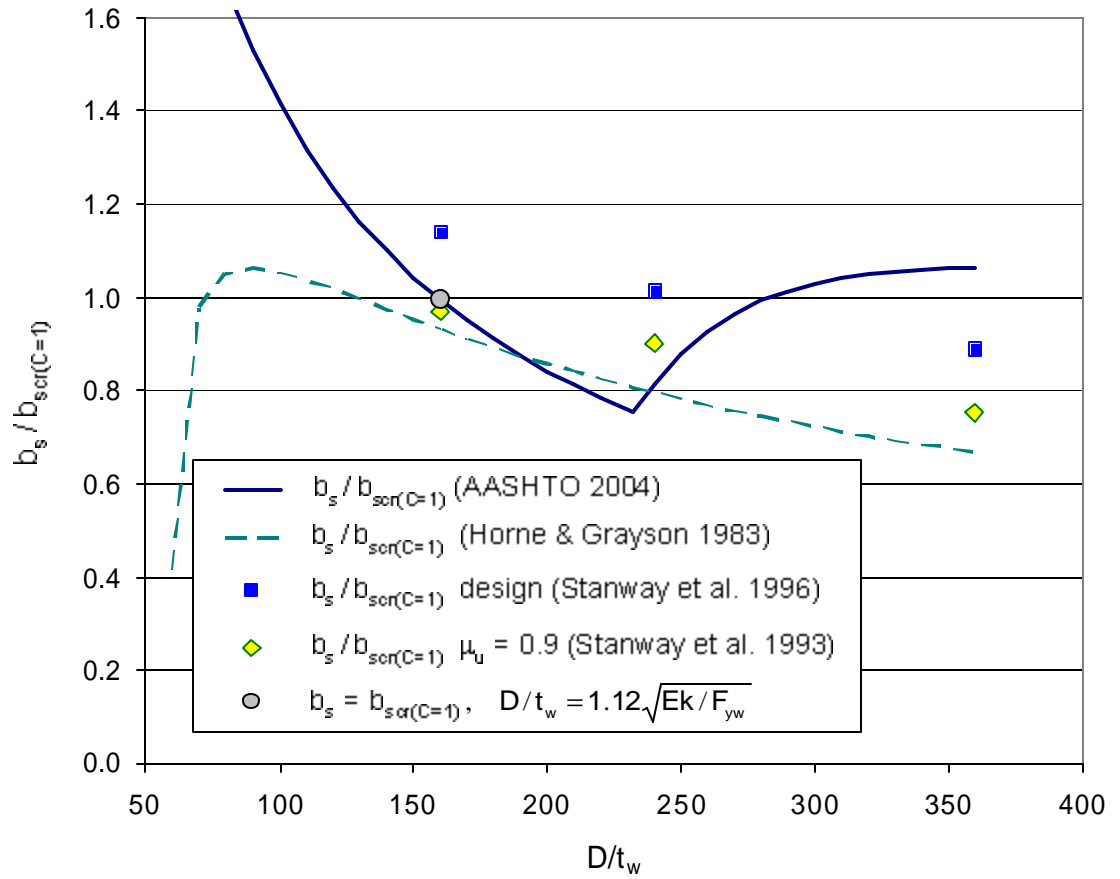


Figure 4.27a. Required stiffener sizes, girders with one-sided stiffeners, $d_o/D = 0.5$, $F_{yw} = 245$ MPa (36 ksi).

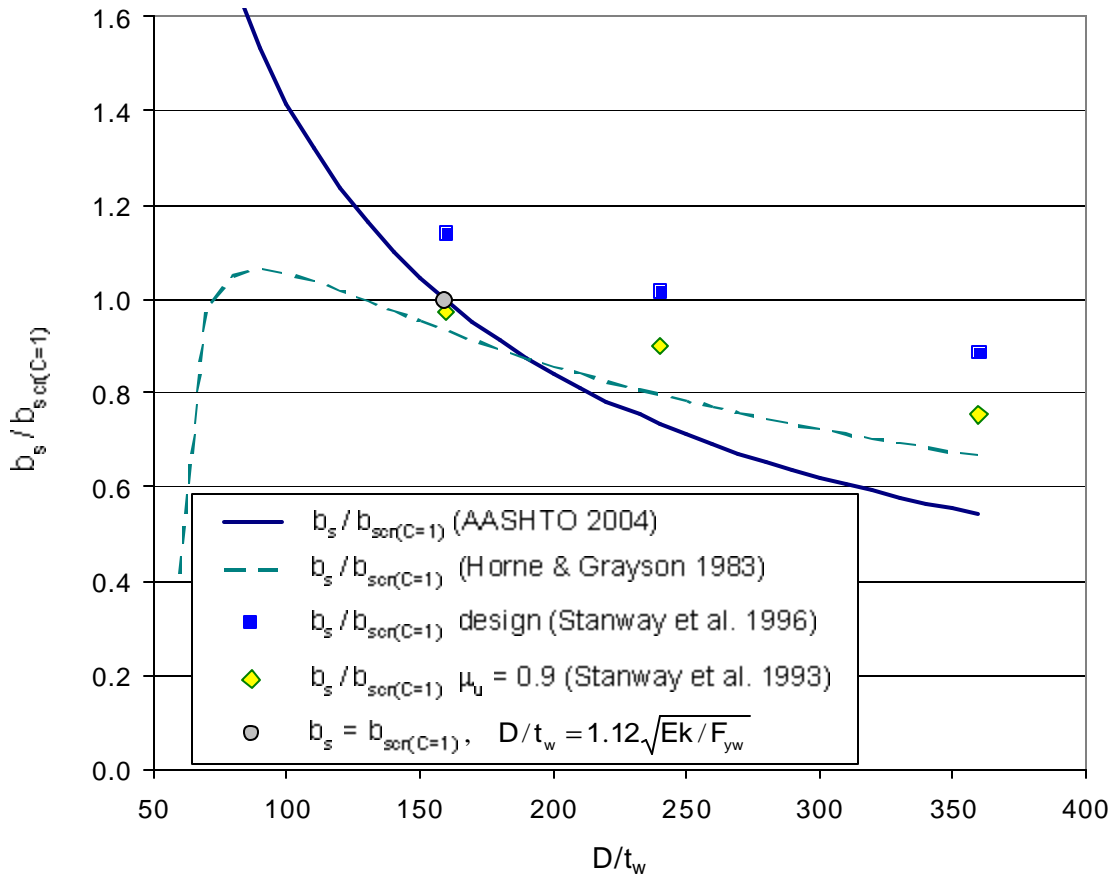


Figure 4.27b. Required stiffener sizes, girders with two-sided stiffeners, $d_o/D = 0.5$, $F_{yw} = 245$ MPa (36 ksi).

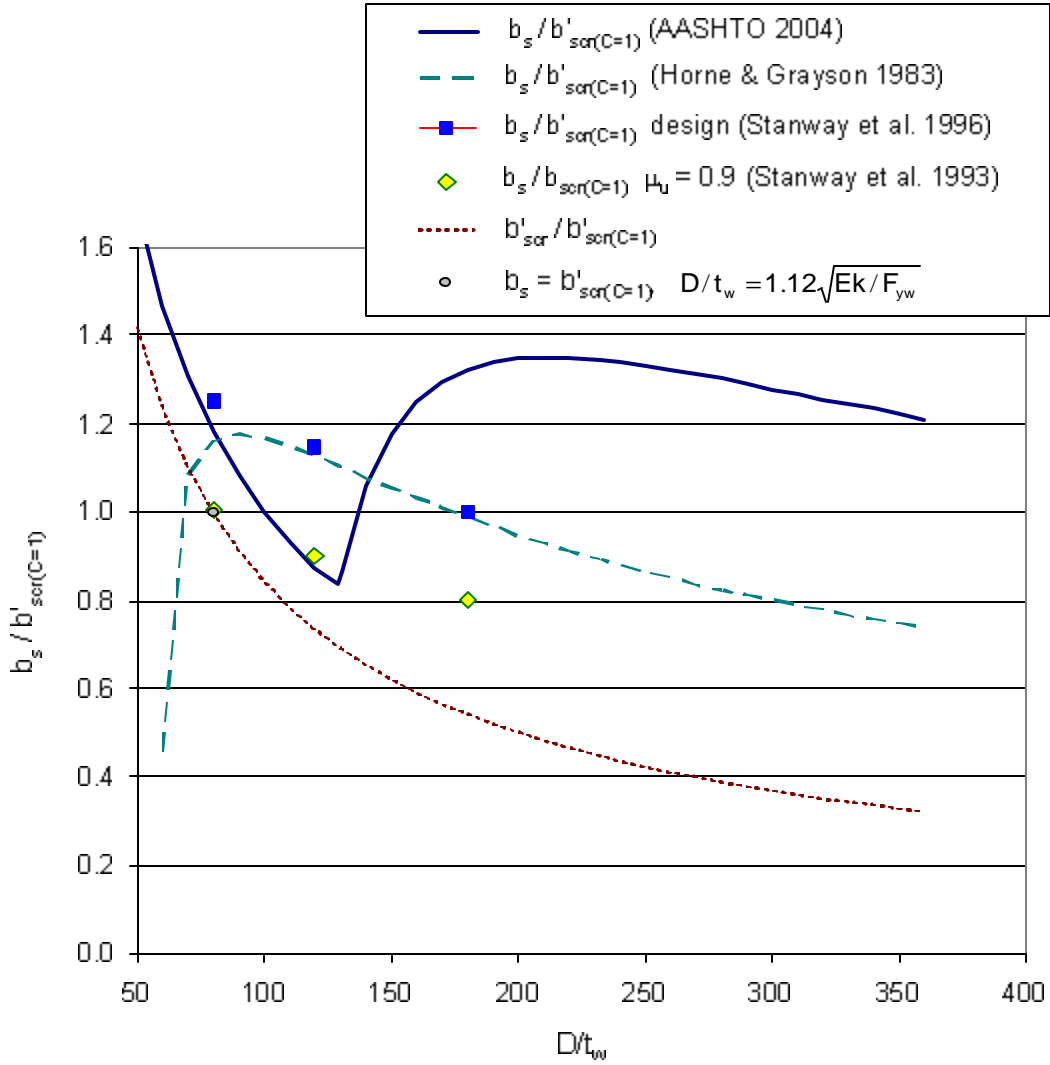


Figure 4.28a. Required stiffener sizes, girders with one-sided stiffeners, $d_o/D = 2$, $F_{yw} = 245 \text{ MPa}$ (36 ksi).

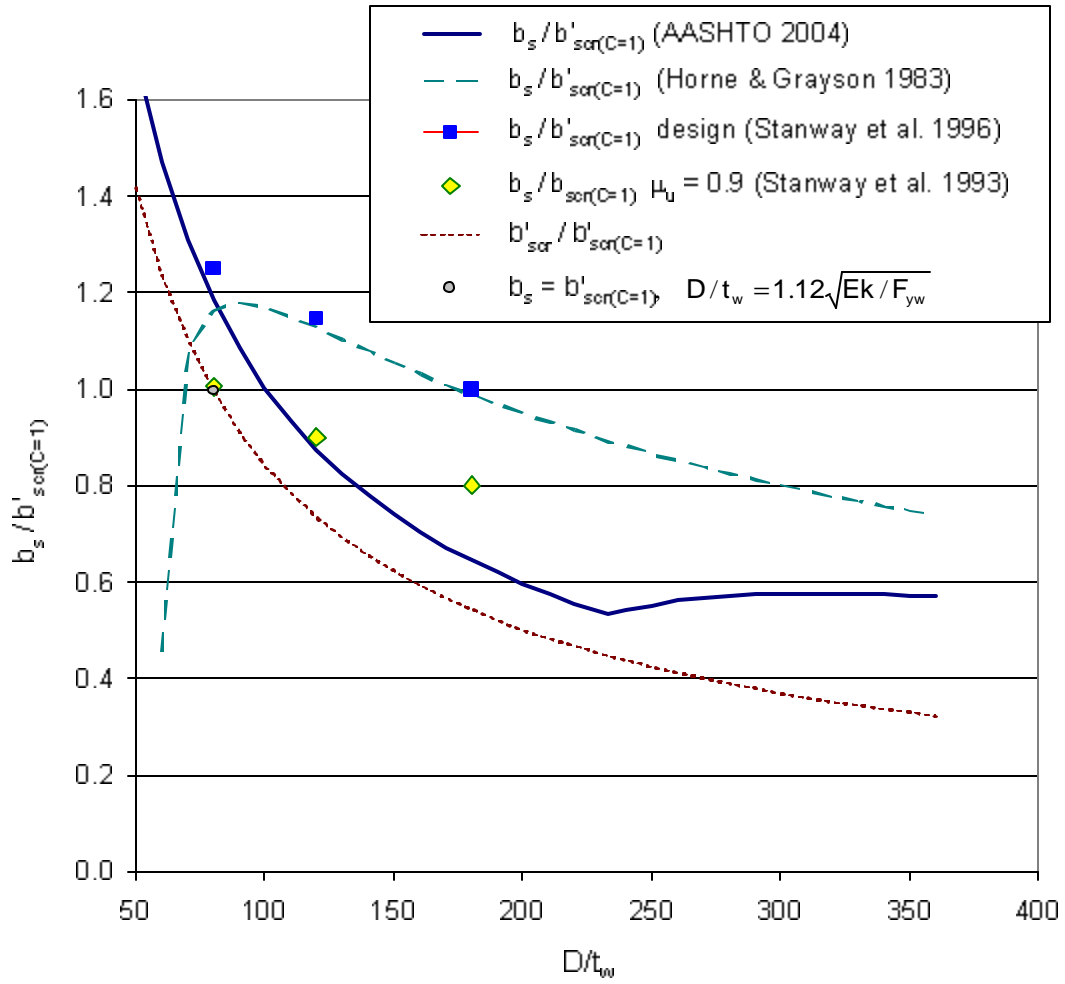


Figure 4.28b. Required stiffener sizes, girders with two-sided stiffeners, $d_o/D = 2$, $F_{yw} = 245$ MPa (36 ksi).

refined FEA solutions (in this case for $\mu_u = 0.9$). Also, it is important to note that Stanway's solutions in these figures indicate that b_s slightly smaller than $b_{scr(C=1)}$ is acceptable at $D/t_w = 80 \leq 1.12 \sqrt{Ek / F_{yw}}$. It is important to note that at small D/t_w values, the differences between the strengths for $I_s = 0$ versus $I_s = \infty$ are somewhat small. This fact is shown clearly in separate FEA solutions presented by Rahal and Harding (1990a) with $F_{yw} = F_{ys} = 355$ MPa. Therefore, the use of $\mu_u = 0.9$ as a criterion for proportioning of the stiffeners allows the web to achieve nearly the strength associated with $I_s = \infty$ at small D/t_w values.

The result that $b_s = b'_{scr(C=1)}$ is adequate to develop the fully-plastic web shear strength at $D/t_w = 1.12 \sqrt{Ek / F_{yw}}$ is also demonstrated in Figures 4.27 and 4.28, where Stanway's solution corresponding to $b/t_w = 80$ is essentially equal to $b'_{scr(C=1)}$. One should note that for $d_o/D = 0.5$, $b/t_w = 80$ corresponds to $D/t_w = 160$. Therefore, Figures 4.27 verify this result for a case in which the web is relatively thin and $V_n = V_p$ is developed by using a relatively small spacing of the transverse stiffeners d_o .

The stiffener design requirement given by Stanway's Equations (2.13), (2.14) and (2.30) to (2.33) and given by Horne and Grayson's Equation (2.15) are significantly larger at small D/t_w compared to Stanway's FEA solutions for $\mu_u = 0.9$ as well as to the data point $(b_s/b_{scr(C=1)}, D/t_w) = (1, 1.12 \sqrt{Ek / F_{yw}})^2$. This is also consistent with the

² The $b_s/b'_{scr(C=1)}$ versus D/t_w curve corresponding to Stanway's equations is not shown in Figures 4.28 through 4.30. This is because the normalized results from these equations in general depend significantly on the values of b_s/D and t_s/t_w (i.e., different $b_s/b'_{scr(C=1)}$ versus D/t_w curves are produced for different b_s/D and/or t_s/t_w), and the values of b_s/D and t_s/t_w for the recommended stiffener sizes obtained by Stanway for the different web slenderness values he studied ($b/t_w = 80, 120$ and 180) are different. The result is that Stanway's $(D/t_w, b_s/b'_{scr(C=1)})$ data points for different D/t_w fall on somewhat different $b_s/b'_{scr(C=1)}$ versus D/t_w curves. In the previous Figures 4.23 to 4.27, the corresponding data points fall on different curves, but these curves are all nearly the same.

results discussed in Section 4.6.2.2.1. Furthermore, Stanway's and Horne and Grayson's equations tend to allow smaller $b_s/b_{scr(C=1)}$ values in all cases for larger D/t_w , as observed previously in Section 4.6.2.2.1. However, the smallest value of $b_s/b'_{scr(C=1)}$ for the FEA solutions shown in Figures 4.26 to 4.28 is 0.75 (see Figures 4.27) whereas the smallest value for the FEA solutions shown in Figures 4.21 to 4.25 is 0.58 (see Figures 4.24).

The AASHTO (2004) solutions shown in Figures 4.26 to 4.28 also exhibit the same characteristics as those illustrated previously in Figures 4.21 to 4.25. Of critical importance, the AASHTO (2004) equations again result in sizes for two-sided stiffeners that are substantially smaller than those needed to develop the shear postbuckling strengths. Conversely, for girders with one-sided transverse stiffeners, the AASHTO (2004) equations result in stiffener sizes that are significantly larger than required by the refined FEA solutions in certain cases. They dip below the requirements indicated by the FEA solutions for $100 < D/t_w < 160$ in Figure 4.26a and for $160 < D/t_w < 250$ in Figure 4.27a.

Figures 4.26 through 4.28 illustrate an important attribute of the AASHTO (2004) equations for $D/t_w < 1.12 \sqrt{E_k / F_{yw}}$. As the web slenderness is reduced relative to the maximum D/t_w value corresponding to $C = 1$, the stiffener size required by the AASHTO (2004) moment of inertia equation increases dramatically. This is due to the fact that the AASHTO (2004) moment of inertia requirement gives the stiffener size needed to develop the *elastic* buckling strength of the web panel, $V_{cr,el}$. However, at $C = 1$, $V_{cr,el} = 1.25V_p$. Furthermore, $V_{cr,el}$ varies with the inverse of $(D/t_w)^2$ and $V_{cr,el}$ becomes substantially larger than V_p for $D/t_w < 1.12 \sqrt{E_k / F_{yw}}$. The transverse stiffener size needed to develop $V_{cr,el}$ is excessive and is not needed at small D/t_w values. This fact is

recognized in AASHTO (2004) by the addition of a provision which states that connection plates in members with

$$\frac{D}{t_w} \leq 2.5 \sqrt{\frac{E}{F_{yw}}} \quad (4.10)$$

need not satisfy the moment of inertia requirement of Equation (2.1). The Engineer should note that the limit in Equation (4.10) is identical to Equation (4.4) but using the AASHTO (2004) value of $k = 5$ for an unstiffened web. The results discussed above indicate that $b_s = b'_{scr(C=1)}$ is sufficient for $D/t_w < 1.12 \sqrt{Ek / F_{yw}}$.

One concern considered regarding the use of $b_s = b'_{scr(C=1)}$ for $D/t_w < 1.12 \sqrt{Ek / F_{yw}}$ is whether an inelastic web buckling failure might occur across multiple web panels in cases with small d_o/D . In as such, the calculation of the inelastic buckling resistance of an infinitely long web panel reinforced by equidistant transverse stiffeners of equal $I_s = I'_{scr(C=1)}$ is considered for an assumed minimum $d_o/D = 0.5$ using the equations in Bleich (1952). It can be shown that the shear buckling coefficient for the above type of girder is smaller for lesser F_{yw} . Therefore, the solution from Bleich with $F_{yw} = 230$ MPa (33 ksi) is employed.

Figure 4.29 shows the shear buckling coefficient as a function of the web slenderness. One can observe that, given the above value of F_{yw} , the shear buckling coefficient decreases from a value larger than specified by Equation (2.7) at $D/t_w = 169$ ($k = 26.74$) to the value 11.7 at $D/t_w = 50$. This is due to the inability of the transverse stiffener with $I_s = I'_{scr(C=1)}$ develop the elastic buckling strength of the web associated with $I_s = \infty$ for $D/t_w < 169$. From Equation (4.10), for $F_{yw} = 230$ MPa (33 ksi), the web fully plastic shear strength can be developed for an unstiffened web at $D/t_w = 75$. Furthermore,

Figure 4.30 shows that the elastic shear buckling strength of the infinitely long stiffened web plate with $d_o/D = 0.5$ increases continuously for $D/t_w < 169$, and at $D/t_w = 50$, $C_{el} = V_{cr,el}/V_p$ is greater than six if stiffeners are provided with $I_s = I'_{scr(C=1)}$. This figure also shows the ratio of the inelastic buckling strength to the fully plastic shear strength of the above plate, V_{cr}/V_p , based on Bleich's inelastic buckling approach.

At $D/t_w = 1.12 \sqrt{Ek / F_{yw}} = 166$, using $k = 25$ from Equation (2.7), the AASHTO (2004) shear strength equations give $C = 1$ whereas Bleich's inelastic buckling solution gives $C = 0.91$. At $D/t_w = 130$, Bleich's solution gives $C = 0.95$. The Engineer should note that Bleich's solution does not account for any incidental restraint from the torsional stiffness of I-girder flanges or the transverse stiffeners. Also, Bleich (1952) assumes a smaller proportional limit of 0.75 compared to 0.80 in the AASHTO (2004) equations, and Bleich assumes a continuous inelastic buckling strength with $C < 1$ for all $D/t_w > 0$ whereas AASHTO (2004) takes the shear strength as $V_n = V_{cr} = V_p$ at $D/t_w <$

$1.12 \sqrt{Ek / F_{yw}} = 166$, assuming that the transverse stiffeners have adequate rigidity. At $D/t_w = 1.12 \sqrt{Ek / F_{yw}} = 166$, AASHTO (2004) requires $I_s = I_{scr} = I'_{scr(C=1)}$ for $d_o/D = 0.5$.

Since this requirement is satisfied by the above hypothetical stiffener, the AASHTO (2004) solution of $C = 1$ is accepted at $D/t_w = 166$ (versus the solution $C = 0.91$ by Bleich's equations). Since Bleich's inelastic buckling solution gives larger C values for $D/t_w < 166$, one can conclude that Bleich's equations confirm that the use of $I_s = I'_{scr(C=1)}$ is sufficient for all D/t_w values less than $1.12 \sqrt{Ek / F_{yw}}$, even for the most critical cases involving a potential web buckling failure across multiple panels.

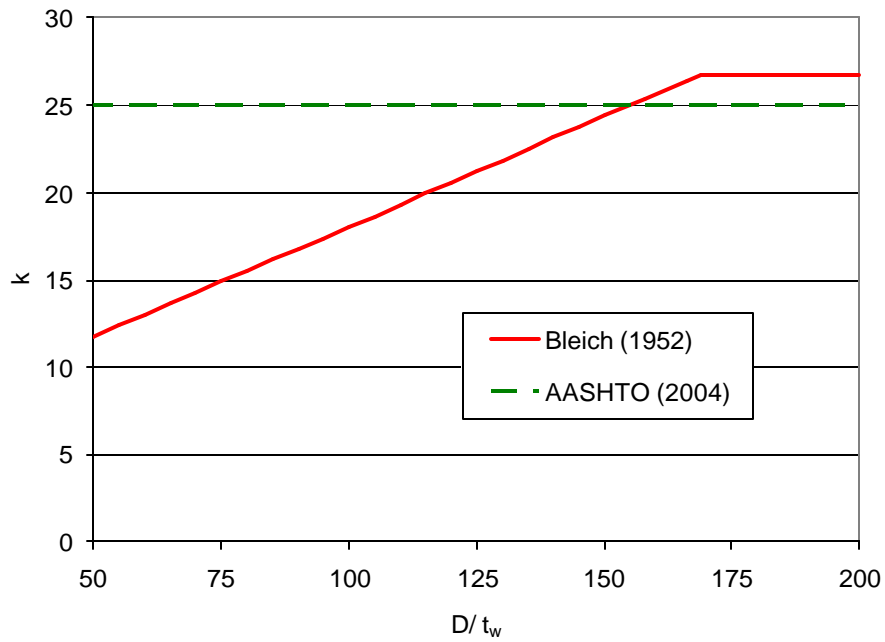


Figure 4.29. Shear buckling coefficient for an infinitely long plate subdivided by equidistant stiffeners with $I_s = I'_{scr(C=1)}$ versus the AASHTO (2004) k value, $d_o/D = 0.5$.

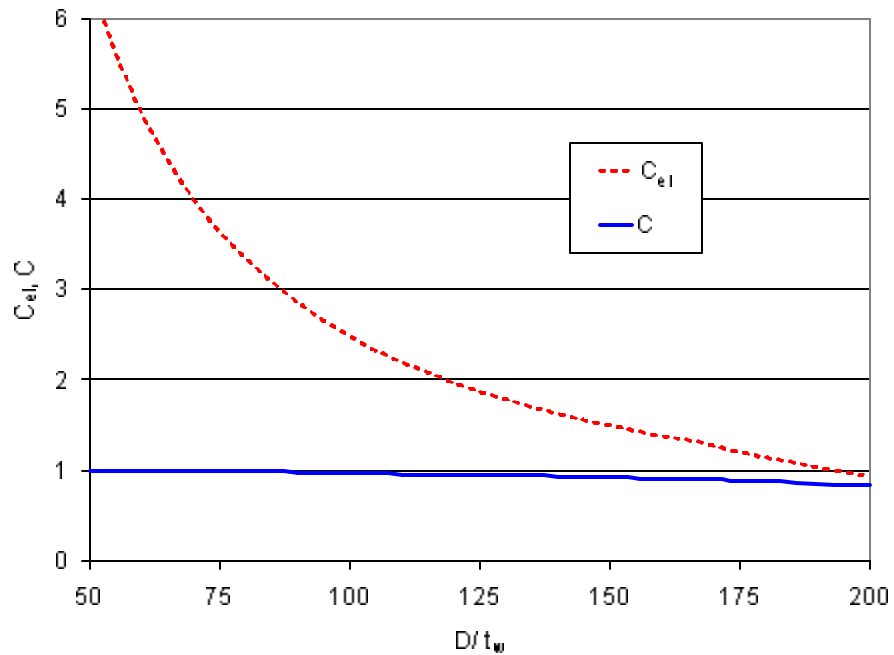


Figure 4.30. Elastic and inelastic buckling solutions $C_{el} = V_{cr,el}/V_p$ and $C = V_{cr}/V_p$ from Bleich (1952) for an infinitely long plate subdivided by equidistant stiffeners with $I_s = I'_{scr(C=1)}$, $d_o/D = 0.5$ and $F_{yw} = 230$ MPa (33 ksi).

4.7. Consideration of General Stiffener Cross-Section Geometry

The FEA studies in this research, as well as in the research by Stanway et al. (1993 and 1996) and by Rahal and Harding (1990a and b, 1991), are based specifically on one- or two-sided plate stiffeners with $b_s/t_s = 10$. For the development of design provisions, it is important to consider the implications of other stiffener geometries. Based on the findings that the stiffener strength behavior is governed more by bending than by axial loading effects, one can conclude that one- and two-sided plate stiffeners with $b_s/t_s < 10$ should be handled conservatively by a stiffener moment of inertia requirement derived from the above studies. This is based on the reasoning that the ratio of the elastic section moduli for two stiffeners with different b_s/t_s , but in which each stiffener provides the same I_s , is

$$\frac{S_{s1}}{S_{s2}} = \left[\frac{(b_s/t_s)_2}{(b_s/t_s)_1} \right]^{1/4} \quad (4.11)$$

Therefore, if stiffener 1 has a smaller width-to-thickness ratio than stiffener 2, it will have a larger elastic section modulus. Similarly, it can be reasoned that angle stiffeners with $b/t < 10$ for the outstanding leg should be handled conservatively.

Conversely, it can be reasoned that requirements based on the above studies may be overly optimistic for b_s/t_s or b/t values greater than 10. However, for $b_s/t_s = 16$, which is the largest stiffener width-to-thickness ratio permitted by AASHTO (2004), Equation (4.11) gives $S_{s1}/S_{s2} = 1.12$. Furthermore, for $F_{ys} > 245$ MPa, the AASHTO (2004) provisions utilize a conservative effective value for the stiffener yield stress given by the elastic local buckling stress F_{crs} previously described by Equation (2.27) for

$$\frac{b_s}{t_s} > 0.56 \sqrt{\frac{E}{F_{ys}}} \quad (4.12)$$

If these provisions are retained from AASHTO (2004), the largest b_s/t_s at which $F_{crs} = F_{ys}$ is 13.5 for $F_{ys} = 345$ MPa (50 ksi). For $b_s/t_s = 13.5$, the ratio of the elastic section modulus relative to an alternate stiffener with $b_s/t_s = 10$ is $S_{s1}/S_{s2} = 1.08$. For larger F_{ys} values, the corresponding stiffener width-to-thickness ratio at which F_{crs} is reduced below F_{ys} is a smaller value. Given the gradual increase in I-girder shear strengths with increasing I_s , and the fact that the final recommended stiffener I_{sR} values are somewhat larger than the knuckle values in Figures 4.1 through 4.7 in all cases with the exception of curved I-girders with $D/t_w = 300$, $d_o/D = 1$ and one-sided stiffeners on the inside, and given that the stiffener section modulus varies with b_s^3 for a given b_s/t_s , the author judges the above S_{s1}/S_{s2} values to be acceptable.

4.8. Stiffeners with $F_{ys} < F_{yw}$

It is also important to consider the potential influence of stiffener yield strengths smaller than F_{yw} . The yield strengths used for stiffeners in bridge I-girders may often be smaller than the web yield strength particularly if $F_{yw} > 345$ MPa (50 ksi). Also, it is important to account for potential local buckling effects if larger values of b_s/t_s within the AASHTO (2004) limits are used with $F_{ys} > 245$ MPa (36 ksi). The use of F_{crs} as an effective yield strength of the stiffener is one way of addressing these effects.

For the moment capacity of a stiffener with a smaller actual or effective F_{ys1} to be the same as an alternate stiffener with $F_{ys2} = F_{yw}$, one must have

$$\frac{S_{s1}}{S_{s2}} = \frac{F_{yw}}{F_{ys1}} \quad (4.13)$$

If these two stiffeners are taken to have the same b_s/t_s (the influence of different values of b_s/t_s is addressed in the previous section), then Equation (4.13) requires

$$\frac{I_{s1}}{I_{s2}} = \left(\frac{F_{yw}}{F_{ys1}} \right)^{4/3} \quad (4.14)$$

4.9. Consideration of Cases with $V_u < \phi V_n$

As discussed in Section 2.3.1, the AASHTO (2004) area requirement (Equation (2.28)) accounts for the fact that the demands on the transverse stiffeners are smaller at shear loads smaller than the shear capacity. This type of rule is not included in the recommended equations for design of transverse stiffeners presented in the following section for the following reasons:

- For the most commonly used stiffener type, a single rectangular plate attached to one side of the web, the recommended equations permit a smaller stiffener size than allowed in AASHTO (2004) as V_u approaches ϕV_n .
- For D/t_w values approaching $1.12 \sqrt{Ek/F_{yw}}$, the recommended transverse stiffener sizes approach the sizes required by AASHTO (2004) for development of the shear buckling strength without the consideration of $V_u/\phi V_n$.
- In some extreme cases, e.g., $d_o/D = 1$ and $D/t_w = 300$ (Figure 4.2), the use of I_s significantly smaller than the knuckle value may result in relatively large stiffener deflections at the strength load level.
- The term $V_u/\phi V_n$ in Equation (2.28) causes the shear resistance to be a continuous function of the applied load level. This can lead to complications in rating of I-girder bridges. If the rating loads are larger than the original design loads, the stiffener may be under-sized. As discussed in the commentary to the AASHTO (2004) provisions

for steel I-girder design, places where the resistance depended upon the applied load level in prior Specifications were eliminated wherever possible. Therefore, it is recommended that the stiffener design requirements should be independent of V_u . If the stiffeners are sized only to develop the shear buckling capacity, the girders would be checked based on the shear buckling capacity in rating. If the stiffeners are sized to develop the web postbuckling shear strength, then the full postbuckling shear strength may be used in rating calculations.

4.10. Summary of Recommendations

Section 4.6.2.2 shows that the stiffener size that satisfies the moment of inertia requirements from Equations (4.1) through (4.3) for development of the shear buckling strength $V_n = V_{cr} = V_p$ ($C = 1$) at $D/t_w = 1.12 \sqrt{Ek / F_{yw}}$ also serves as an accurate to somewhat conservative design to:

- develop the postbuckling shear strength for all larger web slenderness values in straight and curved I-girders and for either one- or two-sided plate stiffeners, and
- develop $V_n = V_p$ for all web slenderness values smaller than $D/t_w = 1.12 \sqrt{Ek / F_{yw}}$.

This stiffener size is defined in terms of a required moment of inertia by Equation (4.5), or in terms of a required stiffener width for a given b_s/t_s by Equation (4.7a). Based on the additional considerations discussed in Sections 4.7 through 4.9, Equation (4.5) may be expressed in the following general form:

$$I_{sR} = \frac{bD^3J}{1.4 \left(\frac{Ek}{F_{yw}} \right)^{1.5} \rho_t^{0.75}} \quad (4.15)$$

where

$$b = \min(d_o, D) \quad (4.16)$$

$$J = \frac{2.5}{\left(\frac{d_o}{D}\right)^2} - 2.0 \geq 0.5 \quad (4.17)$$

$$k = 5 + \frac{5}{(d_o/D)^2} \quad (4.18)$$

$$\rho_t = \max(F_{yw}/F_{crs}, 1) \quad (4.19)$$

and

$$F_{crs} = \frac{0.31E}{\left(\frac{b_s}{t_s}\right)^2} \leq F_{ys} \quad (4.20)$$

Equations (4.15) through (4.20) have the following advantages:

- These equations are based on providing adequate transverse stiffener bending stiffness and strength; the studies in this and prior research demonstrate that this is a more important consideration in developing the I-girder postbuckling shear resistance than the satisfaction of an area or axial force requirement.
- For $F_{ys} = F_{yw}$, these equations give the same result as Equations (4.1) through (4.3) for a web that has a D/t_w equal to the largest slenderness value corresponding to $C = 1$, $D/t_w = 1.12 \sqrt{Ek / F_{yw}}$.
- For webs with larger D/t_w values, these equations provide consistent requirements for one- and two-sided stiffeners, recognizing the fact that either of these stiffener types exhibits similar behavior when their moment of inertia, calculated as defined by Equations (2.4) or Equation (4.6), is the same.

- For webs with larger D/t_w values, Equations (4.15) to (4.20) avoid unconservative predictions by the AASHTO (2004) equations compared to refined FEA solutions and to multiple prior research recommendations in general for two-sided stiffeners and in specific cases for one-sided stiffeners for girders with D/t_w values where the AASHTO area requirement does not govern.
- For webs with larger D/t_w values, these equations avoid conservative predictions by the AASHTO (2004) equations compared to refined FEA solutions and to multiple prior research recommendations in a number of cases with one-sided stiffeners.
- These equations tend to be conservative relative to the refined FEA solutions generated in this work for web slenderness values approaching the maximum AASHTO (2004) limit of $D/t_w = 300$. However, they produce similar results to the equations recommended by Stanway et al. (1996) at these large D/t_w values. Given that the consequences of stiffener failure for reduction in strength and non-ductile post-peak load-deflection response tend to be greater for larger D/t_w values, this apparent greater conservatism for the largest D/t_w values is believed to be justified. For the most critical web aspect ratio ($d_o/D = 1$), the recommended equations give an accurate representation of the requirements determined from the refined FEA solutions generated in this work.
- Equation (4.15) indicates that the transverse stiffener requirements vary as a function of $(F_{yw})^{1.5}$. Interestingly, Rahal and Harding (1990a) conclude independently that the stiffener maximum lateral deflections are proportional to $(F_{yw})^{1.5}$, and in as such, use this form in the development of their recommended stiffener design equations.

For girders that are designed only for the web shear buckling strength, it is recommended that the transverse stiffeners should satisfy the smaller limit defined by:

(a) Equations (4.1) to (4.3), and

(b) Equations (4.15) to (4.20).

In this case, Equations (4.1) to (4.3) govern for $D/t_w > 1.12 \sqrt{E_k / F_{yw}}$, and Equations (4.15) to (4.20) govern for D/t_w smaller than the limit corresponding to $C = 1$. The use of Equations (4.15) to (4.20) for $D/t_w < 1.12 \sqrt{E_k / F_{yw}}$ recognizes the fact that the demands on the transverse stiffeners do not increase dramatically for webs stockier than the limit corresponding to $C = 1$. This fact is already recognized within AASHTO (2004) by the restriction associated with Equation (4.10), which specifies that the I_{scr} equations are not applicable to connection plates in girders having a web slenderness such that $C = 1$ is developed using the shear buckling coefficient for an unstiffened web ($k = 5$). The application of the above recommended rule further relaxes the corresponding transverse stiffener design provisions from prior AASHTO Specifications, removing the conservatism of the prior equations for girders approaching the limit of Equation (4.10).

CHAPTER V

CONCLUSIONS

5.1. Summary

This thesis investigates the behavior of one- and two-sided intermediate transverse stiffeners in straight and horizontally curved steel I-girders by refined full nonlinear finite element analysis. The solutions from these FEA studies are combined with the results from prior research to arrive at new recommendations for design of transverse stiffeners in straight and curved I-girder bridges.

The FEA solutions generated in this research corroborate the findings from multiple prior research studies that transverse stiffeners in straight steel I-girders designed for tension field action are loaded predominantly by bending due to the restraint they provide to lateral deflection of the web panels. Generally, there is evidence of some axial compression in the transverse stiffeners due to the development of the tension field, but even for the most slender web plates permitted for design by AASHTO (2004), the effect of the axial compression transmitted from the postbuckled web plate is typically minor compared to lateral loading effect. This indicates that the stiffener moment of inertia and/or section modulus is a more important design parameter than the stiffener area. The FEA studies of this work also show that in certain cases, significantly larger stiffener bending rigidities are needed to prevent excessive lateral displacement of the stiffeners and reduction of the maximum shear strengths in postbuckled webs compared to the rigidities needed to maintain a line of near zero lateral displacement at the shear buckling load. This is consistent with the findings of a number of prior research studies.

The FEA solutions in this and prior studies indicate that for relatively small stiffener bending rigidities, there is a rapid gain in girder shear strengths V_{\max} with increasing stiffener moment of inertia I_s . However, beyond a certain value of I_s , the shear strength reaches a plateau at which it is relatively constant with additional increases in I_s . The “knuckle” in the V_{\max} versus I_s curves is targeted in this as well as in other prior research as an “optimum” value for the transverse stiffener moment of inertia. It is observed that the V_{\max} versus I_s curves for girders with one- and two-sided stiffeners are slightly different, with the girders with two-sided stiffeners tending to have slightly larger strengths for a given I_s . Nevertheless, these differences are small enough such that they can be neglected and one- and two-sided transverse stiffeners can be designed using the same provisions without any undue penalty. As observed in prior studies, the above consistency in the response of girders with one- and two-sided stiffeners is obtained when I_s is calculated assuming that the neutral axis of the stiffener is located at the web.

Similar conclusions are reached for the V_{\max} versus I_s behavior of horizontally curved versus straight I-girders. The shear strength gain with increasing I_s is noticeably more gradual for some curved I-girders. The strength gain is the most gradual for curved I-girders with one-sided stiffeners and large web slenderness. However, even for girders with the largest web slenderness allowed by AASHTO (2004) ($D/t_w = 300$) and the most critical value of the panel aspect ratio with respect to demands placed on the transverse stiffeners ($d_o/D = 1$), the differences between the different $V_{\max} - I_s$ curves is small enough such that it is feasible to develop one set of requirements for all types of transverse stiffeners in both straight and curved I-girders.

Sections 2.1.3 and 2.2.1 show that for $d_o/D \leq 1$, the I_s required by AASHTO (2004) is an accurate approximation of the moment of inertia, I_{scr} , needed to develop web panel shear buckling strengths equal to the shear buckling resistance of a simply supported flat plate of the same dimensions. However, the AASHTO (2004) equation for I_{scr} is shown to be somewhat conservative for increasing d_o/D values greater than one. These findings are based in large part on the research by Stanway et al. (1993) and by Bleich (1952). A simple modification to the AASHTO (2004) equation is proposed, involving the use of the minimum of the stiffener spacing d_o or the web depth D (i.e., $b = \min(d_o, D)$) within the equation for I_{scr} , rather than d_o . This modified moment of inertia requirement, denoted by the symbol I'_{scr} , is more accurate for $d_o/D > 1$.

Chapter IV shows that the stiffener moment of inertia needed for development of the web shear postbuckling strength varies from I_{scr} to $85I_{scr}$ depending on d_o/D and D/t_w , where I_{scr} is the AASHTO (2004) moment of inertia requirement. However, for a given d_o/D , the stiffener size that gives $I_s = I'_{scr}$ for a web thickness such that $V_n = V_p$ (or $C = 1$) is an accurate to somewhat conservative size for all values of D/t_w . This particular stiffener size is represented in this thesis as the moment of inertia requirement $I'_{scr(C=1)}$ or, for a given b_s/t_s , as the stiffener width requirement $b'_{scr(C=1)}$. The following form of the equation for $I'_{scr(C=1)}$, which includes the additional term $\rho_t^{0.75}$ to account for the potential use of stiffeners with a smaller yield or effective yield strength (based on stiffener local buckling considerations), is recommended for the design of transverse stiffeners in all types of curved and straight bridge I-girders:

$$I_s \geq \left[I_{sR} = \frac{bD^3 J}{1.4 \left(\frac{Ek}{F_{yw}} \right)^{1.5} \rho_t^{0.75}} \right] \quad (5.1)$$

where

$$b = \min (d_o, D) \quad (5.2)$$

and

$$\rho_t = \max(F_{yw}/F_{crs}, 1) \quad (5.3)$$

The term J in Equation (5.1) is the same as the corresponding term in the AASHTO (2004) equation for I_{scr} , the term k in Equation (5.1) is the AASHTO (2004) shear buckling coefficient, and the term F_{crs} in Equation (5.3) is the stiffener effective yield strength accounting for local buckling considerations given by AASHTO (2004).

Stiffeners sized using Equation (5.1) are adequate in terms of both strength and stiffness for development of tension field action in both curved and straight I-girders with $D/t_w > 1.12 \sqrt{Ek/F_{yw}}$, in which case $C = V_{cr}/V_p$ is less than one. Also, stiffeners sized using this equation are adequate to maintain $C = 1$ in web panels where D/t_w is smaller than the above limit corresponding to $C = 1$. In I-girders designed based on the web shear buckling resistance, without consideration of tension field action, the stiffeners may be sized for the smaller of I'_{scr} and I_{sR} . In this case, the I'_{scr} equation governs for $D/t_w \geq 1.12 \sqrt{Ek/F_{yw}}$ whereas Equation (5.1) governs for $D/t_w < 1.12 \sqrt{Ek/F_{yw}}$.

Equation (5.1) has a number of advantages relative to the AASHTO (2004) provisions for design of intermediate transverse stiffeners:

- The AASHTO (2004) equation for the required stiffener area typically does not govern relative to the AASHTO I_{scr} equation when used to check two-sided transverse stiffeners. As noted above, transverse stiffeners with $I_s = I_{scr}$ are in many cases insufficient to develop the web postbuckling strength. In cases where the AASHTO (2004) area requirement governs the design, it tends to result in significantly undersized two-sided transverse stiffeners. Equation (5.1) fixes this unconservatism with the use of a single equation that gives consistent results for both one and two-sided stiffeners.
- The AASHTO (2004) provisions for transverse stiffener design result in one-sided stiffeners that tend to be too small in certain cases where the area requirement does not govern. The cause of this unconservative nature of the AASHTO (2004) provisions is the same as the cause of the above problem for two-sided stiffeners: $I_s = I_{scr}$ is generally not sufficient to develop the web postbuckling strength. However, in one-sided stiffener cases where the AASHTO (2004) area requirement governs, the resulting stiffener size is often conservative relative to the requirements determined from refined FEA solutions in this and other prior research. Equation (5.1) tends to be accurate for all D/t_w values relative to the refined FEA solutions generated in this research for $d_o/D = 1$, whereas it tends to be somewhat conservative relative to the refined FEA solutions at large D/t_w values with other panel aspect ratios. However, in most cases, Equation (5.1) is less conservative than the AASHTO (2004) provisions at these large D/t_w values. Also, Equation (5.1) tends to give an accurate to somewhat conservative estimate of the stiffener size required in procedures forwarded by Horne and Grayson (1983) and by Stanway et al. (1996) at large web

slenderness values. These more conservative solutions are believed to be merited for girders with large D/t_w , since the consequences of stiffener failures are more severe in these cases.

- Since Equation (5.1) is based on $I_s = I'_{scr}$ at the web thickness giving $V_{cr} = V_p$ ($C = 1$), it obviously gives the correct stiffener size in this limit at which the transverse stiffeners are not required to develop any tension field action. The equations proposed by Stanway et al. (1996) generally require a stiffener moment of inertia significantly larger than $I'_{scr(C=1)}$ at this limit of the web thickness. The Horne and Grayson (1983) equation tends to give a slightly more liberal stiffener size at this limit for girders with $d_o/D = 0.5$, but generally requires a larger stiffener at this limit for $d_o/D = 0.8$.
- For webs where d_o/D and D/t_w are small enough such that $C = 1$, i.e., when $D/t_w < 1.12 \sqrt{Ek / F_{yw}}$, Equation (5.1) avoids excessive stiffener sizes obtained using the AASHTO (2004) I_{scr} equation. The AASHTO (2004) I_{scr} equation requires excessively large stiffeners as D/t_w is reduced below the above limit since this equation is based on developing the elastic buckling load of the web plate. However, as D/t_w approaches $2.5 \sqrt{E / F_{yw}}$ (the above limit with $k = 5$), the web is adequate to develop $C = 1$ without any stiffening. Section 4.6.2.2.2 shows an example inelastic buckling solution from Bleich (1952) for a critical case with relatively large D/t_w values, but with small d_o/D and F_{yw} such that $C = 1$. This solution corroborates FEA results indicating that the transverse stiffener moment of inertia does not need to be increased relative to $I'_{scr(C=1)}$ when $D/t_w < 1.12 \sqrt{Ek / F_{yw}}$.

- Equation (5.1) recognizes the fact that one- and two-sided transverse stiffeners with equal I_s exhibit similar performance. This is consistent with prior findings by Horne and Grayson (1983), Rahal and Harding (1990a, 1990b and 1991), Stanway et al. (1993 and 1996), Xie (2000), and Lee et al. (2002 and 2003). However in the cases where the AASHTO (2004) area requirement governs, the resulting moment of inertia I_s is different for one- and two-sided stiffeners. Therefore in these cases, the girder strengths will be different depending on stiffener type (either one- or two-sided).

5.2. Future Work

The present study provides a reasonably comprehensive assessment of the general requirements for the design of one- and two-sided transverse stiffeners in curved and straight I-girder bridges. Nevertheless, a number of additional studies would be worthwhile:

- In this research, b_s/t_s of the transverse stiffeners is set at 10 in all cases. It would be useful to confirm the reasoning discussed in Section 4.7 that the recommendations in this work, based on $b_s/t_s = 10$, are sufficiently accurate for larger b_s/t_s and are not overly conservative for smaller b_s/t_s values.
- In this research and in other prior studies, the influence of $F_{ys} < F_{yw}$ has not been considered explicitly. The adjustment factor given by Equation (5.3) should be evaluated by a number of specific finite element studies. Also, stiffeners with b_s/t_s values such that F_{crs} in Equation (5.3) is less than F_{ys} should be tested to confirm the conservatism of the AASHTO (2004) equivalent yield strength F_{crs} .
- Although the geometric imperfection patterns utilized in this research are believed to provide an adequate representation of the strength behavior, additional studies should

be conducted to verify that there are no precipitous drops in shear strength or significantly larger demands on the transverse stiffeners for other imperfection patterns. For example, the geometric imperfection pattern that Rahal and Harding (1990a) found to be the most critical for $d_o/D = 0.5$, shown in Figure 3.6, should be investigated for the curved and straight I-girders considered in this study. Also, for $d_o/D > 1$, geometric imperfection patterns with multiple waves along the length of the individual panels should be considered.

- Horne and Grayson (1983) observe that when the stiffener bending rigidity is in the region of the “knuckle value” of the V_{\max} versus I_s curve, their solutions involving panels with a single stiffener, similar to the solutions in this study, are essentially the same as solutions involving four panels of equal dimensions, separated by three stiffeners. Rahal and Harding (1990a) also state that the single stiffener model is valid as long as the solution is not within the region of the $V_{\max} - I_s$ curve in which the strength drops rapidly with changes in I_s . In general, if a failure occurs across more than two web panels, or more than one transverse stiffener, the resulting reduction in the shear strength can be much larger than the reduction in the cases considered in this research. It would be useful to determine the V_{\max} versus I_s curves for cases similar to the girders considered in this study with $d_o/D = 1, 2$ and 3 , but with multiple intermediate stiffeners within the middle unbraced length between locations 2L and 2R (see Figure 3.1). It is likely that the girder cross-sections would need to be redesigned for flexure however, since the subdivision of the web by multiple stiffeners will in general significantly increase the shear strength.

- None of the girders considered in this study contained longitudinal stiffeners, although the solutions generated for $D/t_w = 300$ in this research are targeted at the design of these types of members. It is implicitly assumed that the strength of longitudinally stiffened I-girders, and the corresponding demands on their transverse stiffeners, are predicted conservatively by not including the longitudinal stiffeners within the FEA model. Also, it is assumed that the additional AASHTO (2004) requirements on the transverse stiffeners in longitudinally stiffened I-girders would still be applied along with the recommended equations. It is well known that in general, the stability behavior of structures is not always enhanced by adding material. For this reason, as well as for the reason that the demands on the transverse stiffeners in typical longitudinally stiffened I-girders may be smaller due to the presence of a longitudinal stiffener, a number of curved and straight girder studies with typical longitudinal stiffeners included would be useful.
- Lastly, it would be valuable to perform a few experimental tests focused on cases that exhibit the greatest demands on the transverse stiffeners, for example curved girders with $d_o/D = 1$, $D/t_w = 150$ and 300 , and one-sided transverse stiffeners located on the inside. These transverse stiffeners should be sized in the vicinity of the recommended I_{sR} values, the knuckle values determined in the FEA studies as well as somewhat smaller values, to provide a critical validation of the FEA solutions. The girder imperfections should be measured precisely and input into FEA models of the tests.

REFERENCES

- AASHTO (1969). *Standard Specifications for Highway Bridges*, 10th Edition, American Association of State Highway Officials, Washington, D.C.
- AASHTO (1998). *AASHTO LRFD Bridge Design Specifications, 2nd Edition, with 1999, 2000 and 2001 Interims*, American Association of State and Highway Transportation Officials, Washington D.C.
- AASHTO (2003). *Guide Specifications for Horizontally Curved Steel Girder Highway Bridges with Design Examples for I-Girder and Box-Girder Bridges*, American Association of State and Highway Transportation Officials, Washington D.C.
- AASHTO (2004). *AASHTO LRFD Bridge Design Specifications, 3rd Edition, with 2004 Interims*, American Association of State and Highway Transportation Officials, Washington D.C.
- AISC (1999). *Load and Resistance Factor Design Specification for Structural Steel Buildings*, American Institute of Steel Construction, Chicago, IL.
- ASTM (1993). *Standard Specification for High-Yield Strength, Quenched and Tempered Alloy Steel Plate, Suitable for Welding (A514/A514M-93a)*. Philadelphia, PA.
- AWS (2000). *Structural Welding Code–Steel*, AWS D1.1:2000, 17th ed., prepared by AWS Committee on Structural Welding, 450 pp.
- Aydemir, M.A. (2001). “Moment-Shear Interaction in HPS Hybrid Plate Girders,” M.S. Thesis, School of Civil and Environmental Engineering, Georgia Institute of Technology, 208 pp.
- Basler, K., Yen, B.T., Mueller, J.A., and Thurlimann, B. (1960). “Web Buckling Tests on Welded Plate Girders,” WRC Bulletin No. 64, Welding Research Council, New York, NY, 63 pp.

- Basler, K. (1961). "Strength of Plate Girders in Shear," *Journal of Structural Division*, ASCE, 87(ST7), 151-180.
- Bleich, F. (1952). *Buckling Strength of Metal Structures*, McGraw-Hill Book Company, INC., New York, New York.
- CEN (1993). *Eurocode 3: Design of Steel Structures, Part 1.1 – General Rules and Rules for Buildings*, ENV 1992-1-1, European Committee for Standardization, Brussels, Belgium.
- Galambos (1998). *Guide to Stability Design Criteria for Metal Structures*, T.V. Galambos (ed.), Structural Stability Research Council, Wiley Interscience, New York, NY, 911 pp.
- Horne, M.R. and Grayson, W.R. (1983). "Parametric Finite Element Study of Transverse Stiffeners for Webs in Shear," *Instability and Plastic Collapse of Steel Structures*, Proceedings of the Michael R. Horne Conference, L.J.Morris (ed.), Granada Publishing, London, 329-341.
- JSHB (1980). "The Japanese Specification for Highway Bridges," Japanese Road Association, Maruzen, Tokyo, February.
- Jung, S.K. and White, D.W. (2003). "Shear Strength of Horizontally Curved Steel I-Girders – Finite Element Analysis Studies," Final Report to Professional Service Industries, Inc. and Federal Highway Administration, School of Civil and Environmental Engineering, Georgia Institute of Technology, Atlanta, GA, July, 136 pp.
- Krouse, D. (2004). Personal communication, draft ASTM standard for HPS690W steel.
- Lee, S.C. and Yoo, C.H. (1999). "Strength of Plate Girder Web Panels under Pure Shear," *Journal of Structural Engineering*, ASCE, 125(8), 847-853.
- Lee, S.C., Yoo C.H., and Yoon D.Y. (2002). "Behavior of Intermediate Transverse Stiffeners Attached on Web Panels," *Journal of Structural Engineering*, ASCE, 128(3), 337-345.

- Lee, S.C., Yoo C.H., and Yoon D.Y. (2003). "New Design Rule for Intermediate Transverse Stiffeners Attached on Web Panels," *Journal of Structural Engineering*, ASCE, 129(12), 1607-1614.
- Mariani, N., Mozer J.D., Dym, C.L., and Culver, C.G. (1973). "Transverse Stiffener Requirements for Curved Webs," *Journal of Structural Division*, ASCE, 99(ST4), 757-771.
- Nakai, H., Kitada, T., Ohminami R., and Fukumoto K. (1984). "Experimental Study on Shear Strength of Horizontally Curved Girder Bridges," Proc. of JSCE, No. 350/I-2, 269-304.
- Nakai, H., Kitada, T., and Ohminami R. (1985). "A Proposition for Designing Transverse Stiffeners in Web Plate of Horizontally Curved Girders," *Proceeding of JSCE*, 362(I-4), October, 249-257.
- Nakai, H. and Yoo, C.H. (1988). *Analysis and Design of Curved Steel Bridges*, McGraw-Hill, NY, 673 pp.
- Porter, D.M., Rockey, K.C., and Evans, H.R. (1975). "The Collapse Behavior of Plate Girders Loaded in Shear," *The Structural Engineer*, 53(8), 313-325.
- Rahal, K.N. and Harding, J.E. (1990a). "Transversely Stiffened Girder Webs Subjected to Shear Loading – Part 1: Behaviour," *Proceedings of the Institution of Civil Engineers*, Part 2, 89, March, 47-65.
- Rahal, K.N. and Harding, J.E. (1990b). "Transversely Stiffened Girder Webs Subjected to Shear Loading – Part 2: Stiffener Design," *Proceedings of the Institution of Civil Engineers*, Part 2, 89, March, 67-87.
- Rahal, K.N. and Harding, J.E. (1991). "Transversely Stiffened Girder Webs Subjected to Combined In-Plane Loading," *Proceedings of the Institution of Civil Engineers*, Part 2, 91, June, 237-258.
- Rockey, K.C., Valtinat, G., and Tang, K.H. (1981). "The Design of Transverse Stiffeners on Webs Loaded in Shear – An Ultimate Load Approach," *Proceedings of the Institution of Civil Engineers*, Part 2, 71, December, 2425-2441.

- Stanway, G.S., Chapman, J.C., and Dowling, P.J. (1993). "Behaviour of a Web Plate in Shear with an Intermediate Stiffener," *Proceedings of the Institution of Civil Engineers, Structures and Buildings*, 99, August, 327-344.
- Stanway, G.S., Chapman, J.C., and Dowling, P.J. (1996). "A Design Model for Intermediate Web Stiffeners," *Proceedings of the Institution of Civil Engineers, Structures and Buildings*, 116, February, 54-68.
- Stein, M. and Fralich, R.W. (1949). "Critical Shear Stress of Infinitely Long, Simply Supported Plate with Transverse Stiffeners," *NACA Technical Note 1851*, Langley Aeronautical Laboratory, Langley Air Force Base, Va, April, 39 pp.
- Tang, K.H. and Evans, H.R. (1984). "Transverse Stiffeners for Plate Girder Webs – An Experimental Study," *Journal of Constructional Steel Research*, 4, 253-280.
- Timoshenko S.P. and Gere J.M. (1961). *Theory of Elastic Stability*, McGraw-Hill Book Company, INC., New York, New York.
- Vincent, G.S. (1969). "Tentative Criteria for Load Factor Design of Steel Highway Bridges," *AISI Bulletin No. 15*, American Iron and Steel Institute, Washington, D.C., 65 pp.
- White, D.W., Zureick, A.H., Phawanich, N. and Jung, S.K. (2001). "Development of Unified Equations for Design of Curved and Straight Bridge I-Girders," Final Report to American Iron and Steel Institute Transportation and Infrastructure Committee, Professional Service Industries, Inc., and Federal Highway Administration, School of Civil and Environmental Engineering, Georgia Institute of Technology, Atlanta, Georgia, October, 551 pp.
- White, D.W. and Barker, M. (2004). "Shear Strength of Transversely-Stiffened Steel I-Girders," Structural Engineering, Mechanics and Materials Report No. 26, School of Civil and Environmental Engineering, Georgia Institute of Technology, Atlanta, Georgia, May.
- Wright, W.J. (1997). Personal communication, stress-strain data from HPS 70W tension tests.

- Xie, M. (2000). "Behavior and Design of Transversely Stiffened Plates Subject to Combined Shear and Direct In-Plane Loading," PhD Thesis, Department of Civil and Environmental Engineering, Imperial College, London.
- Xie, M. and Chapman, J.C. (2003). "Design of Web Stiffeners: Axial Forces," *Journal of Constructional Steel Research*, 59, 1035-1056.
- Xie M. (2004). Personal communication, development of recommendations for design of transverse stiffeners.
- Yoo C.H., Yoon D.Y., and Lee S.C. (2004). "Mechanics of Diagonal Tension Field Action," *Journal of Structural Engineering*, ASCE, in review.
- Yura, J.A. (1993). "Fundamentals of Beam Bracing," *Is Your Structure Suitably Braced?*, Proceedings, Annual Technical Session, SSRC.
- Yura, J.A. (1995). "Bracing for Stability, State-of-the-Art," *Proceedings*, Structures Congress XIII, ASCE, 88-103.
- Zureick, A.H., White, D.W., Phoawanich, N., and Park, J. (2002). "Shear Strength of Horizontally Curved Steel I-Girders – Experimental Tests," Structural Engineering, Mechanics and Materials Report No. 02-4, Final Report to Professional Services Industries, Inc. and Federal Highway Administration, School of Civil and Environmental Engineering, Georgia Institute of Technology, Atlanta, Georgia, March, 157 pp.